NATIONAL LIBRARY
OTTAWA

BIBLIOTHÈQUE NATIONALE
OTTAWA

NAME OF AUTHOR... *BRYAN JOHN FUHR*

TITLE OF THESIS. *NUCLEAR MAGNETIC RESONANCE*
.... *STUDIES OF THE SOLUTION*
.... *CHEMISTRY OF METAL COMPLEXES*

UNIVERSITY... *UNIVERSITY OF ALBERTA*

DEGREE FOR WHICH THESIS WAS PRESENTED.... *Ph.D.*

YEAR THIS DEGREE GRANTED.... *1974*

Permission is hereby granted to THE NATIONAL LIBRARY

OF CANADA to microfilm this thesis and to lend or sell copies

of the film.

The author reserves other publication rights, and

neither the thesis nor extensive extracts from it may be

printed or otherwise reproduced without the author's

written permission.

(Signed) *Bryan J. Fuhr*

PERMANENT ADDRESS:
Dept. of Medical Cell Biology
University of Toronto
Toronto, Ontario   M5S 1A8

DATED. *November 7,* 1973

THE UNIVERSITY OF ALBERTA

NUCLEAR MAGNETIC RESONANCE STUDIES OF

THE SOLUTION CHEMISTRY OF METAL COMPLEXES

BY

Ⓒ BRYAN JOHN FUHR

A THESIS

SUBMITTED TO THE FACULTY OF GRADUATE STUDIES

AND RESEARCH IN PARTIAL FULFILMENT OF

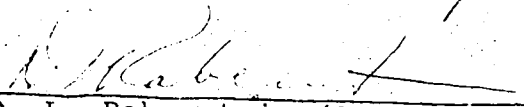THE REQUIREMENTS FOR THE DEGREE OF

DOCTOR OF PHILOSOPHY
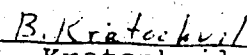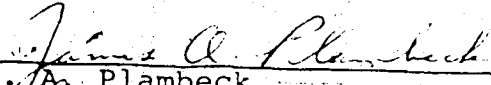
DEPARTMENT OF CHEMISTRY
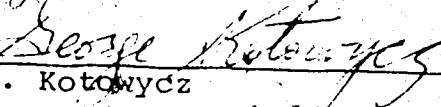
EDMONTON, ALBERTA

SPRING, 1974

THE UNIVERSITY OF ALBERTA

FACULTY OF GRADUATE STUDIES AND RESEARCH

The undersigned certify that they have read,
and recommend to the Faculty of Graduate Studies
and Research, for acceptance, a thesis entitled
NUCLEAR MAGNETIC RESONANCE STUDIES OF THE SOLUTION
CHEMISTRY OF METAL COMPLEXES

submitted by BRYAN JOHN FUHR

in partial fulfilment of the requirements for the
degree of DOCTOR OF PHILOSOPH.

D. L. Rabenstein (Supervisor)

B. Kratochvil

J. A. Plambeck

G. Kotowycz

H. B. Collier

D. W. Margerum
(External Examiner)

DATE: _____, 1973

TO MY WIFE, ARLENE

ABSTRACT

Part I

Proton magnetic resonance (pmr) methods have
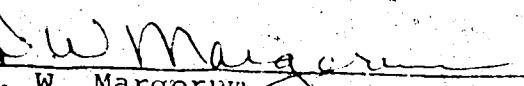been used to determine the average lifetimes of the
nonequivalent acetate methylenic protons before inter-
change in the cadmium and zinc complexes of 1,3-
propylenediaminetetraacetic acid (1,3-PDTA) and of
1,4-butylenediaminetetraacetic acid (1,4-BDTA).
Nonequivalence is indicated by AB multiplet patterns
in the pmr spectra of these complexes. The lifetimes
were determined over a range of temperatures from
the extent of collapse of the AB patterns by matching
experimental spectra with theoretical spectra which
were calculated as a function of the average lifetime
before AB interchange. It is proposed that these
lifetimes are a measure of the rates of partial
dissociation of these complexes. The AB multiplet
patterns in the pmr spectra of the cadmium, zinc
and lead complexes of ethylenediamine-N-N'-diacetic-
N-N'-dipropionic acid (EDDDA) were also investigated
as a function of temperature.

The kinetics of the ligand exchange reactions
of the cadmium, zinc, and lead complexes of 1,3-PDTA
and EDDDA have been studied using pmr line-broadening

methods. Rate constants were obtained for the proton-
assisted dissociation of each of these complexes
and for the displacement of complexed ligand by free
ligand for several of the complexes. The rates of
first order dissociation of all the complexes are
too slow to measure by the pmr technique. Rate
constants for the reaction of cadmium and zinc
with monoprotonated 1,3-PDTA are approximately
equal to those of the analogous reactions with
monoprotonated ethylenediaminetetraacetic acid,
while the rate constants for reaction of cadmium,
zinc and lead with monoprotonated EDDDA are from
2:5 to 10 times slower than the rate constants for
reaction with monoprotonated 1,3-PDTA. Mechanisms
are proposed for the formation reactions of the mono-
protonated ligands.

Part II

The binding of zinc, cadmium, lead and mercury by
the tripeptide glutathione has been investigated
by ^{13}C magnetic resonance spectroscopy. Binding to
the potential coordination sites was monitored as
a function of solution conditions by observing the
chemical shifts of the carbon atoms of glutathione.
The results indicate that each of these metal ions

binds to the potential coordination sites of gluta-
thione with a high degree of specificity. Mercury
binds only to the sulfhydryl group at mercury to
glutathione ratios up to 0.5 and over the entire
accessible pD range. At a metal to glutathione
ratio of 0.5, zinc and cadmium bind to both the
sulfhydryl and amino groups, the extent of binding
to the two different sites being a function of pD,
while lead binds only to the sulfhydryl group.
Some binding of the carboxylic acid groups to
zinc, cadmium and lead was detected in certain pD
regions. The chemical shift data also suggest that
zinc-promoted ionization of the peptide protons
with subsequent binding of zinc to the ionized
peptide nitrogen takes place above pD 10.5. The
results are discussed in terms of the possible
structures of the complexes.

ACKNOWLEDGEMENTS

TABLE OF CONTENTS

CHAPTER

Part I

KINETICS OF METAL COMPLEXES OF AMINO-
CARBOXYLIC ACIDS

LIST OF TABLES

LIST OF FIGURES

PART I

KINETICS OF METAL COMPLEXES OF

AMINOCARBOXYLIC ACIDS

1

CHAPTER I

INTRODUCTION

A. DISSOCIATION KINETICS

Formation and dissociation reactions involving multidentate ligands proceed via stepwise mechanisms in which one of the steps governs the overall rate of the reaction (1). For example, Ahmed and Wilkins (2) found that the kinetic results for the dissociation of the nickel complex of ethylenediamine were consistent with a mechanism involving stepwise rupture of the individual dentate bonds. Margerum and co-workers (3), on the basis of kinetic data for the formation of some nickel-polyamine complexes, proposed a mechanism involving the stepwise formation of the individual coordinate bonds and concluded that the formation of the first nickel-nitrogen bond was the rate-determining step. It was possible for these workers to estimate the values for the stepwise equilibrium constants from their kinetic data.

Stepwise mechanisms have also been proposed for reactions involving the exchange of a multidentate ligand between two different metal ions and of a metal ion between two multidentate ligands (4). For instance, such mechanisms have been inferred from

kinetic data for the reactions of zinc and copper with the nickel complex of ethylenediaminetetraacetic acid (EDTA) and analogs of EDTA (5,6,12,19) and for the reactions of EDTA with several nickel-polyamine complexes (7,8). In particular, the proposed mechanism for the reaction of copper with the nickel complex of EDTA (6) involves the unwrapping of an iminodiacetate fragment from the complex, followed by reaction with copper to give a dinuclear intermediate. For this case, the kinetic data yielded a rate constant for the half-unwrapping of EDTA from nickel.

The preceding work, in which such techniques as isotopic labelling, spectrophotometry and temperature jump relaxation were used, has shown that exchange reactions involving metal complexes of multidentate ligands take place in a stepwise fashion. However, it has only been possible in a few cases, such as in the work of Margerum and coworkers (6), to measure the rate constants for the individual steps.

Proton magnetic resonance (pmr) studies of metal complexes of EDTA (9-11,13-17) and analogs of EDTA (10,13,15-18,20-23) have shown that the complexity of the pmr spectrum of complexes of this type depends on the lability of the individual metal-ligand bonds. Hence pmr may provide a way to study

the kinetics of individual metal-ligand bonds. EDTA contains both oxygen and nitrogen donor groups and, depending on the lability of the various metal-ligand bonds, several situations may arise. The first is the one in which both the metal-oxygen and metal-nitrogen bonds are labile on the pmr time scale. In this case, because of rapid nitrogen inversion, the acetate methylenic protons are all equivalent, and the pmr spectrum for these protons consists of a single resonance peak. An example of a complex giving rise to this type of spectrum is $Sr(EDTA)^{2-}$ (39).

The second case, in which the metal-oxygen bonds are labile but the metal-nitrogen bonds are inert on the pmr time scale, may be illustrated by the following rotational conformers.
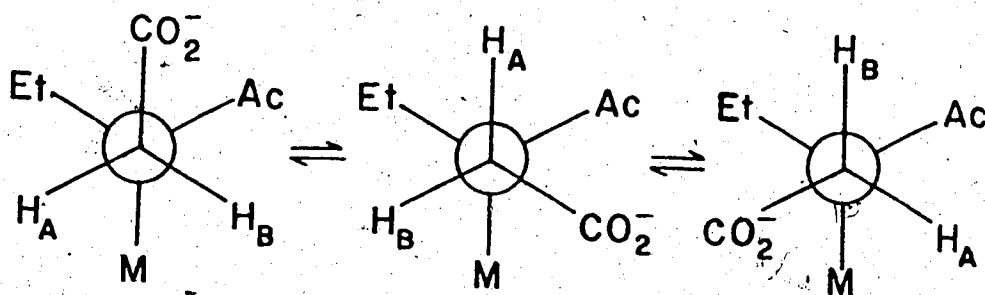
The acetate group is free to rotate about the nitrogen-acetate methylenic carbon bond. Examination reveals that, regardless of the rate of rotation, leading to interchange of the above three conformations, H_A and H_B do

not necessarily experience equivalent environments becau of the asymmetry of the quaternary nitrogen atom. Hence H_A and H_B may have different chemical shifts and if so, their pmr spectrum will consist of a single AB pattern. Interchange of H_A and H_B can occur only by inversion of the nitrogen atom, which presumably is possible only when the nitrogen atom is not metal coordinated. As long as the rate of inter- change of H_A and H_B is less than the chemical shift difference $\Delta\delta_{AB}$ (in sec^{-1}) between H_A and H_B, an AB pattern will be observed. In other words, metal- nitrogen bonding is inert on the pmr time scale. The pmr spectrum of the acetate methylenic protons of $Cd(EDTA)^{2-}$ consists of a single AB pattern such as that described above (24).

 For the situation in which both the metal-oxygen and metal-nitrogen bonding is inert on the pmr time scale, rather complex spectra are expected because the acetate groups are no longer equivalent. In the case of an octahedral complex in which all the ligand atoms are bound, two of the acetate groups are in the plane formed by the metal and the two nitrogen atoms and two are out of the plane. Therefore the acetate groups may be expected to exhibit two different AB patterns in their pmr spectra. The inert bonding

in Co(EDTA)$^{2-}$ results in two different AB patterns in the pmr spectrum for the acetate methylenic protons of this complex (9).

Sudmeier and Reilley (24) obtained evidence for a stepwise mechanism for the reaction of EDTA with Cd(EDTA)$^{2-}$ by monitoring the degree of collapse of the AB pattern in the pmr spectrum of the complex under changing solution conditions. In particular they studied the relative effectiveness of ligands which simulate fragments of EDTA in causing AB interchange. At some point in the overall displacement reaction, the first nitrogen of the complexed EDTA ligand is displaced. Dissociation of this metal-nitrogen bond was studied from the collapse of the AB pattern. It was found that ligands most effective in causing AB interchange contain at least three coordinating groups, a nitrogen and two carboxylate groups. On this basis, it was postulated that formation of the third bond is most effective in breaking the metal-nitrogen bond of the original complex. A stepwise mechanism was proposed with the rate-determining step being the breaking of the first metal-nitrogen bond of the originally complexed ligand and displacement by a carboxylate group of the incoming ligand.

Information about the kinetics of dissociation of the proton from the nitrogen in acidic solutions of tertiary amines of the structure
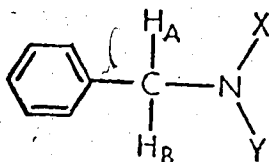
has been obtained from collapse of the AB pattern for the methylenic protons (25-28). When the nitrogen in these types of amines is protonated, it cannot undergo inversion. In this case, the following three rotational conformers are important, assuming rotation about the carbon-nitrogen bond.
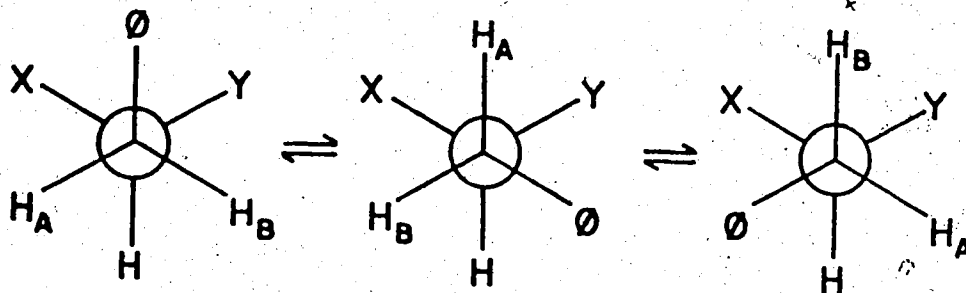
As in the case of the EDTA type complexes, when the rate of nitrogen inversion is slow on the pmr time scale, H_A and H_B will not necessarily experience equivalent environments regardless of the rate of interconversion of the above three conformers. Hence the pmr spectrum for the methylenic protons will

consist of an AB pattern. As the inversion rate is increased by increasing the pH of the solution, thus reducing the fraction of protonated amine in solution, the rate of interchange of H_A and H_B is increased resulting in a collapse of the AB pattern to a single peak. The rate of this AB interchange was determined for a series of tertiary amines by lineshape analysis of the pmr spectra (27). It was shown that if the rate of nitrogen inversion is very much less than the rate of reprotonation of a deprotonated amine, the observed AB interchange rate will be some fraction of the rate of nitrogen inversion. However, if the rate of inversion is very much greater than the rate of reprotonation, the observed AB interchange rate will be one-half the rate of proton exchange.

The work of Sudmeier and Reilley (24) and that on the tertiary amines (27,28) indicates that from a lineshape analysis of AB patterns it may be possible to obtain detailed information about the dissociation kinetics of complexes of multidentate ligands. By analogy with the work on tertiary amines, collapse of the AB pattern by inversion of a nitrogen atom in a complexed aminocarboxylic acid ligand may be governed by the rate of metal-nitrogen bond dissociation and/or the rate of inversion of the noncoordinated nitrogen

atom. If dissociation of the metal-nitrogen bond governs the rate of collapse, the presence of an AB pattern is an indication of inert metal-nitrogen bonding and potentially can provide information about the partial dissociation kinetics of the complex.

In Chapter II, the results of a pmr temperature study of the AB multiplet patterns arising from the acetate methylenic protons of the cadmium and zinc complexes of 1,3-propylenediaminetetraacetic acid (1,3-PDTA),

$$HO_2CCH_2\diagdown \quad \diagup CH_2CO_2H$$
$$NCH_2CH_2CH_2N$$
$$HO_2CCH_2\diagup \quad \diagdown CH_2CO_2H$$
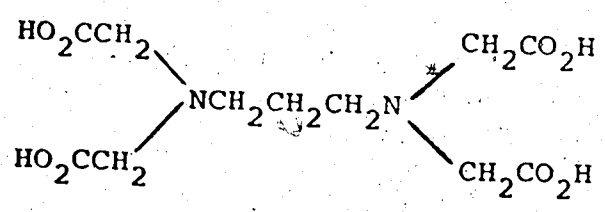
1,3-PDTA

and of 1,4-butylenediaminetetraacetic acid (1,4-BDTA) are presented and discussed (29,30). These particular

$$HO_2CCH_2\diagdown \quad \diagup CH_2CO_2H$$
$$NCH_2CH_2CH_2CH_2N$$
$$HO_2CCH_2\diagup \quad \diagdown CH_2CO_2H$$
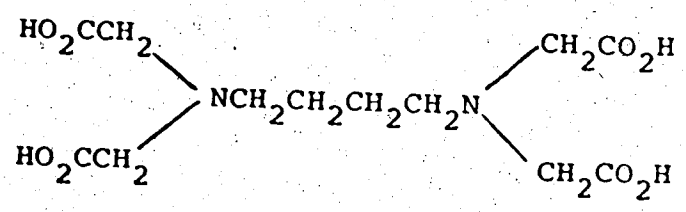
1,4-BDTA

ligands were chosen since they are structurally
similar to EDTA whose cadmium complex, as noted above
(24), exhibits an AB pattern in its pmr spectrum.
It was thought that the different sizes of the nitrogen-
metal-nitrogen chelate rings in the metal complexes
of 1,3-PDTA and 1,4-BDTA might affect the lability
of the metal-nitrogen bonds. The mutliplet patterns
for the acetate methylenic protons of the cadmium,
zinc and lead complexes of ethylenediamine-N,N'-
diacetic-N,N'-dipropionic acid (EDDDA) were also studied
as a function of temperature.

$$HO_2CCH_2CH_2 \diagdown \qquad \diagup CH_2CH_2CO_2H$$
$$NCH_2CH_2N$$
$$HO_2CCH_2 \diagup \qquad \diagdown CH_2CO_2H$$
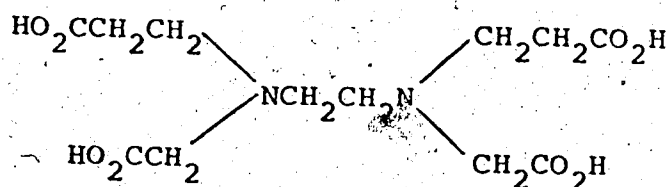
EDDDA

The main objective of this work was to determine what
kinetic information can be obtained from the multi-
plet patterns of the methylenic protons in complexes
of this type.

B. FORMATION KINETICS

According to the dissociative mechanism for the

react ... of an aquated metal ion with a ligand to form a metal complex (31-33,20), the metal ion and the ligand first diffuse together to form an outer-sphere complex. A water molecule then dissociates from the aquated metal ion and a donor group of the ligand coordinates with the metal ion at the vacated site. When steric and electrostatic effects are negligible, the rate-determining step in this reaction mechanism is water loss from the aquated metal ion. For a monodentate ligand this mechanism may be depicted as

$$M(H_2O)_6^{2+} + X^- \underset{k_{-x}}{\overset{k_x}{\rightleftharpoons}} M(H_2O)_6^{2+} \cdots X^-$$

$$\overset{k^{-H_2O}}{\longrightarrow} M(H_2O)_5 X^+ + H_2O$$
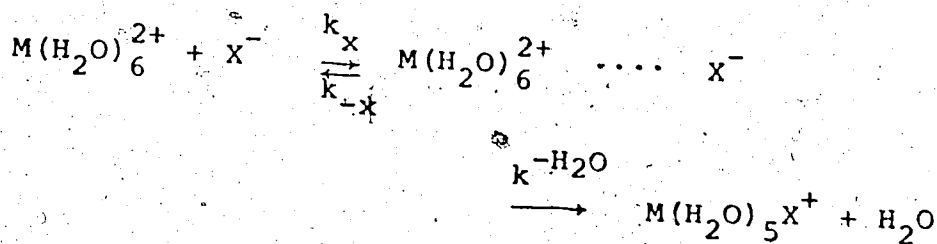
For a multidentate ligand, this reaction scheme has to be modified to account for the stepwise nature of complex formation with multidentate ligands (2,7,8). This is illustrated by the reaction scheme for a bidentate ligand.

$$M(H_2O)_6^{2+} + \overset{X}{\underset{X}{|}} \rightleftharpoons M(H_2O)_6^{2+} \cdots X{-}X \underset{k_{-1}H_2O}{\overset{k_1 H_2O}{\rightleftharpoons}}$$

$$M(H_2O)_5 X{-}X \overset{k_2}{\rightarrow} M(H_2O)_4 (X{-}X)$$

As in the case of a monodentate ligand, the bidentate ligand forms an outer-sphere complex with the metal ion, followed by water loss from the metal ion and formation of the first metal-ligand bond. A second water molecule then dissociates from the metal ion in a position cis to the first metal-ligand bond, and the second metal-ligand bond forms. The rate of this second bond formation process is represented by k_2 in the above reaction sequence. Depending upon the relative magnitudes of $k_{-1}^{H_2O}$ and k_2, the formation of the first or second bond to the bidentate ligand determines the overall rate of complex formation. For multidentate ligands, such as EDTA, the reaction sequence for complex formation would include steps for each successive bond formation.

It has been found for the majority of complex formation reactions involving multidentate ligands, that the formation of the first metal-ligand bond is rate-determining (70), its rate being governed by the rate of water dissociation from the aquated metal ion in the outer-sphere complex. For example, the rate of complexation of divalent cadmium, zinc, cobalt, copper and nickel by the monoprotonated form of EDTA (15,24,34,36-38).

$$M^{2+} + HEDTA^{3-} \rightarrow M(EDTA)^{2-} + H^+$$
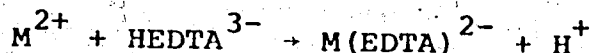
are all/approximately equal to those predicted by the dissociative mechanism.

Other studies have shown, however, that the rates of complexation of calcium and strontium by the tetraanion of EDTA are factors of 2.5×10^2 and

$$M^{2+} + EDTA^{4-} \rightarrow M(EDTA)^{2-}$$
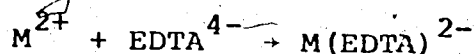
1.6×10^3 greater than their rates of complexation by $HEDTA^{3-}$ (39,40). Similarly, the rates of complexation of nickel (41) and cadmium (42,44) by the trianion of nitrilotriacetic acid (NTA) are 7×10^4 times

$$M^{2+} + NTA^{3-} \rightarrow M(NTA)^-$$
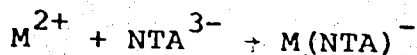
greater than their rates with $HNTA^{2-}$, while the rates of reaction of zinc (44) and lead (43) with $HNTA^{2-}$ are three to four orders of magnitude less than the approximate values predicted by the dissociative mechanism.

In one of the mechanisms proposed to account for these decreased rates, a small amount of the mono-protonated ligand is considered to be present in the carboxylate-protonated form along with the nitrogen-protonated form. This carboxylate-protonated form is considered to be the reactive species due to the blocking of the nitrogen atom by the proton (44-46).

A second reaction mechanism to account for the decreased rates of reaction of M^{2+} with HL^{3-} for ligands of the EDTA type may be illustrated by reference to Figure 1. Reaction proceeds by dissociation of water molecules followed by metal-ligand bond formation to yield intermediate (III) in which the three dentates of one end of the ligand are metal coordinated while co-ordination of the other end is blocked by the proton on the nitrogen. For further coordination to occur, the proton must be transferred to a carboxylate oxygen or a solvent molecule before the intermediate dissociates to the reactants. A slow proton transfer step relative to dissociation of the intermediate back to reactants would account for the decreased rates mentioned above.

The size of a chelate ring formed in many complexation reactions may also affect the overall rate of the reaction. For instance, the rate of reaction of cobalt(II) with α-alanine, in which a five-membered ring is formed, is an order of magnitude greater than that for the similar reaction with β-alanine, in which a six-membered ring is formed (47). Similarly, the rates for the reactions of nickel and cobalt with α-aminobutyric acid were found to be about an order of magnitude greater than the corresponding
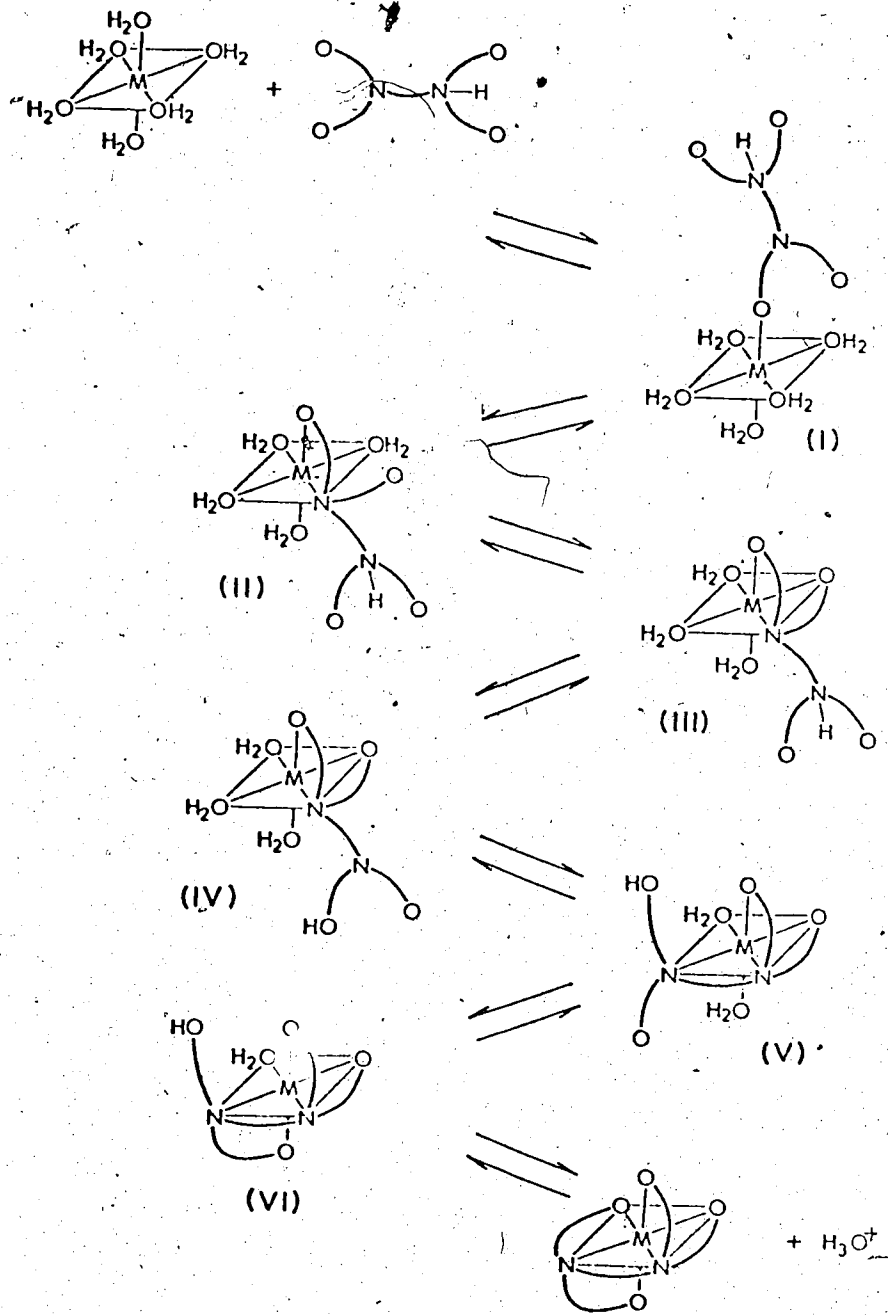
Figure 1: Proposed stepwise reaction mechanism for the
formation of ML^{2-} complexes from M^{2+} and HL^{3-}.
HL^{3-} is the monoprotonated form of EDTA type
ligands.

rates with the β-amino acid (48). The results with
the α-amino acids are consistent with the dissociative
mechanism. With the β-amino acids, however, the results
are consistent with a mechanism in which ring closure
is the rate-determining step. The latter mechanism
implies that the repossession of the vacated coordination
site by a water molecule is a faster process than ring
closure.

The size of chelate rings formed may also be an
important factor governing the rates of the formation
reactions of EDTA type complexes from the mono-
protonated form of the ligand. For example, the larger
the chelate ring which must be formed in going from
intermediates (IV) to (V) in Figure 1, the more
likely the vacated coordination site is to be reoccupied
by a water molecule before ring closure can occur.
The stability of certain intermediates may also affect
the overall rates of these formation reactions. For
instance, the less stable intermediate (III) is, the
more likely it is to dissociate to reactants before
proton transfer and bonding of the second nitrogen
can occur. In order to see if these two factors do
have an effect on the rates of certain complexation
reactions, a pmr line-broadening study of the kinetics
of the ligand exchange reactions of the cadmium, zinc

and lead complexes of 1,3-PDTA and EDDDA was undertaken (49). The results of this study are described in Chapter III. The predominant pathways by which the ligands exchange between free and complexed forms are established and their rate constants measured. The results are discussed with emphasis on the mechanism of formation of the complexes from the monoprotonated forms of the ligands.

CHAPTER II

PARTIAL DISSOCIATION KINETICS OF METAL COMPLEXES

OF AMINOCARBOXYLIC ACIDS

In this chapter, the results of a study of the temperature dependence of the AB multiplet patterns in the pmr spectra of certain metal complexes of aminocarboxylic acids are presented and discussed. In particular, the cadmium and zinc complexes of both 1,3-PDTA and 1,4-BDTA and the cadmium, zinc and lead complexes of EDDDA were investigated. A central purpose of this work was to ascertain what kinetic information can be obtained from the nonequivalence of the acetate methylenic protons in complexes of this type.
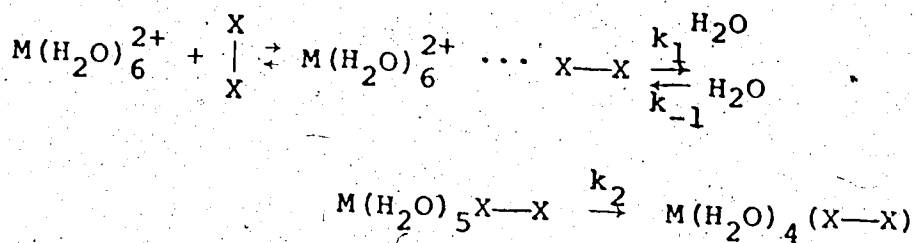
A. RESULTS

Analysis of Multiplet Patterns

The 60 MHz pmr spectrum of the acetate methylenic protons of $Zn(1,3-PDTA)^{2-}$ in aqueous solution at 25° is shown in the lower left hand side of Figure 2. The pH of the solution was 8.7 at 25°. The spectrum consists of an AB pattern, the upfield peak of which is obscured by a broad triplet due to the two methylene groups bonded to the nitrogen atoms in the

Figure 2: Representative experimental (left) and theoretical (right) 60 MHz pmr spectra of the acetate methylenic protons of an aqueous solution of $Zn(1,3-PDTA)^{2-}$.

propylene part of the ligand. Analysis of this AB

pattern by standard methods (35) yielded the values

for $\Delta\delta_{AB}$ and J_{AB} listed in Table I. $\Delta\delta_{AB}$ is the

chemical shift difference between the A and B protons

and J_{AB} is the spin-spin coupling constant. The

value for this geminal coupling constant was assumed

to be negative (17).

The 100 MHz pmr spectrum of the acetate methylenic

protons of $Cd(1,3-PDTA)^{2-}$ in D_2O solution at 10° is

shown in Figure 3. The pD of the solution was 7.5

at 25°. This multiplet pattern is more complicated

than that for the zinc system because of the ^{111}Cd

and ^{113}Cd isotopes which have a nuclear spin quantum

number of 1/2 and are present at a combined natural

abundance of 25.0%. The multiplet consists of the

AB part of an ABX pattern superimposed on an AB

pattern. The AB pattern arises from the complexes

of the cadmium isotopes whose spin numbers are zero,

while the AB part of an ABX pattern is due to the

^{111}Cd and ^{113}Cd complexes. The broad triplet just

upfield from the multiplet pattern arises from the

two methylene groups bonded to the nitrogen atoms

in the propylene part of the ligand. Analysis of the

AB pattern from slow exchange spectra of the type shown

in Figure 3 at several temperatures in the range

Table I

Pmr Spectral Parameters for the Acetate Methylenic

Protons of the Indicated Metal Complexes

	$\Delta\delta_{AB}$ (ppm)	J_{AB} (Hz)	$|J_{AX}|$	$|J_{BX}|$
Cd(1,3-PDTA)$^{2-}$	0.192	-16.3	11.8	15.0
Zn(1,3-PDTA)$^{2-}$	0.220	-16.3		
Pb(1,3-PDTA)$^{2-}$			19.2	
Cd(1,4-BDTA)$^{2-}$	0.141	-16.2	17.3	17.7
Zn(1,4-BDTA)$^{2-a}$	0.204	-16.3		
Cd(EDDDA)$^{2-}$	b	b	13.5	12.5
Zn(EDDDA)$^{2-}$	0.453	-18.3		
Pb(EDDDA)$^{2-}$	0.221	-16.7	22.6	17.5

(a) From reference 30.

(b) Could not be determined from the spectrum.
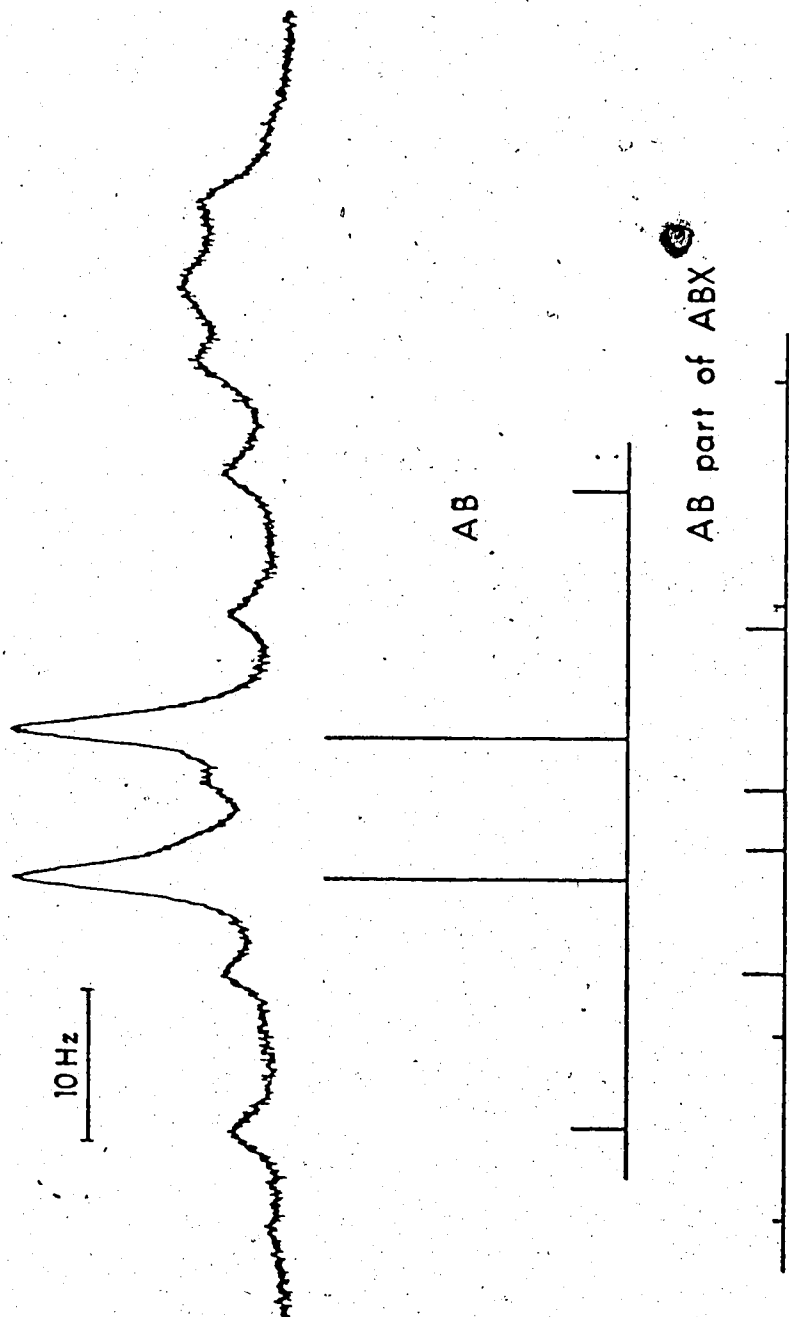
Figure 3: The 100 MHz pmr spectrum of the acetate methylenic protons of a D$_2$O solution of Cd(1,3-PDTA)$^{2-}$.

3 to 26° yielded the value for J_{AB} listed in Table I.
The chemical shift difference was found to decrease
linearly as the temperature was increased, and a
least squares analysis of the data yielded the
following relati :

$$\Delta\delta_{AB}(ppm) = -5.00 \times 10^{-4} T + 0.205 \qquad I$$

where T is the temperature in degrees centigrade.
Analysis of the AB part of the ABX pattern using the
value determined for J_{AB} gave a value of 3.2 Hz for
$|J_{AX} - J_{BX}|$, where J_{AX} and J_{BX} are the coupling
constants between the cadmium nuclei with spin numbers
1/2 and H_A and H_B. The values for $|J_{AX}|$ and $|J_{BX}|$
shown in Table I were determined by varying them and
calculating spectra until the best fit between
experimental and calculated spectra was obtained (35),
assuming the signs of the coupling constants to be
the same. No significant variation of these coupling
constants with temperature was found. The stick
spectra presented in the bottom part of Figure 3 were
calculated from the chemical shift and coupling
constants obtained above.

The 60 MHz spectrum of the acetate methylenic
protons of a solution of Pb(1,3-PDTA)$^{2-}$ at 25° and
pH 7.9 consists of a single resonance flanked symmet-

rically by two satellite peaks; the width of the central resonance is 1.2 Hz. The satellites arise from proton coupling to the ^{207}Pb isotope which has a nuclear spin quantum number of 1/2 and a natural abundance of 22.6%; the magnitude of the coupling constant J_{AX} is given in Table I. At both 100 and 220 MHz, the basic pattern of the spectrum of Pb(1,3-PDTA)$^{2-}$ is the same as that at 60 MHz. The lack of an AB pattern could be due to more labile lead-nitrogen bonding resulting in averaging of the resonances (9) or to accidental equivalence of the methylenic proton chemical shifts (15).

The 220 MHz spectrum of the acetate methylenic protons of Cd(1,4-BDTA)$^{2-}$ at 5° is shown at the bottom of Figure 4. The pH of this solution was 7.6 at 25°. The spectrum consists of the AB part of an ABX pattern superimposed on an AB pattern; analysis of the multiplet yielded the values listed in Table I.

The 60 MHz spectrum of the acetate protons of Zn(1,4-BDTA)$^{2-}$ at 62° consists of a simple AB pattern; the results of an analysis are given in Table I. This work was done in collaboration with Dr. G. Blakney (30).

The acetate proton spectrum of Cd(EDDDA)$^{2-}$ at 220 MHz and 5° is shown at the bottom left of Figure 5.
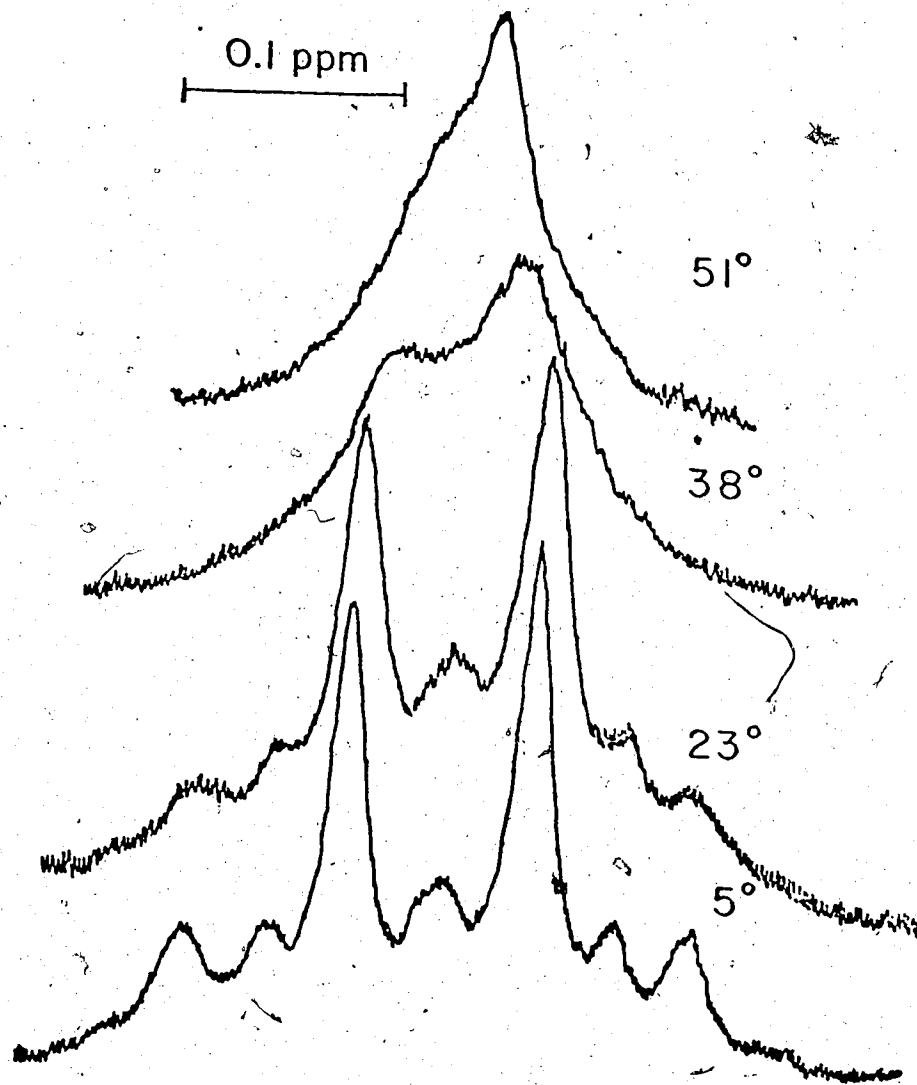
Figure 4: 220 MHz pmr spectra of the acetate methylenic
protons of an aqueous solution of
Cd(1,4-BDTA)$^{2-}$ at the indicated temperatures.
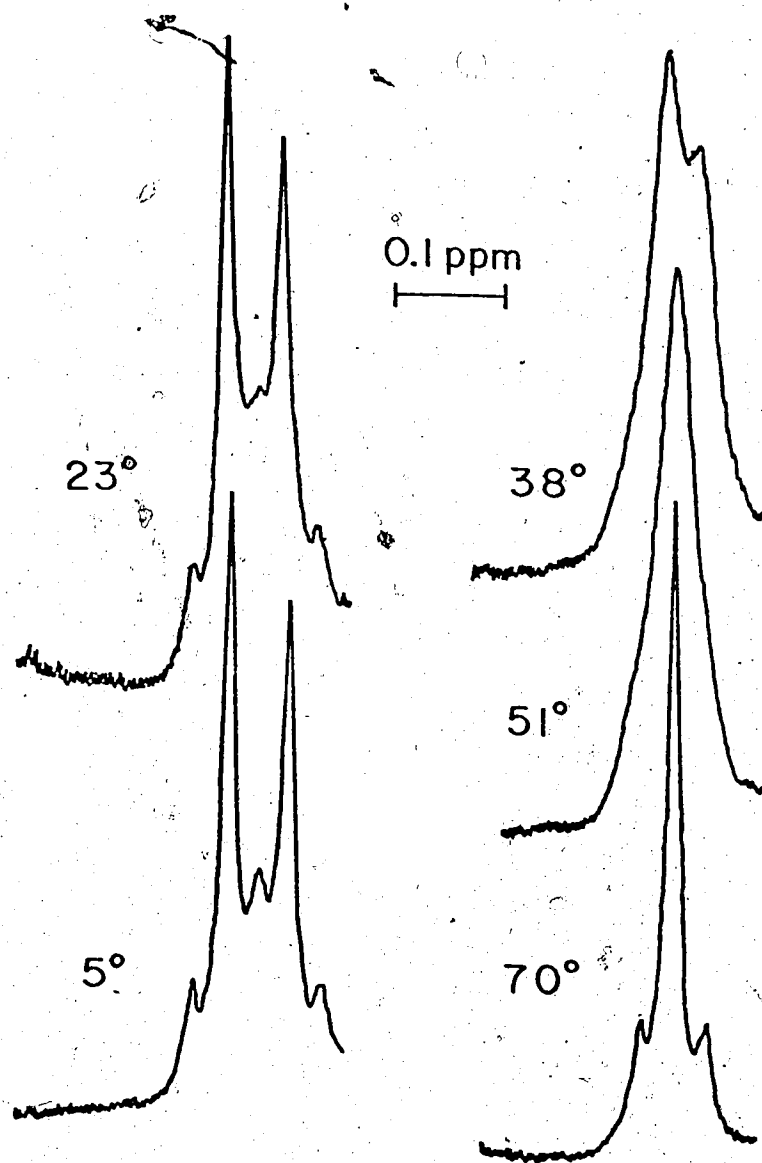
Figure 5: 220 MHz pmr spectra of the acetate methylenic protons of an aqueous solution of Cd(EDDDA)$^{2-}$ at the indicated temperatures.

It is believed to consist of the AB part of an ABX spectrum superimposed on an AB pattern. The two low intensity peaks of the AB pattern are too weak to be observed and hence, $\Delta\delta_{AB}$ and J_{AB} could not be calculated. Values for $|J_{AX}|$ and $|J'_{BX}|$ were estimated directly from the spectrum and are listed in Table I.

At 60 MHz and 25°, the acetate methylenic portion of the $Zn(EDDDA)^{2-}$ spectrum consists of a simple AB pattern. The results of an analysis of this spectrum are shown in Table I.

The 220 MHz spectrum of the acetate methylenic protons of $Pb(EDDDA)^{2-}$ at 5° consists of the AB part of an ABX spectrum superimposed on an AB spectrum. The AB part of an ABX spectrum arises from those complexes containing the ^{207}Pb isotope. Analysis of this multiplet pattern yielded the results shown in Table I.

AB Interchange Rates for the 1,3-PDTA and 1,4-BDTA Complexes

The lineshape of the multiplet pattern for the acetate methylenic protons of $Cd(1,3-PDTA)^{2-}$ is temperature dependent, as shown by the 60 MHz spectra in Figure 6 for a solution of the complex which was pH 8.0 at 25°. The two low intensity peaks of the
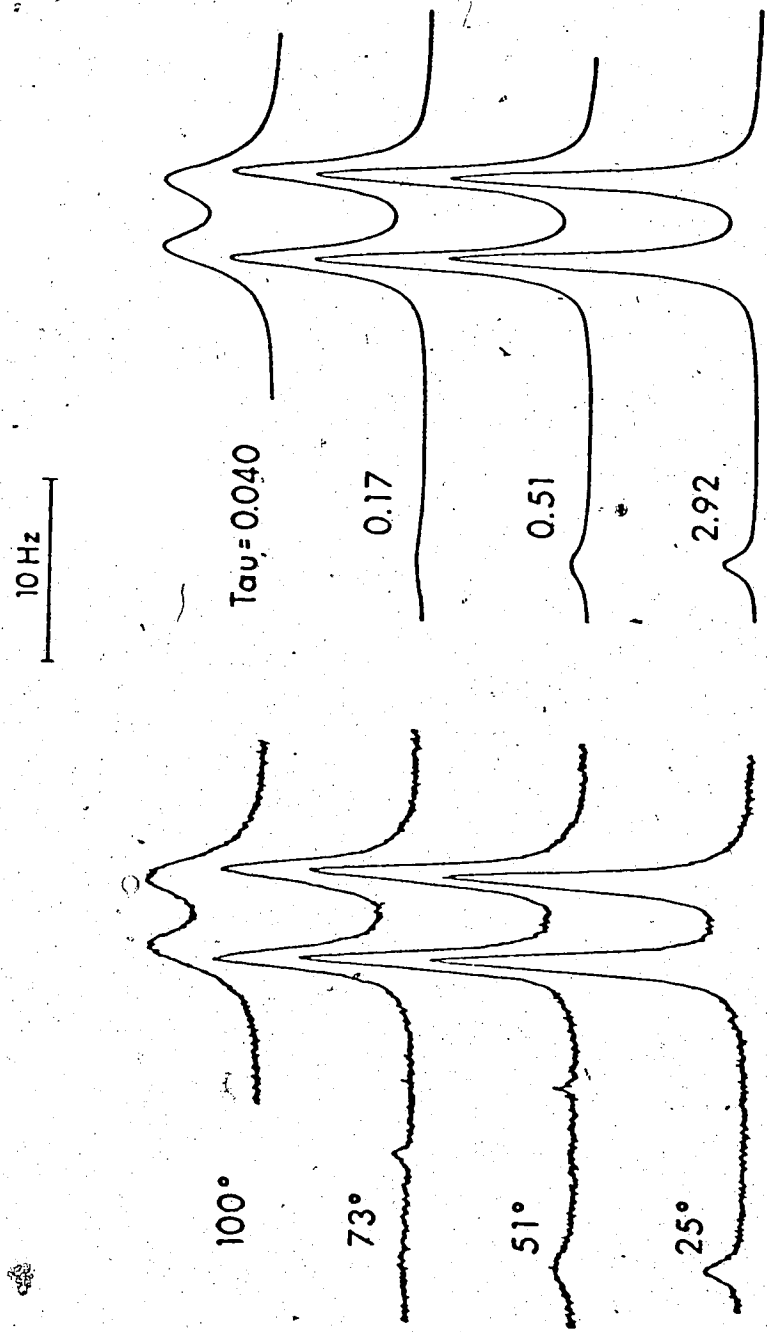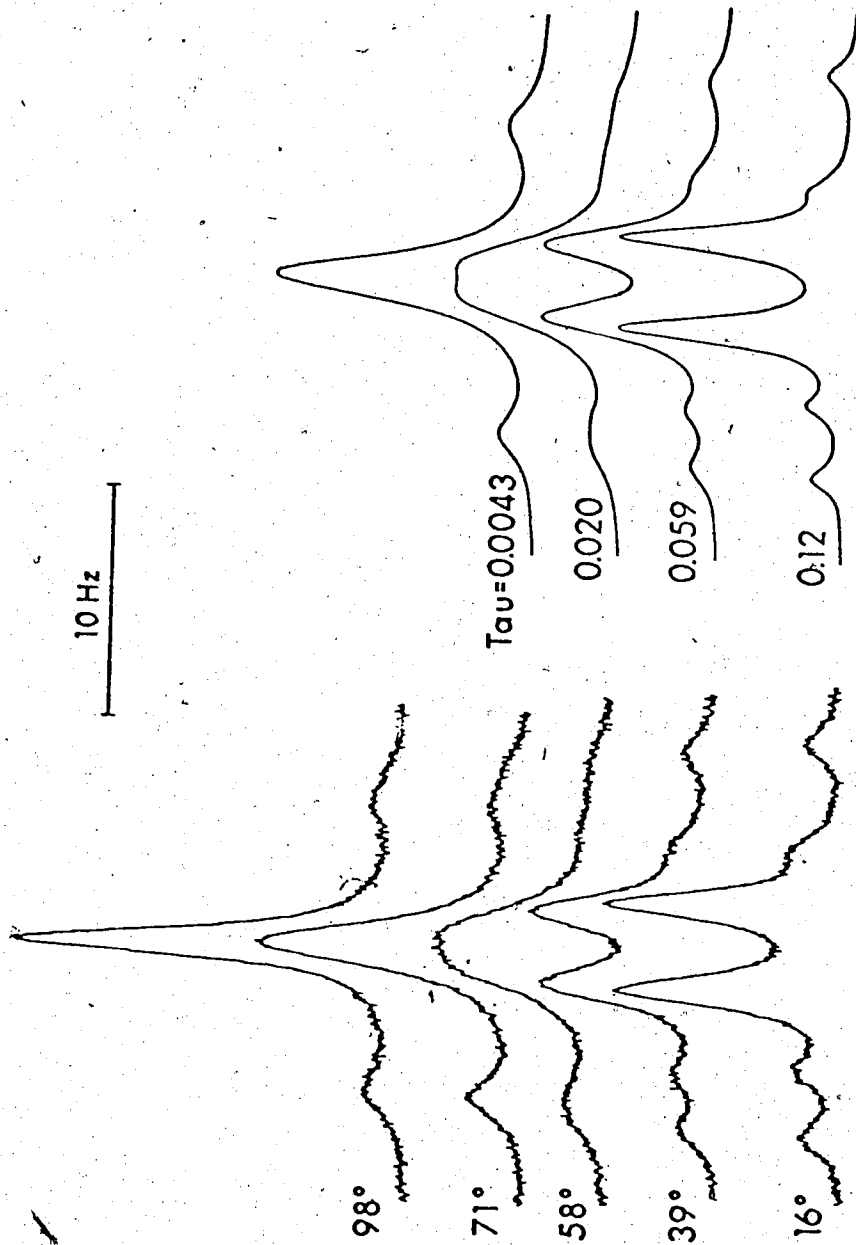
Figure 6: Representative experimental (left) and theoretical (right) 60 MHz spectra of the acetate methylenic protons of an aqueous solution of Cd(1,3-PDTA)$^{2-}$.

10 Hz

Tau=0.0043

0.020

0.059

0.12

98°

71°

58°

39°

16°

AB pattern are barely visible at 16° and are not

shown in the figure. As the temperature is increased,

the AB pattern collapses to a single, averaged resonance

while the AB part of an ABX pattern collapses to the

A part of an A_2X pattern. The 98° spectrum clearly

illustrates the limit of rapid interchange of the A

and B protons of a given methylenic group on the pmr

time scale. The coupling to the ^{111}Cd and ^{113}Cd

isotopes at 98° indicates that complete dissociation

of the complex must be occurring slowly on the pmr

time scale, since metal-proton coupling in multi-

dentate ligand complexes is not collapsed as long as

chelated ligand does not exchange rapidly with free

ligand (9). The metal-proton coupling would be observed

even if the ligand partially unwraps from the metal

and then re-bonds because all nuclei remain in the

same spin states and the coupling is not relaxed.

The upper limit of the rate of first order dissociation

of the complex at 98° is $2\pi |J_{AX}| \approx 87$ sec^{-1}, where

$|J_{AX}|$ is the average value of the magnitude of the

cadmium-proton coupling constant in the limit of fast

AB interchange. The slight broadening of the

satellite peaks at 98° suggests that at this temperature

the rate of complete dissociation is just becoming

appreciable on the pmr time scale (43); that is,

the rate must be of the order of $\frac{2}{a}\pi|J_{AX}|$.

Average lifetimes before AB interchange were determined by lineshape analysis of spectra of which those in Figure 6 are representative. The density matrix method (78,79) was used to simulate spectra theoretically as a function of τ, the average lifetime before interchange. Other parameters used in the calculation were $\Delta\delta_{AB}$ (Hz), J_{AB}, J_{AX}, J_{BX} and T_2, where T_2 is the effective spin-spin relaxation time. $\Delta\delta_{AB}$ at a given temperature was calculated with the aid of Equation I; similar chemical shift functions have been used previously in lineshape treatments (57). A constant T_2 calculated from an assumed natural linewidth of 1.0 Hz was used; the natural linewidth could not be measured directly because some exchange-broadening was observed even at the lowest temperatures attainable. Typical linewidths in similar complexes are about 1.0 Hz.

The computer program used to simulate the spectra (51) was modified so that it first calculated the lineshape of the AB spectrum and then the AB part of the ABX spectrum for a given set of parameters. It then normalized the intensities for the two sets of spectra so that the AB part of the ABX pattern represented 25.0% of the total intensity,

since this part of the pattern arises from the complexes of the isotopes of cadmium with spin numbers of 1/2 which are present at a combined natural abundance of 25.0%. The normalized spectra were combined to give a spectrum which was compared to the experimental spectrum. For a given set of input parameters, τ was varied until the computed and experimental spectra matched. In the slow and rapid exchange regions the criterion for matching was the linewidth of the resonance peaks; in the intermediate exchange region it was the peak-to-valley ratio of the two central peaks. The terms slow, intermediate, and fast exchange will be explained in Chapter IV. The spectra shown in Figure 6 are typical of the fits obtained. Average lifetimes before AB interchange determined by this matching procedure over a range of temperatures are listed in Table II. The experimental error in the lifetime determinations was from ± 5 to ± 10% due mainly to difficulties in matching computed and experimental spectra.

A pH of 8.0 was chosen for the Cd-1,3-PDTA lineshape study to minimize the contributions of reactions involving hydrogen or hydroxide ion to the overall rate of AB interchange. To determine the

Table II

Average Lifetimes of the Acetate Methylenic Protons
of $Cd(1,3-PDTA)^{2-}$ and $Cd(1,4-BDTA)^{2-}$

Before AB Interchange

Temp. ($^{\circ}$C)	τ (sec.)	
	$Cd(1,3-PDTA)^{2-a,b}$	$Cd(1,4-BDTA)^{2-c,d}$
5		0.10
16	0.12	
23	0.085	0.050
31	0.070	
38		0.012
39	0.059	
45	0.042	
51	0.029	0.0055
58	0.020	
64	0.011	
71	0.0043	

(a) pH 8.0 at 25°.

(b) Lifetimes determined by lineshape analysis of 60 MHz
spectra.

(c) pH 7.6 at 25°.

(d) Lifetimes determined by lineshape analysis of 220
MHz spectra.

magnitude of any pH dependence, samples at pH's

7.2, 8.4 and 9.1 (at 25°) were studied over the

same temperature range. The spectra obtained were

identical, at the same temperatures, with those from

which the results in Table II were obtained,

indicating no pH dependence of the rate within this

pH range.

.To determine if the lineshape treatment is

dependent on the spectrometer frequency, lifetimes

were determined by the above procedure for a D_2O

solution of Cd(1,3-PDTA)$^{2-}$ at pD 7.5 over a range

of temperatures from both 60 and 100 MHz spectra.

D_2O was used as the solvent rather than H_2O because

with H_2O as the solvent, the water resonance caused

locking problems on the 100 MHz spectrometer.

The results shown in Table III indicate that the

lifetimes are independent of the measuring frequency

within experimental error. The results in Tables

II and III also show that, on the average, the

rates of AB interchange for the D_2O solution are

0.6 times as fast as those for the H_2O solution.

These results are discussed in a later section of

this chapter.

The 60 MHz pmr spectrum of the acetate methylenic

protons of Zn(1,3-PDTA)$^{2-}$ in aqueous solution is

Table III

Comparison of Average Lifetimes of the Acetate

Methylenic Protons of Cd(1,3-PDTA)$^{2-}$ [a] Before

AB Interchange Determined from 60 MHz

and 100 MHz Spectra

	τ (sec.)	
Temp. (°C)	60 MHz	100 MHz
23	0.12	
26		0.12
31	0.10	
39		0.094
45	0.065	
47		0.056
51	0.043	
56		0.034
58	0.028	
60		0.026

(a) D_2O solution of pD 7.5 at 25°.

shown as a function of temperature in Figure 2.
As the temperature is increased, the AB pattern
begins to collapse; however the extent of collapse
and hence the rate of AB interchange is somewhat
less than that for $Cd(1,3-PDTA)^{2-}$. Average lifetimes
before AB interchange were determined by matching
computer-simulated and experimental spectra in the
same way as for the cadmium complex as described
above. The chemical shift difference and coupling
constant used in the computer-simulation were found
to be independent of temperature in the range
which they could be measured (25 to 62°). The life-
times obtained are listed in Table IV, and some of
the calculated spectra are shown in Figure 2.

The temperature dependence of the lineshape of
the multiplet pattern for the acetate protons of
$Cd(1,4-BDTA)^{2-}$ at 220 MHz is shown in Figure 4.
As observed for $Cd(1,3-PDTA)^{2-}$, the AB pattern
collapses to a single resonance as the temperature
is increased and the AB part of the ABX pattern is
just beginning to become the A part of an A_2X pattern
by 70°. In the intermediate interchange region,
the lineshape is slightly asymmetric with one side
of the multiplet sharper than the other. Average
lifetimes before AB interchange were determined by

Table IV

Average Lifetimes of the Acetate Methylenic Protons

of $Zn(1,3-PDTA)^{2-}$ and $Zn(1,4-BDTA)^{2-}$

Before AB Interchange

Temp. (°C)	τ (sec.) [a]	
	$Zn(1,3-PDTA)^{2-}$ [b]	$Zn(1,4-BDTA)^{2-}$ [c]
25	2.9	
39	1.2	
51	0.51	
56		0.50
62	0.25	0.30
73	0.17	0.20
80	0.12	0.095
87	0.084	0.063
93	0.060	0.047
100	0.040	0.035

(a) Determined by lineshape analysis of 60 MHz spectra.

(b) pH 8.7 at 25°.

(c) pH 7.8 at 25°.

the matching procedure used for the 1,3-PDTA complexes, but disregarding the asymmetry. The chemical shift and coupling constant values used in the calculation are given in Table I and a T_2 assuming a natural linewidth of 2.5 Hz obtained from the 220 MHz spectra was used. The lifetimes which were obtained are shown in Table II for comparison with those for $Cd(1,3-PDTA)^{2-}$. The error introduced into the lifetime calculations for the 1,4-BDTA complex by the presence of the asymmetry in the intermediate exchange spectra is estimated to be ± 20%.

The temperature dependence of the lineshape for the acetate protons of $Zn(1,4-BDTA)^{2-}$ at 60 MHz is shown by the spectra in Figure 7 (30). Average lifetimes before AB interchange determined by matching computer-simulated spectra with experimental spectra obtained above 48° are given in Table IV for comparison with the results for $Zn(1,3-PDTA)^{2-}$.

Below 48° for $Zn(1,4-BDTA)^{2-}$, the individual lines of the multiplet pattern broaden at different rates, resulting in an asymmetrical AB pattern as shown in Figure 7. Each half of the spectrum is broadened further at 100 and 220 MHz, indicating that the broadening results from a second kinetic process. One possibility is relatively slow exchange
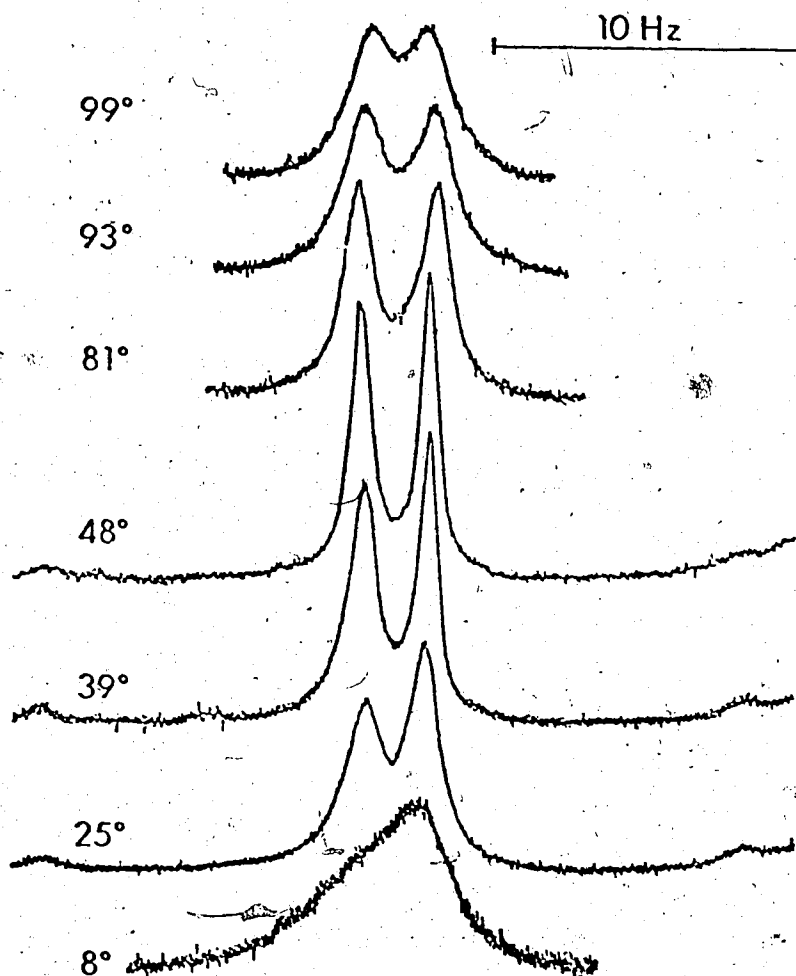
Figure 7: 60 MHz pmr spectra of the acetate methylenic protons of an aqueous solution of $Zn(1,4-BDTA)^{2-}$ at the indicated temperatures.

of the acetate groups between the site in the plane
formed by the metal and the two nitrogen atoms and
the site out of the plane. Such a process would
yield an asymmetrical pattern if J_{AB}, δ_A, and δ_B are
different for the in-plane and out-of-plane acetate
groups, as in the cobalt(III) and rhodium(III)
complexes of EDTA (9,14,16,17), and if $\delta_{A(in-plane)}$ -
$\delta_{A(out-of-plane)}$ is different from $\delta_{B(in-plane)}$ -
$\delta_{B(out-of-plane)}$. It is possible that the asymmetry
observed in the intermediate exchange spectra for
$Cd(1,4-BDTA)^{2-}$ also results from in-plane to out-of-
plane exchange of acetate dentates. However, in this
case, the chemical shift differences between the in-
plane and out-of-plane sites must be very small,
since in the slow exchange spectrum only a slightly
greater intensity of one of the peaks can be observed.

Temperature Dependence of the AB Multiplet Patterns
for the EDDDA Complexes

The multiplet pattern for the acetate methylenic
protons of $Cd(EDDDA)^{2-}$ at 220 MHz broadens asymmet-
rically as the temperature is increased as can be
seen by the spectra in Figure 5. At 70° it consists
of a single resonance flanked symmetrically by the
A part of an A_2X pattern due to the proton coupling

to the ^{111}Cd and ^{113}Cd isotopes. The temperature dependence of this multiplet pattern could not be quantitatively studied because the chemical shift difference and coupling constants could not be obtained from the slow exchange spectra.

The AB pattern for Zn(EDDDA)$^{2-}$ at 60 MHz broadens little at the highest temperatures studied, indicating only a slight degree of AB interchange. Lifetime determinations were not made because of the small temperature range (90 to 100°) over which broadening was observed.

The multiplet pattern for Pb(EDDDA)$^{2-}$ at 220 MHz also broadens as the temperature is increased, indicating AB interchange. In the intermediate exchange region the broadened pattern is asymmetrical. Severe interference from the water resonance in this exchange region prevented a quantitative rate study from being undertaken.

Pmr Spectra of the EDTA Complexes

The 60 MHz pmr spectrum of the acetate methylenic protons of an aqueous solution of Cd(EDTA)$^{2-}$ at a neutral pH consists of the AB part of an ABX pattern superimposed on an AB pattern (9), similar to that observed for Cd(1,3-PDTA)$^{2-}$. In contrast to the

1,3-PDTA system, however, the lineshape of the

multiplet pattern of the EDTA complex is temperature

invariant up to 100°.

It has previously been observed that the acetate

methylenic proton resonances of the zinc and lead

complexes of EDTA (9,52) at 60 MHz consist of

single peaks. Pmr measurements at 220 MHz (15),

however, have revealed AB patterns for these two

complexes.

B. DISCUSSION

Partial Dissociation Kinetics of the Complexes of

1,3-PDTA and 1,4-BDTA

The multiplets in the pmr spectra for the acetate

methylenic protons of Cd(1,3-PDTA)$^{2-}$, Zn(1,3-PDTA)$^{2-}$

and Cd(1,4-BDTA)$^{2-}$ at 25° and of Zn(1,4-BDTA)$^{2-}$ at

62° consist of single AB patterns (or the AB part

of an ABX pattern superimposed on a single AB

pattern). The single AB patterns indicate that the

four acetate groups of a given complex are equivalent

on the pmr time scale. If it is assumed that coordina-

tion around the metal ion is octahedral and that all

six dentates of the ligands are coordinated, two

acetate groups are in the plane formed by the metal

and two nitrogen atoms and two are out of the plane ,

in the instantaneous structures of the complexes.
If a given structure is long-lived on the pmr time
scale, the environments experienced by the acetate
groups in the in-plane and out-of-plane sites
must be equivalent to observe a single AB pattern.
Pmr spectra of the nonlabile rhodium(III) (14) and
cobalt(III) complexes of EDTA (9,16,17) suggest it
is unlikely that the in-plane and out-of-plane
environments will be equivalent and rather that the
single AB patterns for the 1,3-PDTA and 1,4-BDTA
complexes result from rapid exchange of acetate
dentates between the two sites. Exchange could be
by a sequence of reactions involving dissociation of
labile metal-oxygen bonds (9) or by a twist mechanism
of the type proposed by Bailar (18,53).

The AB patterns reveal that, for the given solution
conditions, each nitrogen atom of the 1,3-PDTA
and 1,4-BDTA complexes is permanently in one of its
two possible inversion states on the pmr time scale.
Increasing the temperature results in inversion of
the nitrogen atom becoming more rapid, as evidenced
by the collapse of the multiplet patterns for these
complexes.

A series of stepwise reactions which could lead
to interchange of nonequivalent acetate protons in

complexes of EDTA and its homologs via inversion of a nitrogen atom is shown schematically in Figure 8. The ligand is shown as being hexadentate in at least some of the complex, but the conclusions from the following discussion are not dependent on this assumption. It is assumed, however, that a metal-nitrogen bond can dissociate making possible nitrogen inversion only after dissociation of the metal bonds to the two acetate groups of the given nitrogen atom. If K_1 ($= k_1/k_{-1}$) and K_2 ($= k_2/k_{-2}$) are rapid pre-equilibria on the pmr time scale, the rate-determining step for AB interchange via the reaction sequence in Figure 8 is either nitrogen inversion or metal-nitrogen bond dissociation. Qualitatively, if $k_{-3} \gg k_i$, the metal-nitrogen bond dissociates and re-forms many times on the average before the noncoordinated nitrogen atom inverts, so that the rate-determining step is the nitrogen inversion. On the other hand, if $k_i \gg k_{-3}$, once the metal-nitrogen bond has broken the noncoordinated nitrogen atom inverts many times before the bond re-forms and the rate-determining step is metal-nitrogen bond dissociation. In the latter case, there is statistically a 50% chance that the nitrogen atom will be in an inverted state when it re-bonds to the metal,

Bonding of Nitrogen and Carboxylate Oxygens
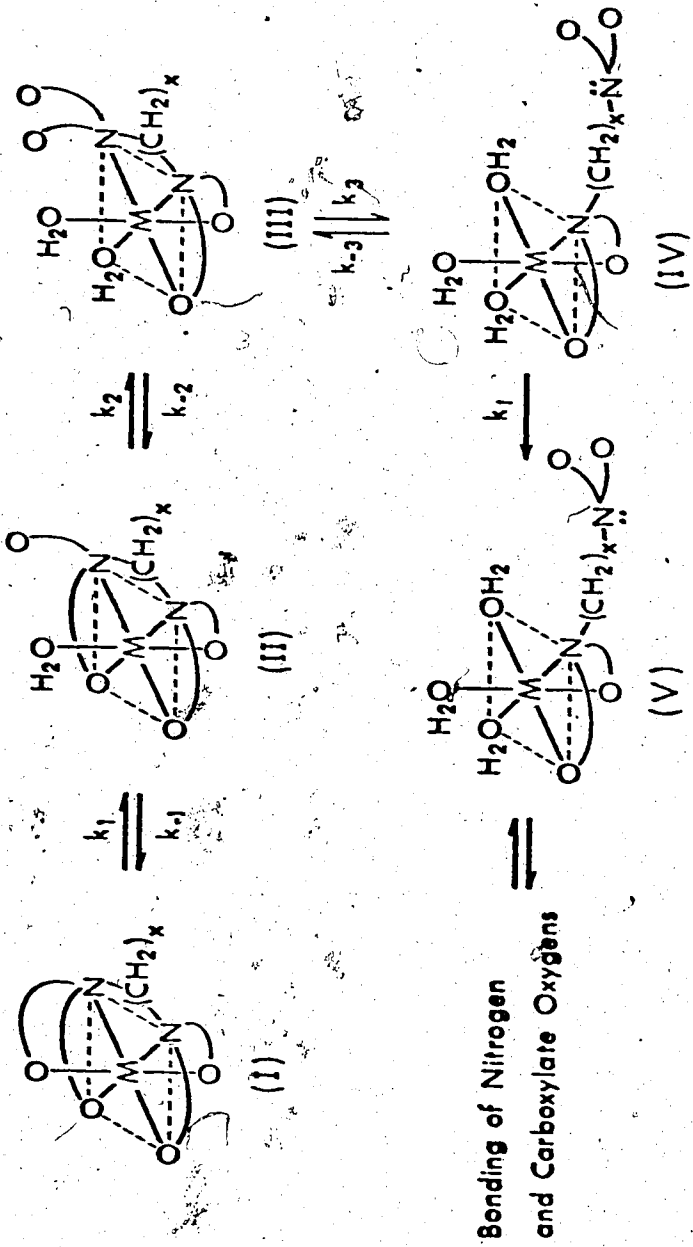
Figure 8: Possible stepwise reactions that can lead to the A to B interchange observed by the pmr method for the acetate methylenic protons in complexes of EDTA and its homologs.

so that the observed rate of AB interchange will be
half the rate of dissociation to species (IV) in
Figure 8.

Inversion rates of nitrogen atoms in multidentate
ligands of the type studied here are not known;
however, they have been estimated to be 10^8 to 10^9
$\sec^{-1}$ for nitrogen atoms in tertiary amines of the
type described earlier (26-28). In the absence of
more appropriate inversion rate constants, k_i for
nitrogen atoms in multidentate ligands of the EDTA
type will be assumed to be of this magnitude in the
following discussion.

The upper limit for the rate of formation of
the metal-nitrogen bond described by the rate constant
k_{-3}, is the rate of dissociation of the water molecule
occupying the coordination site if the reaction
occurs by the Eigen dissociative mechanism (31-33,70).
In terms of this mechanism, a water molecule will
first be released from a site cis to the site of
coordination to the other nitrogen atom, and the
noncoordinated nitrogen atom will then bond to the
metal ion at the vacated coordination site. The
rates of water release from totally aquated cadmium
and zinc are 4×10^8 and 5×10^7 $\sec^{-1}$ respectively
(54). The rates of water release from these metal ions

will be considered as the upper limits for k_{-3} in the following discussion.

For k_{-3} to equal the rate of water release, the rate at which the noncoordinated nitrogen atom in species (IV) of Figure 8 coordinates to an unoccupied site has to be significantly larger than the rate at which a water molecule reoccupies the site. This requires that the nitrogen atom be properly oriented for bonding at the time the water molecule dissociates. Previous investigations of a number of fast complexation reactions of multidentate ligands would suggest that the rate at which the nitrogen atom will coordinate to the unoccupied site will be less when the chelate ring formed is six-membered than when it is five-membered. For example, Kustin and coworkers observed that the formation rate constants of the β-alanine complex of cobalt(II) is almost one order of magnitude less than that for the α-alanine complex (47). The difference was attributed to the difficulty in forming the six-membered chelate ring. Similar differences were observed for the nickel and cobalt(II) complexes of α- and β-aminobutyric acids (48). These results suggest that, for $Cd(1,3-PDTA)^{2-}$ and $Zn(1,3-PDTA)^{2-}$, k_{-3} may be somewhat less than the rates of water release from species (IV) in Figure 8 due to the

formation of a six-membered chelate ring. If so, k_i would be somewhat greater than k_{-3} for these complexes. On this basis, it is proposed that the AB patterns observed for these complexes are indicative of relatively inert metal-nitrogen bonding on the pmr time scale, and that the inverses of the lifetimes before AB interchange, which are listed in Tables II and IV, are half the first order rate constants for partial dissociation of the complexes to species (IV) at the indicated temperatures. If this proposal is correct, the lifetimes before AB interchange indicate that the relative order of lability of the metal-nitrogen bonds in the two metal complexes of 1,3-PDTA is cadmium > zinc.

The rate at which the metal-nitrogen bond in the 1,4-BDTA complexes dissociates should be the same or slightly faster than in the 1,3-PDTA complexes since it may be easier to open the larger seven-membered chelate ring (47,48); while the rate at which the bond re-forms is predicted to be less since a seven-membered ring is formed (1,58). There-fore, if k_i is somewhat greater than k_{-3} for the 1,3-PDTA complexes, the rates of interchange in the 1,4-BDTA complexes of cadmium and zinc should be the same or slightly faster than in the 1,3-PDTA

complexes. The results in Tables II and IV indicate this to be the case. Furthermore, the lifetimes before AB interchange indicate that the order of lability of the metal-nitrogen bonds for the complexes of 1,4-BDTA is cadmium > zinc.

To determine if the rate constants calculated from the lifetimes in Tables II and IV are reasonable for the reaction represented in Figure 8, comparison can be made with the rate constant k_d, for dissociation of one N-methyliminodiacetic acid (MIDA) ligand from the complex $Zn(MIDA)_2^{2-}$,

$$CH_3 - N \begin{array}{c} CH_2CO_2H \\ \\ CH_2CO_2H \end{array}$$

MIDA

$$Zn(MIDA)_2^{2-} \xrightarrow{k_d} Zn(MIDA) + MIDA^{2-}$$
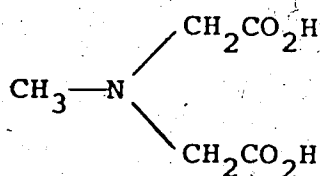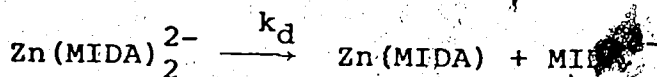
which has previously been determined by pmr line-broadening measurements (30). The value for k_d is 40 ± 5 sec^{-1} at 25°. Taking the inverse of the life-times before AB interchange to be half the first order rate constants for partial dissociation to species (IV) in Figure 8, the partial dissociation rate constant

for $Zn(1,3-PDTA)^{2-}$ is 0.69 ± 0.14 sec^{-1} at $25°$.
The difference between k_d for $Zn(MIDA)_2^{2-}$ and this value
is of the magnitude expected if the energy barrier
associated with the necessary twisting of the ali-
phatic chain in $Zn(1,3-PDTA)^{2-}$ is accounted for (1).

The results in Tables I and II which indicate
that the rate of AB interchange in $Cd(1,3-PDTA)^{2-}$
is different in H_2O and D_2O, can be accounted for if
the fraction of the complex that exists in the various
partially coordinated forms, shown in Figure 8, is
different in these two solvents. This would be the
case if the rate at which H_2O and D_2O dissociate
from the metal complex is different. For example,
K_1 ($= k_1/k_{-1}$) would be different in H_2O and D_2O if
the rate of dissociation of H_2O from species (II)
is different from the rate dissociation of D_2O.

Temperature Dependence of the AB Multiplet Patterns
of the EDDDA Complexes

The multiplet patterns observed for the acetate
methylenic protons of the cadmium, zinc and lead
complexes of EDDDA indicate an inertness on the pmr
time scale of the metal-nitrogen bonds. The collapse
of these patterns with increasing temperature indicates
that partial dissociation of these complexes is

occurring on the pmr time scale. The different degrees of collapse of the multiplet patterns for these complexes suggest that the relative order of lability of the metal-nitrogen bond is cadmium > lead > zinc.

Assuming that coordination in the EDDDA complexes is octahedral and that all six dentates are coordinated to the metal ion, three instantaneous structures are possible depending on whether the acetate or propionate groups are in-plane or out-of-plane (59).
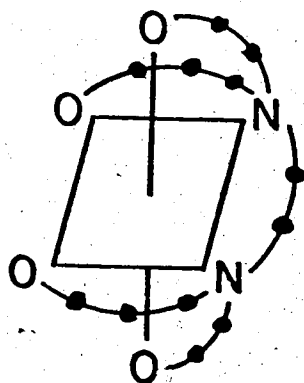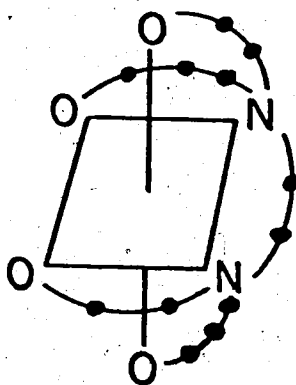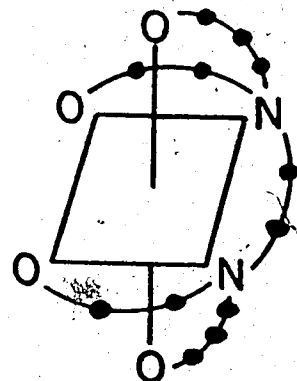
(I)   (II)   (III)

The single AB pattern observed in the pmr spectrum for $Zn(EDDDA)^{2-}$ suggests rapid exchange of the carboxylate dentates, but the values for J_{AB} and $\Delta\delta_{AB}$ indicate that one of the above structures is pre-dominant. The magnitude of the geminal coupling constant J_{AB} is approximately the same for all the

complexes listed in Table I except that for $Zn(EDDDA)^{2-}$.

Sudmeier and coworkers (17) have reported the magnitude

of the geminal coupling constants of the methylenic

protons of the in-plane and out-of-plane acetate groups

in the inert cobalt(III) complexes of EDTA type

ligands to be 16 ± 0.5 Hz and 18 ± 0.5 Hz respectively.

Since geminal coupling is sensitive to the electro-

negativity of substituents, the magnitudes of in-plane

and out-of-plane coupling constants of aminocarboxylic

acid ligands coordinated to divalent metal ions may

be different. Assuming the relative magnitudes to

be in the same direction as those for the cobalt

complexes, the results in Table I suggest that

$Zn(EDDDA)^{2-}$ exists predominantly as structure (III)

shown above. Support for this structure also comes

from the observation of Legg and coworkers (60) that

$\Delta\delta_{AL}$ for out-of-plane acetate groups of cobalt(III)-

aminocarboxylic acid complexes is larger than for

in-plane groups, and the results of Byers and

Douglas (59) which show the structure of one isomer

of $Co(EDDDA)^{-}$ be similar to the one proposed

here for $Zn(E \quad 2-$.

If the preceding conclusions are correct, the geminal

coupling constant reported for the AB pattern of $Pb(EDDDA)^{2-}$

as the temperature is increased might then be explained

by a temperature dependence of the populations of the above three structures. The value for J_{AB} could not be determined from the multiplet pattern for $Cd(EDDDA)^{2-}$, but the asymmetric broadening of this pattern might also be explained by a temperature dependence of the populations of the given structures.

The lack of broadening in the multiplet for $Cd(EDTA)^{2-}$ up to 100° indicates that the rate of AB interchange is significantly less than the rate in $Cd(1,3-PDTA)^{2-}$. This difference could result from more inert cadmium-nitrogen bonding in $Cd(EDTA)^{2-}$, as predicted by the observation that it is easier for a six-membered chelate ring to open than for a five-membered ring (1,58), or it may indicate that $k_{-3} \gg k_i$. Bond re-formation, the reaction step described by the rate constant k_{-3}, is predicted to be faster for $Cd(EDTA)^{2-}$ than for the 1,3-PDTA complex since a five-membered chelate ring is being formed (47,48). Considering the EDDDA results, the rate of partial dissociation to yield species (IV) in Figure 8 is predicted to be larger for $Cd(EDDDA)^{2-}$ than for the EDTA complex on the basis that intermediates in the stepwise sequence will be present at higher concentrations while the rate of cadmium-nitrogen bond re-formation is assumed to

be the same. Thus, if the AB pattern of $Cd(EDTA)^{2-}$ is due to the cadmium-nitrogen bond re-forming before inversion occurs, the AB pattern of $Cd(EDDDA)^{2-}$ should be temperature invariant. Rather the ti-plet for the acetate methylenic protons of the EDDDA complex is completely collapsed to a single resonance flanked by the A part of an A_2X pattern at 70°, indicating rapid AB interchange on the pmr time scale. These considerations provide support for the proposal of Day and Reilley (9) that the multiplet pattern for $Cd(EDTA)^{2-}$ results from inert cadmium-nitrogen bonding.

CHAPTER III.

LIGAND EXCHANGE KINETICS OF METAL COMPLEXES
OF 1,3-PDTA AND EDDDA

In this chapter, the results of a pmr line-
broadening study of the ligand exchange kinetics
of the 1,3-PDTA and EDDDA complexes of cadmium, zinc
and lead are presented. These systems were investi-
gated with the objective of elucidating the mechanisms
of ligand exchange reactions of cadmium, zinc and
lead complexes of aminocarboxylic acid ligands with
emphasis on the formation reactions of the mono-
protonated forms of the ligands. These two particular
ligands were chosen in order to observe the effects
of slight structural changes on the rates of reactions
of aminocarboxylic acids of the EDTA type.

A.   RESULTS

pH Dependence of the Chemical Shifts

The pmr spectrum of 1,3-PDTA consists of a sharp
singlet for the acetate methylenic protons, a broad
triplet-like pattern for the protons of the two
nitrogen-bonded methylenic groups of the propylene
part of the ligand and a broad quintet-like pattern
for the central methylenic protons over the pH range
2 to 13. The lack of any broadening of the exchange-

averaged acetate methylenic resonance indicates that
exchange of the acidic carboxylate and nitrogen protons
is fast on the pmr time scale. The resonances due
to the propylene protons, which form an A_4B_2 spin
system, were not used in the ligand exchange studies
because of their complexity.

The chemical shif of the 1,3-PDTA resonances
are pH dependent as illustrated by curve A for the
acetate methylenic protons in Figure 9. By analogy
with EDTA, the two nitrogen atoms of the tetraanion
of 1,3-PDTA are protonated first, followed by
protonation of the carboxylate groups (61-63). From
the chemical shift vs. pH data, values were determined
for the third and fourth ionization constants of
1,3-PDTA, defined by Equations II and III, by methods
described previously (44,67) and are given in

$$K_3 = \frac{a_H[HL^{3-}]}{[H_2L^{2-}]} \qquad \text{II}$$

$$K_4 = \frac{a_H[L^{4-}]}{[HL^{3-}]} \qquad \text{III}$$

Table V. These constants are mixed mode constants
involving hydrogen ion activity and 1,3-PDTA con-
centrations.
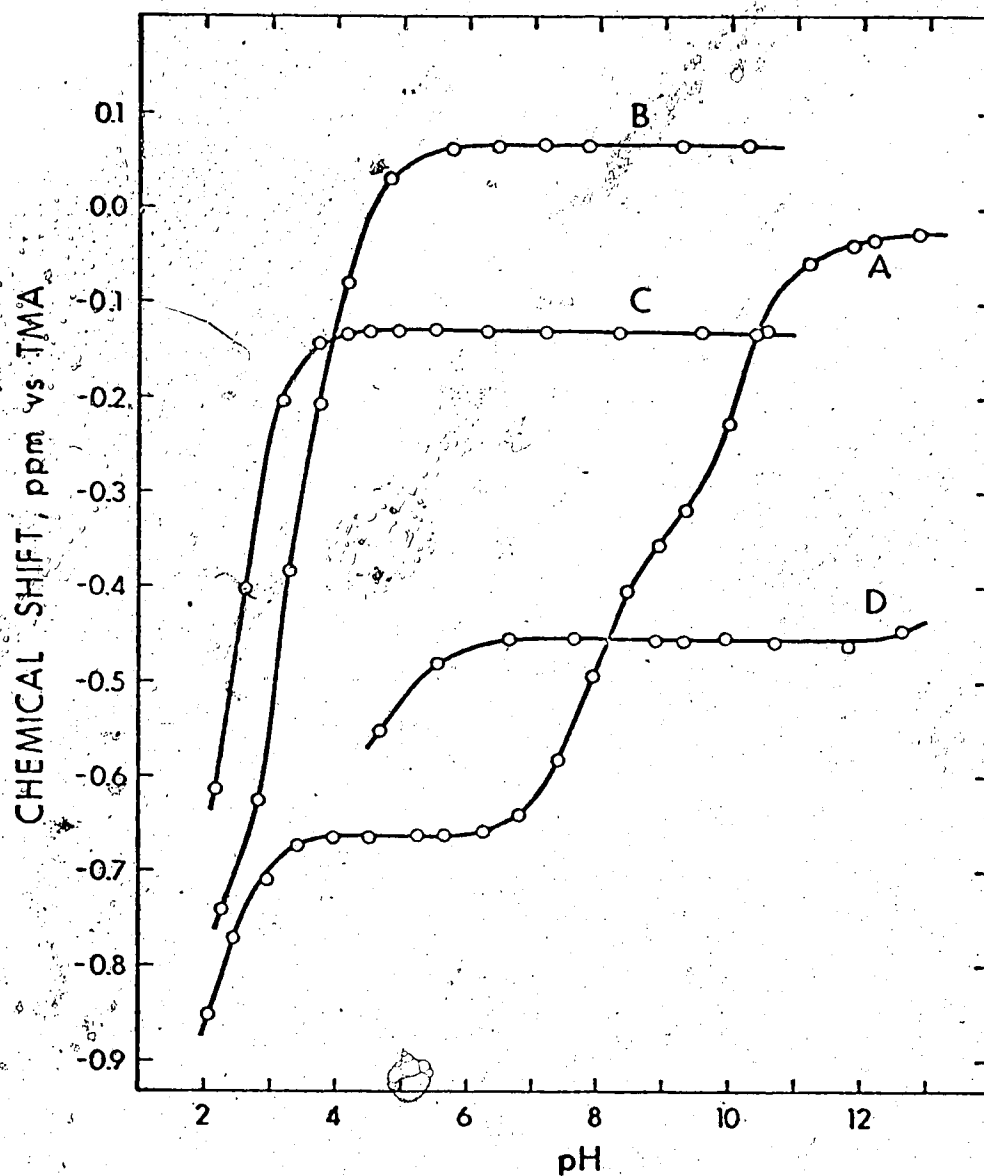
Figure 9:   pH dependence of the chemical shift of the
acetate methylenic protons of 1,3-PDTA.
Curve A, 0.20 $\underline{M}$ 1,3-PDTA; curve B, 0.20 $\underline{M}$
$Cd(1,3-PDTA)^{2-}$; curve C, 0.20 $\underline{M}$ Zn(1,3-
$PDTA)^{2-}$; curve D, 0.20 $\underline{M}$ $Pb(1,3-PDTA)^{2-}$.

Table V

Acid Ionization Constants of 1,3-PDTA and EDDDA

| | 1,3-PDTA | | EDDDA | |
	This work[a]	lit.[b]	This work[a]	lit.[c]
pK_1		1.88		3.00
pK_2		2.57		3.79
pK_3	7.93	8.02	6.00	5.98
pK_4	10.25	10.46	9.88	9.83

(a) 25°C, ionic strength ≈ 0.6 M.

(b) References 64 and 65, ionic strength = 0.1 M, mixed mode constants.

(c) Reference 66, ionic strength = 0.1 M, mixed mode constants.

Over the pH range 3 to 13, the pmr spectrum of
EDDDA consists of a sharp singlet for the acetate
methylenic protons, a sharp singlet for the ethylenic
protons between the two nitrogen atoms and a complex
multiplet pattern for the carbon-bonded protons of
the two propionate groups. The spectrum at pH 10
has been described previously (59). On the basis
of chemical shift data for other structurally-
related aminocarboxylic acids (62,63,68), the down-
field singlet was assigned to the acetate methylenic
protons. The chemical shifts of the EDDDA resonances
are pH dependent as illustrated by curve A for the
acetate methylenic protons in Figure 10. The third
and fourth ionization constants were determined from
these data; the results are given in Table V.

The spectra of the acetate methylenic protons of
the cadmium, zinc and lead complexes of 1,3-PDTA
and EDDDA are reported in Chapter II. In most cases
they consist of complex multiplet patterns due to
inert metal-nitrogen bonding. To a first approximation,
the resonances of the remaining carbon-bonded protons
of these two complexed ligands appear the same as
those of the uncomplexed ligands, but have different
chemical shifts.

The chemical shifts of the acetate methylenic
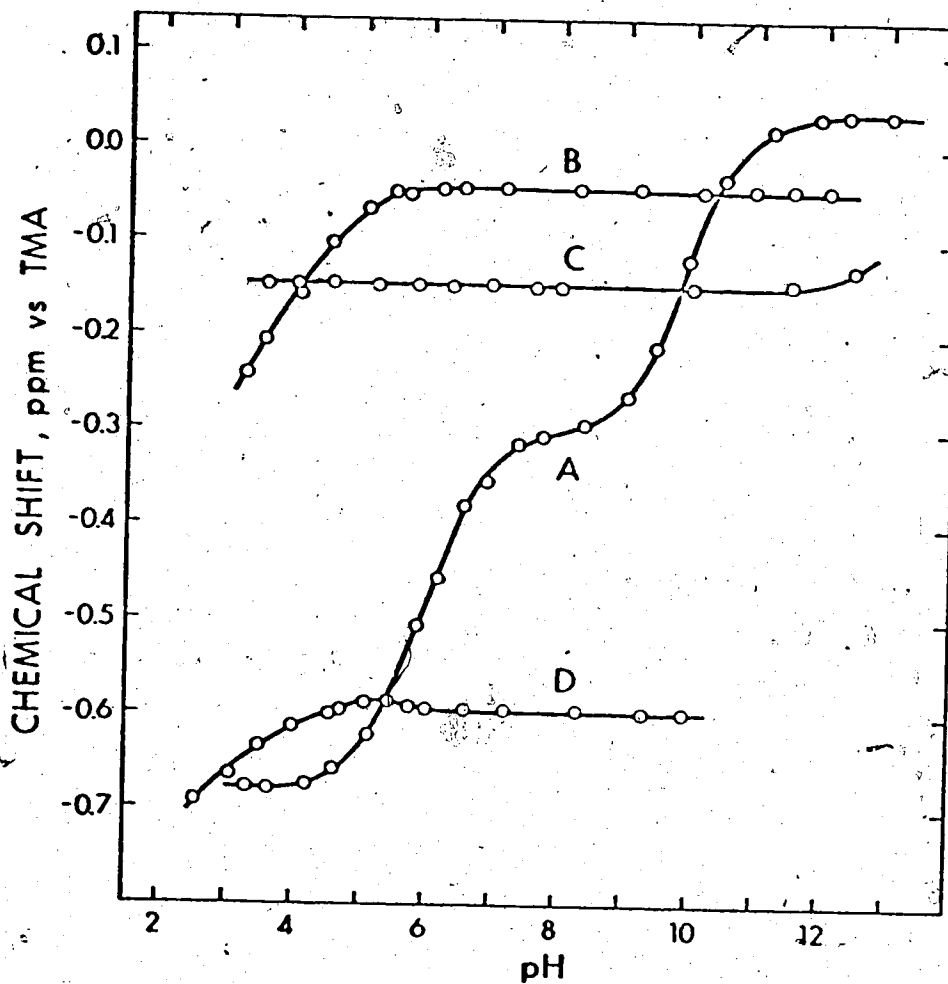
Figure 10: pH dependence of the chemical shift of the acetate methylenic protons of EDDDA. Curve A, 0.20 $\underline{M}$ EDDDA; curve B, 0.20 $\underline{M}$ Cd(EDDDA)$^{2-}$; curve C, 0.20 $\underline{M}$ Zn(EDDDA)$^{2-}$; curve D, 0.20 $\underline{M}$ Pb(EDDDA)$^{2-}$.

protons of the cadmium, zinc and lead complexes of 1,3-PDTA and of EDDDA are pH dependent as shown by curves B, C and D in Figures 9 and 10. These data were obtained from solutions made up from equimolar quantities of both metal nitrate and ligand. For those complexes in which an AB pattern was observed, the chemical shift values used in these curves were the chemical shifts at the centres of the patterns. For all the metal complexes studied, the chemical shifts remain constant above a certain pH, corresponding to the chemical shifts of the 1:1 complexes. Below this pH, the resonances move towards those of the free ligand and are exchange-broadened. Calculations of the species present in solution for the 1,3-PDTA systems using the literature ionization constants in Table V and the literature formation constants (64-66) indicate that dissociation of the 1:1 complexes and formation of protonated complexes is occurring at those pH's when the resonances are shifting and are broadened. For example, calculations indicate that in a solution with a cadmium to 1,3-PDTA ratio of one, dissociation of the 1:1 complex and formation of a protonated complex begin to take place at pH less than 5.5. It is also below this pH that broadening and shifting of the resonance begins to take place

as can be seen from Figure 9. For the EDDDA systems, no formation constants are available for the protonated complexes, but such species are indicated by the exchange-broadening and the chemical shift data shown in Figure 10.

An attempt was made to calculate formation constants for the nonprotonated and the protonated complexes from the chemical shift data presented in Figures 9 and 10 using the method described previously (44). These formation constants would have been useful in subsequent calculations since they would have been obtained under ionic strength conditions similar to those used in all experiments reported in this work. This attempt, however, yielded inconsistent results, possibly because of the uncertainties in the chemical shift values of the observed resonances and those of the protonated complexes. The observed resonances are broad and hence it was difficult to measure their chemical shift positions. The chemical shift values of the protonated complexes could not be measured directly, but had to be approximated in the attempted calculation of formation constants. Therefore, in the subsequent rate constant deter- minations it was necessary to use literature values of the formation constants (64,65). However, the

error involved using these literature values is within the experimental error of the lifetime measure‑ ments.

Ligand Exchange Kinetics of the 1,3-PDTA Complexes

Exchange-broadening was observed in the pmr spectra of each of the 1,3-PDTA complexes under conditions where some noncomplexed ligand was present. From the broadening for a given set of experimental conditions, the mean lifetime τ between events which lead to exchange of the ligand from the free form to the complexed form or vice·versa may be determined. The following reactions are considered to be pathways by which exchange can occur:

$$ML^{2-} \underset{k_{-1}}{\overset{k_1}{\rightleftharpoons}} M^{2+} + L^{4-} \qquad\qquad IV$$

$$H^+ + ML^{2-} \underset{k_{-2}}{\overset{k_2}{\rightleftharpoons}} M^{2+} + HL^{3-} \qquad\qquad V$$

$$L^{4-} + \overset{*}{M}L^{2-} \overset{k_3}{\rightleftharpoons} \overset{*}{L}^{4-} + ML^{2-} \qquad\qquad VI$$

$$HL^{3-} + \overset{*}{M}L^{2-} \overset{k_4}{\rightleftharpoons} H\overset{*}{L}^{3-} + ML^{2-} \qquad\qquad VII$$

$$H_2L^{2-} + \overset{*}{M}L^{2-} \overset{k_5}{\rightleftharpoons} H_2\overset{*}{L}^{2-} + ML^{2-} \qquad\qquad VIII$$
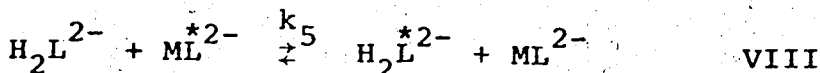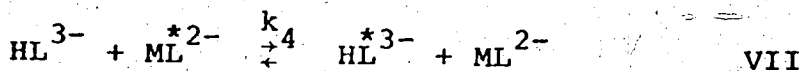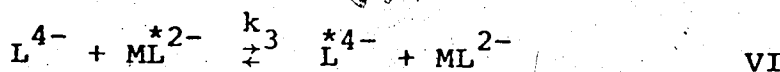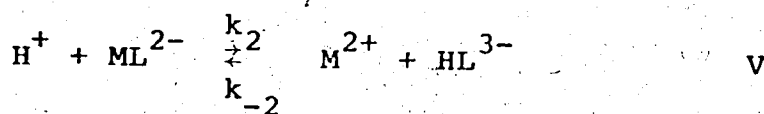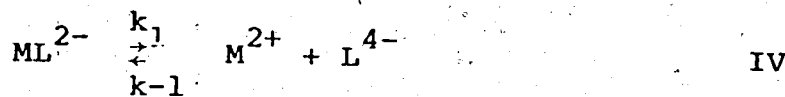
The AB multiplet patterns observed for the acetate

methylenic protons of Cd(1,3-PDTA)$^{2-}$ and Zn(1,3-PDTA)$^{3-}$ at intermediate pH values in the absence of non-complexed ligand, which were discussed in detail in Chapter II, indicate that for these conditions the mean lifetimes before AB interchange are greater than 0.1 sec. This value was obtained by computer-simulating spectra by the method described in Chapter II. Since AB interchange may occur even when the complex is partially bonded, the above lifetime is a lower limit for the mean lifetime of the complex before it completely dissociates via the reaction represented by Equation IV and indicates that the rate of this reaction is too slow to be measured by the pmr line-broadening method. Similarly the metal-proton coupling observed for the cadmium and lead complexes in the absence of noncomplexed ligand indicates that for these complexes the reaction represented by Equation IV contributes a negligible amount to the exchange-broadening (43). Neglecting this reaction, the rate equation for exchange of ligand from the free form to the complexed form is

$$\frac{-d[L_f]}{dt} = k_{-2}[M^{2+}][HL^{3-}] + k_3[L^{4-}][ML^{2-}] + k_4[HL^{3-}][ML^{2-}]$$
$$+ k_5[H_2L^{2-}][ML^{2-}] \qquad\qquad IX$$

where $[L_f]$ represents the sum of the concentrations of the free ligand in the various protonated forms. The reciprocal of the mean lifetime of the free form, $1/\tau_{L_f}$, is related to the exchange rate, $-d[L_f]/dt$, by

$$\frac{1}{\tau_{L_f}} = - \frac{d[L_f]}{dt} \frac{1}{[L_f]} \qquad \qquad X$$

which yields

$$\frac{1}{\tau_{L_f}} = k_{-2}\alpha_3[M^{2+}] + k_3\alpha_4[ML^{2-}] + k_4\alpha_3[ML^{2-}] + k_5\alpha_2[ML^{2-}]$$

$$XI$$

where $\alpha_2 = [H_2L^{2-}]/[L_f]$, $\alpha_3 = [HL^{3-}]/[L_f]$ and $\alpha_4 = [L^{4-}]/[L_f]$. Expressing the concentrations in terms of fractional concentrations and the term for the contribution from the reaction represented by Equation V in terms of $[ML^{2-}]$ by the relation $k_{-2}[M^{2+}] = k_2[H^+][ML^{2-}]/\alpha_3[L_f]$ yields

$$P_{L_f}/(\tau_{L_f}P_{ML}) = k_2[H^+] + (k_3\alpha_4 + k_4\alpha_3 + k_5\alpha_2)[L_f] \qquad XII$$

where P_{L_f} and P_{ML} are the fractional concentrations of ligand in the free and complexed forms ($P_{L_f} + P_{ML} = 1$). The individual rate constants were evaluated from the dependence of τ_{L_f} on $[H^+]$ and $[L_f]$.

A typical example of the spectra obtained as a
function of pH for a solution 0.10 $\underline{M}$ in both Cd(1,3-
PDTA)$^{2-}$ and free 1,3-PDTA is given in Figure 11.
At pH 6.42 separate acetate methylenic proton
resonances are observed for both the free and the
complexed forms of 1,3-PDTA; only the two strong
central peaks of the AB pattern for the complexed
form can be seen. An increase in the pH results in
broadening of the resonances indicating faster
exchange. Since the linewidth of the free ligand
resonance for most of the systems in this study
could easily be measured over a wide range of solution
conditions, τ_{L_f} was calculated using Equation
XVIII, the slow exchange expression, which will be
discussed in more detail in Chapter IV. The errors
involved in determining the values of $1/\tau_{L_f}$ arise
mainly from the linewidth measurements and are
estimated to be between $\pm$ 5% and $\pm$ 15%.

Lifetime data are given in Table VI for the
Cd-1,3-PDTA system for experiments in which the pH
was held constant at six different values and the
concentration of free ligand was varied at each
value. A typical plot using the data at pH 6.51 is
shown in Figure 12. According to Equation XII, the
slope of a plot of $P_{L_f}/(\tau_{L_f} P_{ML})$ vs. [L_f] at constant
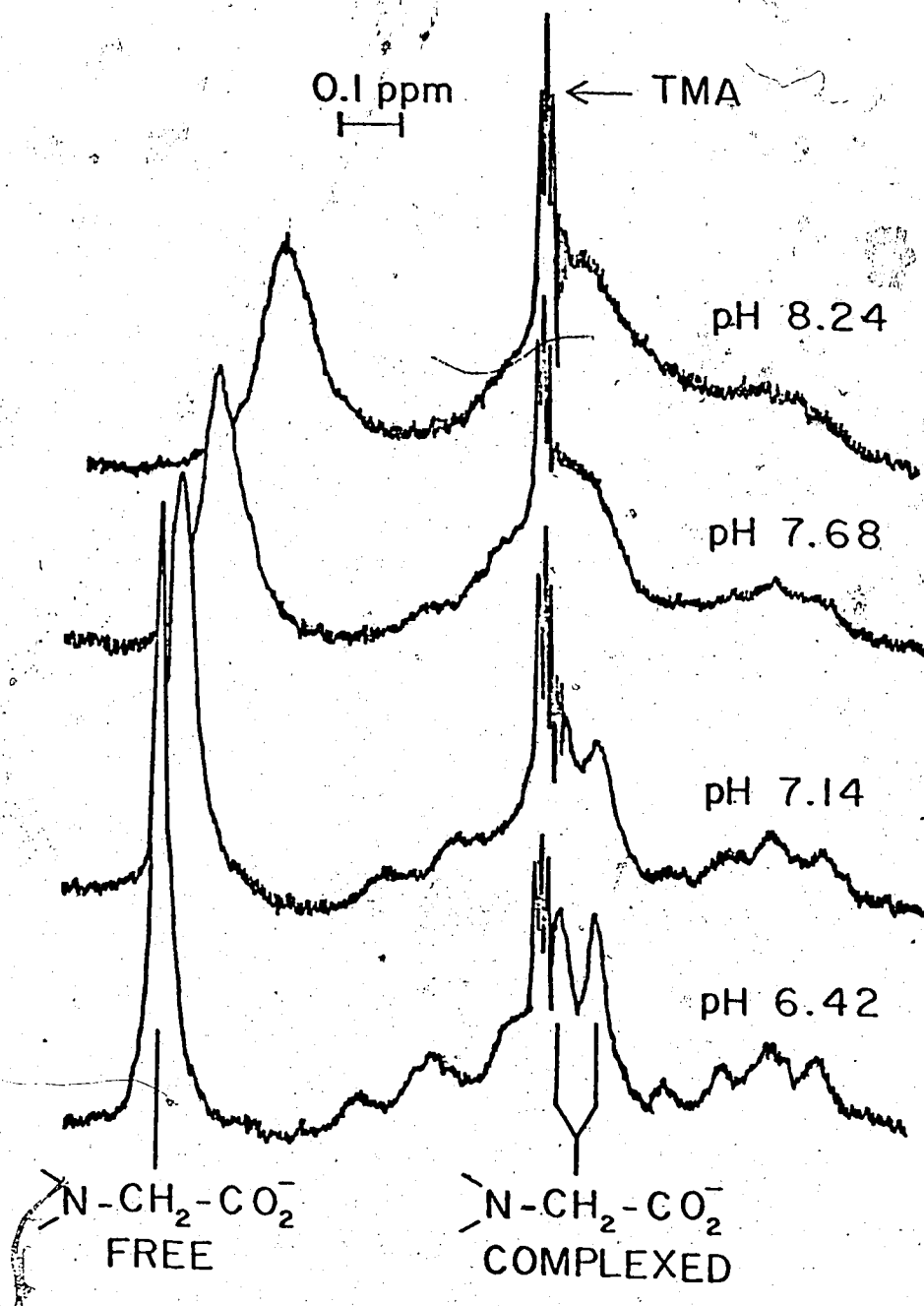
Figure 11: 60 MHz pmr spectra showing the acetate
methylenic resonances for an aqueous
solution containing both free 1,3-PDTA
and $Cd(1,3-PDTA)^{2-}$ at the indicated pH
values. The solution was 0.1 M in both
free 1,3-PDTA and $Cd(1,3-PDTA)^{2-}$.

Table VI

Kinetic Data for the Cd-1,3-PDTA System at Constant
pH Values as a Function of Free Ligand Concentration[a,b]

pH	$[L_f]$ (M)	P_{L_f}/P_{ML}	$W'_{1/2}$ (Hz)	$1/\tau_{L_f}$ (sec^{-1})
5.52	0.180	11.5	1.05	0.816
	0.162	5.28	1.26	1.48
	0.143	3.15	1.54	2.36
	0.125	2.10	1.87	3.39
	0.107	1.46	2.16	4.30
	0.090	1.04	2.49	5.34
	0.073	0.726	2.83	6.41
	0.057	0.497	3.37	8.10
5.72	0.180	11.5	0.99	0.691
	0.161	5.25	1.16	1.22
	0.143	3.16	1.39	1.95
	0.125	2.08	1.59	2.57
	0.107	1.45	1.74	3.05
	0.090	1.03	2.13	4.27
	0.073	0.724	2.38	5.06
	0.055	0.476	2.76	6.25

(Table VI, continued)

pH	$[L_f]$ ($\underline{M}$)	P_{L_f}/P_{ML}	$W'_{1/2}$ (Hz)	$1/\tau_{L_f}$ (sec^{-1})
6.00	0.163	5.67	1.08	0.879
	0.145	3.39	1.18	1.19
	0.127	2.19	1.32	1.63
	0.109	1.53	1.51	2.23
	0.092	1.08	1.70	2.83
	0.075	0.763	1.87	3.36
	0.058	0.515	2.23	4.49
6.51	0.162	5.35	1.12	1.10
	0.143	3.13	1.33	1.76
	0.125	2.08	1.48	2.23
	0.107	1.45	1.74	3.05
	0.091	1.05	1.96	3.74
	0.074	0.742	2.15	4.33
	0.058	0.510	2.35	4.96
7.09	0.181	11.76	1.17	0.88
	0.162	5.32	1.50	1.92
	0.145	3.29	1.80	2.86
	0.127	2.18	2.00	3.49
	0.109	1.51	2.31	4.46
	0.092	1.08	2.55	5.21
	0.075	0.758	2.90	6.31
	0.059	0.527	3.16	7.33

(Table VI, continued)

pH	$[L_f]$ ($\underline{M}$)	P_{L_f}/P_{ML}	$W'_{1/2}$ (Hz)	$1/\tau_{L_f}$ (sec^{-1})
8.03	0.182	12.43	1.78	2.79
	0.162	5.41	2.68	5.62
	0.144	3.21	3.48	8.13
	0.125	2.12	4.15	10.2
	0.108	1.48	4.73	12.1
	0.091	1.05	5.46	14.4
	0.074	0.740	6.00	16.1
	0.057	0.510	6.90	18.9

(a) 25°.

(b) $W_{1/2}$ of free ligand resonance for no ligand exchange is 0.73 Hz.
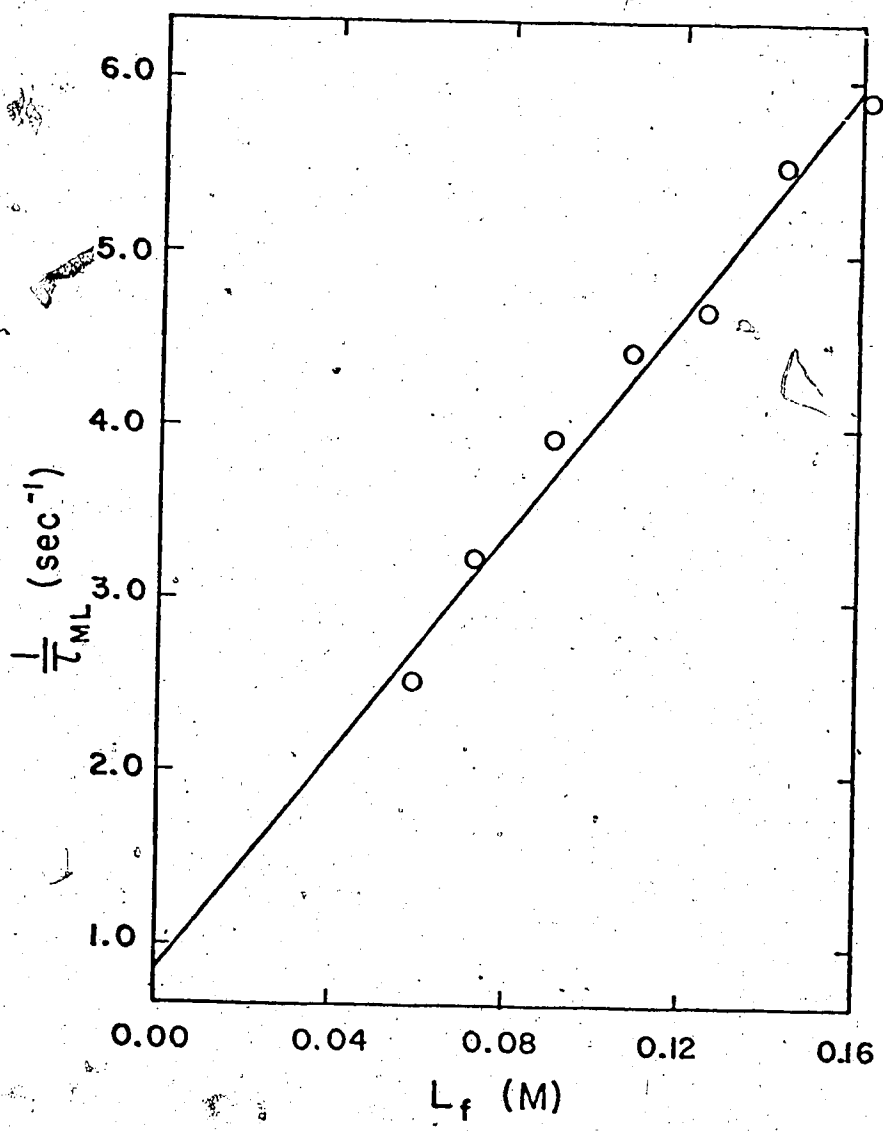
Figure 12: Pmr rate data for the Cd-1,3-PDTA system at pH 6.51 as a function of the free 1,3-PDTA concentration.

pH is equal to $k_3\alpha_4 + k_4\alpha_3 + k_5\alpha_2$ and the intercept is equal to $k_2[H^+]$. At the pH values listed in Table VI, α_3 ranges from factors of 10^5 to 3×10^2 greater than α_4 while k_3 has been found to be only 10 to 20 times larger than k_4 in similar reactions of EDTA complexes (39,40), suggesting that the term $k_3\alpha_4$ contributes a negligible amount to the slopes of the $P_{L_f}/(\tau_{L_f}P_{ML})$ vs. $[L_f]$ plots. Assuming the slope $\underline{m}$ to be equal to $k_4\alpha_3 + k_5\alpha_2$, Equation XIII can be derived.

$$\underline{m}/\alpha_2 = k_4(\alpha_3/\alpha_2) + k_5 \qquad\qquad XIII$$

Rate constants k_4 and k_5 were evaluated from the slope and intercept of a plot of $\underline{m}/\alpha_2$ vs. α_3/α_2; the values for α_2 and α_3 were calculated from the literature dissociation constants listed in Table V. A linear least squares analysis was used for this and all subsequent determinations of slopes and intercepts. The rate constants and their standard deviations are given in Table VII. The uncertainty in the intercepts of the plots of $P_{L_f}/(\tau_{L_f}P_{ML})$ vs. $[L_f]$ for which the data are given in Table VI, was too large to allow evaluation of k_2.

Lifetime data are given in Table VIII as a function of pH for a solution 0.10 $\underline{M}$ in both

Table VII

Experimentally Determined Ligand Exchange Rate Constants for 1,3-PDTA and EDDDA Complexes [a]

	k_2 ($M^{-1}sec^{-1}$)	k_{-2}	k_3	k_4	k_5
Cd(1,3-PDTA)$^{2-}$	9.1($\pm$0.3)x10^5	4.1($\pm$0.1)x10^9		3.0($\pm$0.1)x10^2 [b]	3.6($\pm$1.0)x10 [b]
Pb(1,3-PDTA)$^{2-}$	2.0($\pm$0.1)x10^7	6.8($\pm$0.3)x10^{10}	2.0($\pm$0.9)x10^4	2.5($\pm$0.1)x10^2 [c]	3.2($\pm$0.3)x10 [c]
Zn(1,3-PDTA)$^{2-}$	3.9($\pm$0.1)x10^4	4.0($\pm$0.1)x10^9		1.5($\pm$0.2)x10^3	1.7($\pm$0.4)x10^2
Cd(EDDDA)$^{2-}$	4.8($\pm$0.2)x10^6	4.0($\pm$0.2)x10^8	1.5($\pm$0.3)x10^3	6.5 $\pm$ 0.2	2.5($\pm$0.1)x10
Pb(EDDDA)$^{2-}$	1.2($\pm$0.1)x10^7	2.5($\pm$0.2)x10^{10}	2.0($\pm$0.1)x10^4		
Zn(EDDDA)$^{2-}$	2.0($\pm$0.1)x10^4	8.3($\pm$0.4)x10^8			

(a) 25°.

(b) From experiments at constant pH and varying L_f.

(c) From experiments at constant L_f and varying pH.

Table VIII

Kinetic Data as a Function of pH for the Cd-1,3-PDTA System[a,b,c]

pH	$W'_{1/2}$ (Hz)	$1/\tau_{L_f}$ (sec^{-1})
4.80	6.23	17.3
4.99	4.78	12.7
5.23	3.53	8.80
5.49	2.84	6.64
5.76	2.20	4.62
6.00	2.04	4.12
6.24	1.95	3.84
6.42	1.85	3.51
6.51	1.95	3.84
6.84	2.35	5.09
7.14	2.73	6.28
7.68	4.58	12.1
8.24	6.25	17.3

(a) 0.10 M Cd(1,3-PDTA)$^{2-}$ and 0.10 M free 1,3-PDTA.

(b) $W_{1/2}$ of free ligand resonance for no ligand exchange is ___ Hz.

(c) 25°.

Cd(1,3-PDTA)$^{2-}$ and free 1,3-PDTA. As can be seen

from these data and from the spectra in Figure 11,

the rate of ligand exchange decreases as the pH

is increased from 4.8, goes through a minimum at

pH 6.4 and then increases, as the pH is increased

further. Above pH 8.5, the exchange rate is so

fast that the lineshapes are of the intermediate

to fast types. Since exchange occurs between a

single line, an AB pattern, and the AB part of an

ABX pattern, the theory is quite complicated and

no attempt was made to evaluate lifetimes from data

at pH's greater than 8.5.

Rate constant k_2 was obtained from the data in

Table VIII at pH less than 6.4. At these pH's,

α_4 is negligible relative to α_2 and α_3, and the

contribution to the total exchange by the reaction

represented by Equation VI may be neglected. Since

P_{L_f} equals P_{ML}, rearrangement of Equation XII leads

to

$$\frac{1}{\tau_{L_f}} - (k_4\alpha_3 + k_5\alpha_2)[L_f] = k_2[H^+] \qquad \text{XIV}$$

The value given in Table VII for k_2 was obtained from

the slope of a plot of $1/\tau_{L_f} - (k_4\alpha_3 + k_5\alpha_2)[L_f]$ vs.

$[H^+]$ using the data in Table VIII and the values

determined above for k_4 and k_5. This plot is shown in Figure 13. Rate constant k_{-2} was obtained from k_2 using the relation $k_{-2} = k_2 K_4 K_f$ where K_f is the formation constant of Cd(1,3-PDTA)$^{2-}$ (64-66).

Rate constants k_4 and k_5 were also determined from the data in Table VIII in the pH range 6.4 to 8.2. In this pH range, calculations using the value of k_2 show the amount of ligand exchange via the reaction represented by Equation V to be negligible. The reaction represented by Equation VI has also been neglected for reasons given above, leading to

$$\frac{1}{\tau_{L_f} [L_f] \alpha_2} = k_4 \frac{\alpha_3}{\alpha_2} + k_5 \qquad \text{XV}$$

by rearrangement of Equation XII. The values obtained for k_4 and k_5 from the slope and intercept of a plot of $1/(\tau_{L_f} [L_f] \alpha_2)$ vs. α_3/α_2 are given in Table VII.

Above pH 8.5, the rate of ligand exchange increases, as evidenced by the intermediate to fast exchange spectra, presumably due to increased contributions from the reactions represented by Equations VI and VII.

Lifetime data are given in Table IX as a function of pH for a solution 0.10 M in both Zn(1,3-PDTA)$^{2-}$ and free 1,3-PDTA. Slow exchange spectra were obtained throughout the whole pH range studied and Equation
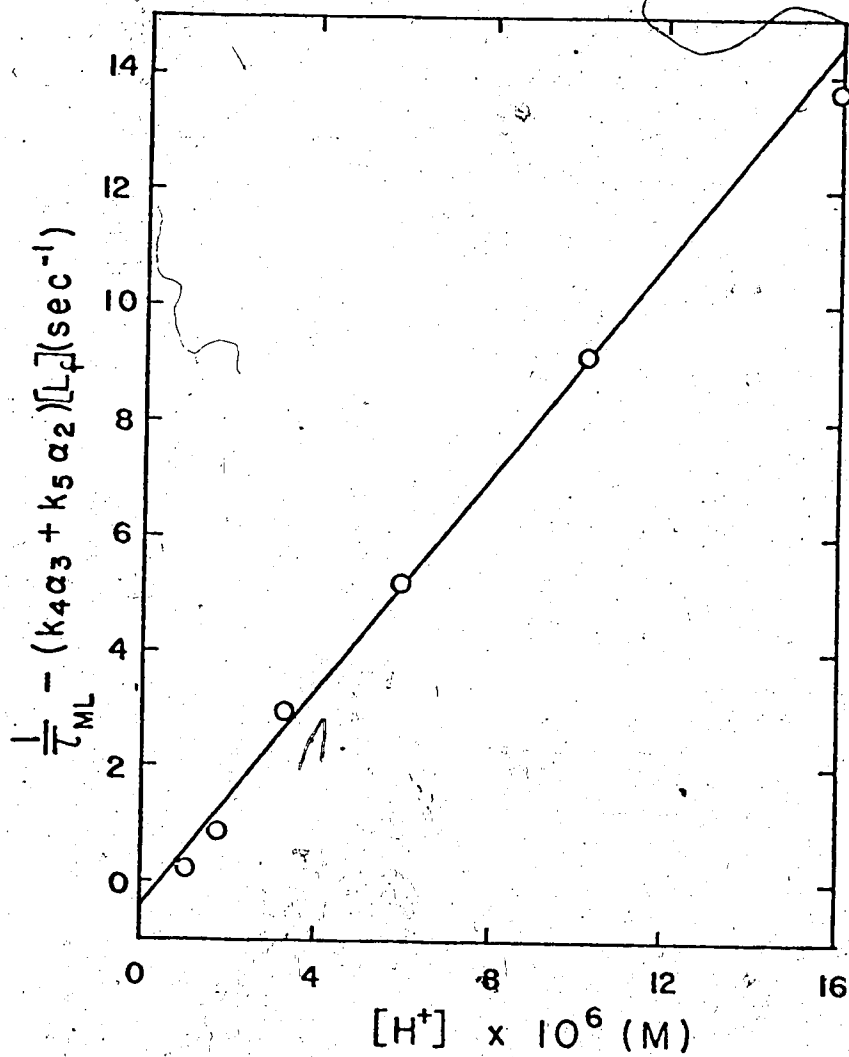
Figure 13: Pmr rate data for the Cd-1,3-PDTA system as a function of [H$^+$].

Table IX

Kinetic Data as a Function of pH for the Zn-1,3-PDTA System [a,b,c]

pH	$W'_{1/2}$ (Hz)	$1/\tau_{L_f}$ (sec^{-1})
3.64	4.35	11.34
4.03	2.72	6.22
4.65	1.90	3.64
4.97	1.75	3.17
5.60	1.55	2.54
6.03	1.53	2.48
6.34	1.55	2.54
6.68	1.49	2.36
7.02	1.44	2.20
7.53	1.35	1.92
7.95	1.25	1.60
8.38	1.12	1.19
9.01	0.98	0.75

(a) 0.10 $\underline{M}$ Zn(1,3-PDTA)$^{2-}$ and 0.10 $\underline{M}$ free 1,3-PDTA.

(b) $W_{1/2}$ of free ligand resonance for no ligand exchange is 0.73 Hz.

(c) 25°.

XVIII was used to calculate the lifetime τ_{L_f} from the acetate methylenic proton resonance of the free 1,3-PDTA. As in the Cd-1,3-PDTA system, the rate constants k_4 and k_5 were obtained from the slope and intercept of a plot of $1/(\tau_{L_f} [L_f] \alpha_2)$ vs. α_3/α_2 using the kinetic data at pH's greater than 7. The value for k_2 was obtained from the slope of a plot of $1/\tau_{L_f} - (k_4\alpha_3 + k_5\alpha_2)[L_f]$ vs. $[H^+]$ using the lifetime data at pH less than 6 and the values of k_4 and k_5 determined above. All rate constants so obtained are listed in Table VII.

Intermediate to fast exchange spectra for the acetate methylenic protons are exhibited by the Pb-1,3-PDTA system; examples of such spectra are shown on the left hand side of Figure 14 for a 0.10 $\underline{M}$ solution of Pb(1,3-PDTA)$^{2-}$ at pH 7.00 which contained the indicated concentrations of free 1,3-PDTA. Because of the complexity of this exchange case, kinetic data were obtained from the experimental spectra by comparison with computer-simulated spectra. The simulation was accomplished with a four-site exchange program (43) formulated using modified Bloch equations. The four sites are free 1,3-PDTA and 1,3-PDTA complexed to lead in three different nuclear spin states, +1/2 and -1/2 for ^{207}Pb and
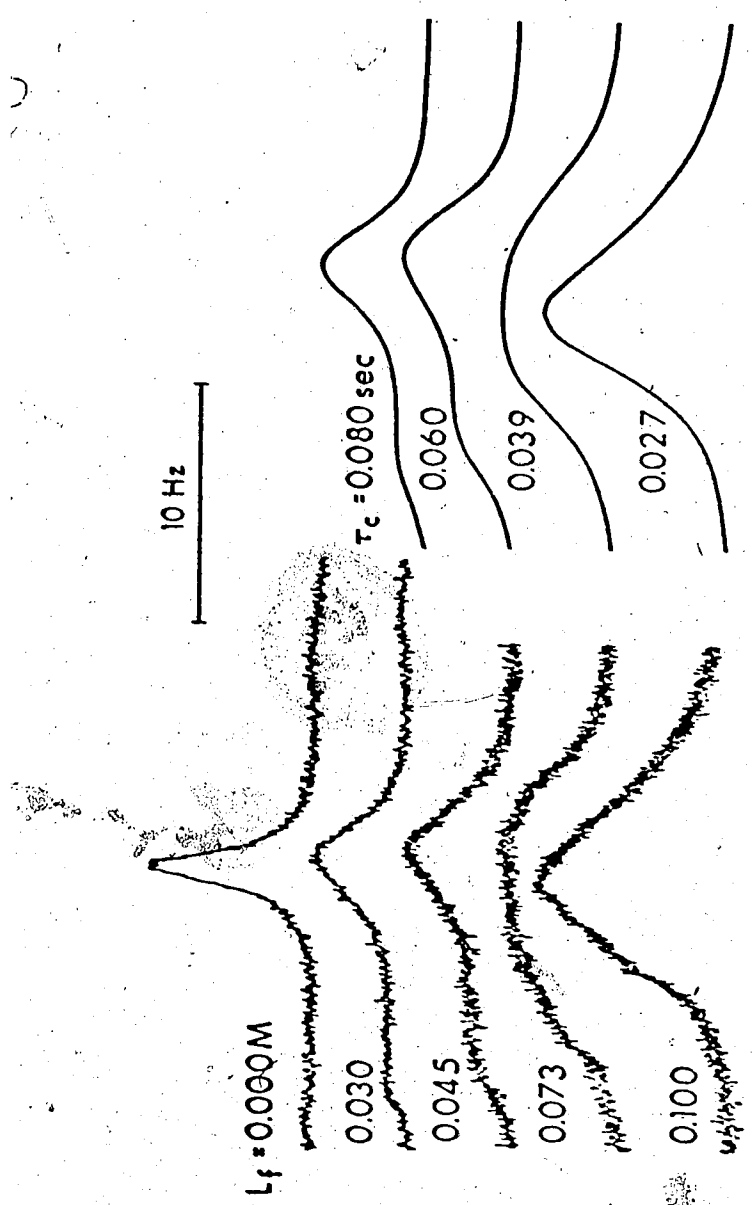
Figure 14: Representative experimental (left) and theoretical (right) 60 MHz pmr spectra of the acetate methylenic protons of an aqueous solution of Pb(1,3-PDTA)$^{2-}$ containing the indicated concentrations of free 1,3-PDTA at pH 7.00.

zero for all the other lead isotopes. The procedure
was to simulate a series of spectra as a function of
the mean lifetime of the Pb-1,3-PDTA complex before
ligand exchange τ_{ML}, using the following input para-
meters: populations, chemical shifts and natural
linewidths at each of the four sites. The individual
lifetimes for given solution conditions were then
obtained by comparing the linewidths of the resonance
peaks and by superimposing the experimental and
calculated spectra.

The lifetime data presented in Table X were ob-
tained from experiments in which the pH was held
constant and the free ligand concentration was varied.
The matched experimental and computer-simulated
spectra shown in Figure 14 are typical of the fits
obtained in such experiments. Applying Equation XII
to the above lifetime data, the slopes of the plots
of $P_{L_f}/(\tau_{L_f} P_{ML})$ vs. $[L_f]$ yielded the values for k_3,
k_4 and k_5 listed in Table VII. The intercepts of such
plots gave an approximate value of 2.2×10^7 $M^{-1}sec^{-1}$
for k_2.

A more precise value for k_2 was obtained using the
data given in Table XI which gives the pH dependence
of $1/\tau_{L_f}$ for a solution 0.10 $\underline{M}$ in both $Pb(1,3-PDTA)^{2-}$
and free 1,3-PDTA. Equation XIV was applicable in

Table X

Kinetic Data for the Pb-1,3-PDTA System at
Constant pH Values as a Function of Free
Ligand Concentration.[a]

pH	$[L_f]$ $(\underline{M})$	P_{L_f}/P_{ML}	$1/\tau_{L_f}$ (sec^{-1})[b]
6.00	0.015	0.153	163
	0.030	0.307	93.2
	0.044	0.468	69.2
	0.058	0.634	52.5
	0.073	0.808	45.9
	0.087	0.980	39.6
	0.100	1.15	36.5
	0.114	1.34	33.1
7.00	0.015	0.155	32.3
	0.030	0.314	39.8
	0.045	0.479	34.9
	0.059	0.639	35.7
	0.073	0.808	31.7
	0.087	0.984	31.7
	0.100	1.16	29.2
	0.113	1.33	27.9
9.03	0.015	0.157	79.6
	0.030	0.314	290
	0.045	0.474	201
	0.059	0.645	174
	0.074	0.814	189
	0.089	1.00	185
	0.103	1.18	212

(a) 25°.
(b) Determined by matching experimental and computer-
simulated spectra.

Table XI

Kinetic Data as a Function of pH for the

Pb-1,3-PDTA System [a,b]

pH	$1/\tau_{L_f}$ (sec^{-1}) [c]
4.64	465
4.87	303
5.31	108
5.83	50.0
6.71	31.9

(a) 0.10 $\underline{M}$ Pb(1,3-PDTA)$^{2-}$ and 0.10 $\underline{M}$ free 1,3-PDTA.

(b) 25°.

(c) Determined by matching experimental and computer-simulated spectra.

this case, so that the slope of a plot of

$1/\tau_{L_f} = (k_4\alpha_3 + k_5\alpha_2)[L_f]$ vs. $[H^+]$ yielded the value

for k shown in Table VII. Rate constant k_{-2} was

obtained from the relation $k_{-2} = k_2 K_4 K_f$.

Ligand Exchange Kinetics of the EDDDA Complexes

The reactions represented by Equations IV to VIII

were considered to be the predominant pathways by

which EDDDA exchanges between the free and complexed

forms for the solution conditions used in this work.

As in the 1,3-PDTA systems, the AB multiplet patterns

observed for the acetate methylenic protons of the

EDDDA complexes at intermediate pH values in the

absence of noncomplexed ligand indicate that the mean

lifetime of the complexes before first-order dis-

sociation by the reaction represented by Equation IV

is greater than 0.1 sec. Thus, this reaction can be

neglected in the kinetic analysis of the data. Free

ligand lifetimes were determined from the linewidths

of the exchanged-broadened acetate resonance of the

free ligand using Equation XVIII.

Lifetime data for the Cd-EDDDA system for experi-

ments in which the pH was held constant and the free

ligand concentration was varied are given in Table

XII. Using Equation XII, the slopes obtained from

Table XII

Kinetic Data for the Cd-EDDDA System at

Constant pH Values as a Function of

Free Ligand Concentration [a,b]

pH	$[L_f]$ $(\underline{M})$	P_{L_f}/P_{ML}	$W'_{1/2}$ (Hz)	$1/\tau_{L_f}$ (sec^{-1})
8.20	0.160	5.02	1.28	0.82
	0.140	2.92	1.40	1.19
	0.121	1.93	1.57	1.73
	0.102	1.29	.75	2.30
	0.084	0.898	1.87	2.67
	0.066	0.613	2.04	3.20
8.50	0.160	4.95	1.57	1.82
	0.141	2.94	1.85	2.70
	0.122	1.95	2.16	3.68
	0.103	1.31	2.31	4.15
	0.084	0.894	2.63	5.15
	0.066	0.608	3.18	6.88

(a) 25°.

(b) $W_{1/2}$ of free ligand resonance for no ligand exchange
     is 1.03 Hz.

plots of $P_{L_f}/(\tau_{L_f} P_{ML})$ vs. $[L_f]$ yielded the value for k_3 listed in Table VII and values of zero within experimental error for k_4 and k_5, indicating that the latter rate constants are too small to be measured by the pmr method. From the lifetime data as a function of pH for a solution 0.10 $\underline{M}$ in both Cd(EDDDA)$^{2-}$ and free EDDDA shown in Table XIII, the value for k_2 was determined. Over the pH range studied, Equation XII could be reduced to

$$\frac{1}{\tau_{L_f}} = k_2 [H^+] \qquad\qquad\qquad \text{XVI}$$

The terms in k_4 and k_5 were neglected because it was shown above that their exchange contributions are too small to be detected by pmr line-broadening methods. Knowing the value of k_3, calculations indicated that the term containing this rate constant could also be neglected. For the given solution conditions $P_{L_f} = P_{ML}$, and the slope of the plot of $1/\tau_{L_f}$ vs. $[H^+]$ yielded the value for k_2 shown in Table VII.

Lifetime data for the Pb-EDDDA system at constant pH varying the free ligand concentration are presented in Table XIV. Using Equation XII the slopes obtained from plots of $P_{L_f}/(\tau_{L_f} P_{ML})$ vs. $[L_f]$ yielded the value of k_3 listed in Table VII and values of zero within

Table XIII

Kinetic Data as a Function of pH for the

Cd-EDDDA System [a,b,c]

pH	$W'_{1/2}$ (Hz)	$1/\tau_{L_f}$ (sec^{-1})
5.60	5.28	13.3
5.74	4.09	9.61
5.90	3.44	7.57
5.99	3.13	6.59
6.15	2.63	5.02
6.37	2.04	3.17
6.67	1.59	1.76
7.03	1.32	0.91

(a) 25°C.

(b) 0.10 $\underline{M}$ Cd(EDDDA)$^{2-}$ and 0.10 $\underline{M}$ free EDDDA.

(c) $W_{1/2}$ of free ligand resonance for no ligand exchange is 1.03 Hz.

Table XIV

Kinetic Data for the Pb-EDDDA System at Constant pH Values as a Function of Free Ligand Concentration [a,b]

pH	$[L_f]$ ($\underline{M}$)	P_{L_f}/P_{ML}	$W'_{1/2}$ (Hz)	$1/\tau_{L_f}$ (sec^{-1})
7.20	0.178	9.87	1.26	0.818
	0.156	4.37	1.56	1.76
	0.135	2.49	1.84	2.64
	0.113	1.59	2.16	3.64
	0.0924	1.04	2.43	4.50
	0.0727	0.70	2.85	5.81
	0.0530	0.44	3.18	6.85
7.50	0.178	9.88	1.50	1.60
	0.159	4.81	1.91	2.91
	0.141	2.94	2.26	3.9
	0.123	1.98	2.64	5.19
	0.105	1.38	3.02	6.39
	0.0875	0.981	3.33	7.35
	0.0702	0.685	3.66	8.40
	0.0534	0.460	4.55	11.2

(a) 25°C

(b) $W_{1/2}$ of free ligand resonance for no ligand exchange is 1.03 Hz.

experimental error for k_4 and k_5. Data as a function
of pH for this system are given in Table XV. In
the determination of k_2 from these data, Equation XII
was reduced to

$$\frac{1}{\tau_{L_f}} + k_3 \alpha_4 [L_f] = k_2 [H^+] \qquad XVII$$

In this case the term containing k_3 was too large
to be neglected over the pH range shown in Table XV.
Therefore, a plot of $1/\tau_{L_f} - k_3 \alpha_4 [L_f]$ vs. $[H^+]$
yielded the value of k_2 given in Table VII.

For the Zn-EDDDA system it was found that the
rates of the reactions represented by Equations VI
to VIII are too slow to be measured by pmr line-
broadening methods. The value for k_2, however, was
determined from the slope of a plot of $1/\tau_{L_f}$ vs.
$[H^+]$ using the lifetime data in Table XVI.

B. DISCUSSION

Mechanism of Formation of the $M(1,3-PDTA)^{2-}$ and
$M(EDDDA)^{2-}$ Complexes

In the present investigation, the rate constants
for the complexation of cadmium and zinc by mono-
protonated 1,3-PDTA (k_{-2} in Table VII) were found
to be essentially the same as those with mono-

Table XV

Kinetic Data as a Function of pH

for the Pb-EDDDA System [a,b,c]

pH	$W'_{1/2}$ (Hz)	$1/\tau_{L_f}$ (sec^{-1})
6.30	3.08	6.15
6.50	2.50	4.34
6.77	2.27	3.62
6.97	2.25	3.77

(a) 25°C.

(b) 0.10 $\underline{M}$ Pb(EDDDA)$^{2-}$ and 0.10 $\underline{M}$ free EDDDA.

(c) $W_{1/2}$ of free ligand resonance for no ligand exchange is 1.03 Hz.

Table VI

Kinetic Data as Function of pH

for the EDDDA System [a,b,c]

pH	$W'_{1/2}$ (Hz)	$1/\tau_{L_f}$ (sec^{-1})
3.48	2.99	6.28
3.67	2.46	4.62
3.87	1.88	2.80
4.06	1.59	1.89
4.26	1.31	1.01
4.46	1.16	0.54

(a) 25°C.

(b) 0.10 M Zn(EDDDA)$^{2-}$ and 0.10 M free EDDDA.

(c) $W_{1/2}$ of free ligand resonance for no ligand exchange is 1.03 Hz.

protonated EDTA (15,24,34). This finding contrasts with that of Pearson and de Wit (69) who determined that the rate of the reaction of zinc with monoprotonated EDTA was less than that with monoprotonated 1,3-PDTA using stopped-flow kinetic measurements. Their results can only be considered approximate, however, since the observed rates were just at the detection limits for their stopped-flow apparatus. The rate constants for complexation of cadmium, zinc and lead by monoprotonated EDDDA are from 2.5 to 10 times smaller than the corresponding ones with monoprotonated 1,3-PDTA.

In the dissociative mechanism (1,70) of complex formation, the reaction takes place in a stepwise fashion, with metal ion and ligand first diffusing together to form an outer-sphere complex. A water molecule then dissociates from the aquated metal ion and a donor group of the multidentate ligand coordinates at the vacated site. When a second water molecule dissociates at a position cis to the metal-ligand bond the second metal-ligand bond forms. The reaction continues with a separate step for each of the bonds. Depending on the structure of the ligand, the rate of formation of a specific metal-ligand bond will govern the complexation rate. For the majority of complexes whose formation kinetics have been studied,

formation of the first bond is rate-determining, its rate being governed by the rate of water dissociation from the aquated metal ion in the outer-sphere complex (70).

A possible sequence for the stepwise reaction of aquated metal ions with monoprotonated hexadentate ligands of the EDTA type is shown in Figure 1. Reaction proceeds by dissociation of water molecules followed by metal-ligand bond formation to yield an intermediate in which the three dentates of one end of the ligand are metal-coordinated while coordination at the other end is blocked by the proton on the nitrogen. For further coordination to occur, the second metal-nitrogen bond has to form before the intermediate dissociates to reactants. Presumably the second metal-nitrogen bond can form only after the proton has been transferred to a carboxylate oxygen or to a solvent molecule.

The similarity of the rate constants for the reaction of monoprotonated EDTA and 1,3-PDTA with aquated cadmium and zinc (k_{-2}) suggests that, once the nitrogen-protonated intermediate has formed with these ligands, coordination of the remaining dentates is not rate-determining. If it were rate-determining, it is likely the overall complexation rate constants

for monoprotonated 1,3-PDTA would be less than those for monoprotonated EDTA due to closure of the six-membered ring which is necessary in the former complexes. Kustin and coworkers (47,48) have found that when ring closure is the rate-determining step, the rates of certain complex formation reactions are slower when six-membered rings are involved than when five-membered rings must be closed. The present results are consistent with the rate-determining step being formation of one of the first three metal-ligand bonds, its rate being governed by the rate of water loss from the metal ion.

The smaller rate constants for reaction with mono-protonated EDDDA (k_2) suggest that the rate-determining step is different in these reactions. It is possible that, when the first ligand dentate to bond is a propionate carboxylate oxygen, the rate of formation of the metal-nitrogen bond to close the six-membered chelate ring is less than when the first ligand dentate to bond is an acetate carboxylate oxygen. If this were the only factor responsible for the smaller rate constants, the rates of complexation with monoprotonated EDDDA should be at least half those with monoprotonated 1,3-PDTA.

A larger decrease, the magnitude of which would

be metal ion dependent, might result if the rates
of dissociation of the nitrogen-protonated inter-
mediates in the EDDDA reactions are sufficiently
large that a significant amount of intermediate
dissociates to reactants prior to proton transfer
from the nitrogen atom. Kinetic data are not available
for model tridentate complexes from which the rates
of dissociation of the nitrogen-protonated, tri-
dentate intermediates of 1,3-PDTA and EDDDA can be
obtained. However, assuming the rate constants for
formation of the nitrogen-protonated intermediates
to be equal to the rate constants for the reaction
with monoprotonated 1,3-PDTA (k_{-2}) and the formation
constants for the intermediates to be approximately
those of complexes of model tridentate ligands, order
of magnitude rates of intermediate dissociation can
be predicted. The dissociation rate constant is
given by k_{-2}/K_f, where K_f is the formation constant.
Using the formation constants of the iminodiacetic
acid (IDA) complexes (71) as approximate values for
tridentate coordination to monoprotonated 1,3-PDTA
and assuming the analogous formation constants with
monoprotonated EDDDA to lie between those for IDA
and iminodipropionic acid, the predicted value for
the dissociation rate constant of the cadmium inter-

mediate with 1,3-PDTA is 1.8×10^4 sec^{-1} while that with EDDDA is between 1.8×10^4 and 1.1×10^6 sec^{-1}. The predicted value for the dissociation rate constant of the zinc intermediate with 1,3-PDTA is 3.7×10^2 sec^{-1} while that with EDDDA is between 3.7×10^2 and 4.5×10^4 sec^{-1}. The formation constant of the lead complex of iminodipropionic acid is not available.

The reaction by which the proton leaves the nitrogen to permit formation of the second metal-nitrogen bond could involve either direct transfer to solvent water or migration to a neighbouring carboxylate group. The kinetics of these two reactions for the nitrogen-protonated isomer of neutral glycine have been studied by Sheinblatt and Gutowsky (72), who report a pseudo first order rate constant of 5 sec^{-1} for the transfer of the nitrogen-bonded proton to water and a rate constant of 175 sec^{-1} for migration of the proton to the carboxylate group. The rate constants for proton transfer in the nitrogen-protonated intermediates of 1,3-PDTA and EDDDA would probably be somewhat larger than either of those for glycine because of charge-charge interaction between the metal ion and the proton and the additional carboxylate group to which proton transfer can occur.

The preceding considerations suggest that the
rates of dissociation of the metal ions from the
EDDDA intermediates are larger than from the cor-
responding 1,3-PDTA intermediates, and that they may
be comparable to the rate of proton transfer from
the nitrogen atom. If so, there is a greater chance
that EDDDA intermediates will dissociate before
proton transfer and formation of the second metal-
nitrogen bon can take place, and consequently k_{-2}
would be less for the EDDDA complexes. The preceding
considerations also suggest that the rate of reaction
with cadmium should be decreased more than with zinc,
as observed experimentally. If these conclusions
are correct, a further decrease would be predicted
for the formation reactions of the monoprotonated
form of ethylenediaminetetrapropionic acid. Pearson
and de Wit (69) found this to be the case for the
zinc complex.

Second Order Ligand Displacement Reactions

The reactions represented by Equations VI to
VIII are second order ligand displacement reactions.
The mechanism (7,24,73) for similar EDTA type ligand
exchange reactions has been demonstrated to involve
the bound ligand being successively displaced by

the incoming ligand with intermediates present in which both ligands simultaneously bound in varying degrees to the metal ion. The mechanism for the ligand displacement reactions studied in this chapter is probably similar. Comparison of the rate constants k_3, k_4 and k_5 in Table VII for the cadmium and lead complexes of 1,3-PDTA shows a decrease in the values with increasing degree of protonation of the incoming ligand, indicating that proton transfer might be a rate-determining step in these reactions. Similar results have been found for other systems (7,39,40,44,73).

CHAPTER IV

EXPERIMENTAL

A. CHEMICALS

1,3-PDTA was synthesized by the method of Weyh and Hamm (74). The following analytical data were obtained for the ligand: Calculated for $C_{11}H_{18}N_2O_8$: C, 43.1; H, 4.9; N, 9.1. Found, C, 42.9; H, 5.1; N, 9.1. The 1,4-BDTA was prepared by Dr. George Blakney by a procedure analogous to that used for 1,3-PDTA. EDDDA (Lamont Laboratories) was used without further purification. No impurities could be detected in the pmr spectra of solutions of each of these ligands. Reagent grade metal nitrate salts were used as received. Tetramethylammonium (TMA) hydroxide (Eastman Organic Chemicals), tertiary-butanol (t-butanol) and 1,4-dioxane (Fisher Scientific) were used as received.

B. SOLUTIONS

A stock solution of TMA nitrate, used as a reference for some of the chemical shift measurements, was prepared by titration of a 25% aqueous solution of TMA hydroxide with nitric acid to a neutral pH.

The solutions used in the pmr measurements were prepared in either triply distilled water or in D_2O from the appropriate amounts of metal salt and ligand at concentrations varying between 0.10 and 0.20 $\underline{M}$. For making chemical shift measurements TMA or t-butanol was added at concentrations of 0.01 $\underline{M}$ and 0.03 $\underline{M}$ respectively to serve as a reference. To avoid dilution, the pH or pD was adjusted with concentrated HNO_3, KOH or KOD and samples of about 0.5 ml were withdrawn at appropriate pH or pD values. When kinetic measurements were being made at constant pH as a function of free ligand (or metal nitrate) concentration, the requisite amount of ligand (or metal nitrate) was added, the pH adjusted and a sample withdrawn. More ligand was added to the solution and the same procedure followed for all samples at this pH. The concentrations were corrected for the decreasing solution volume. Since high concentrations are necessary in the pmr experiment, no attempt was made to control the ionic strength.

C. pH MEASUREMENTS

All pH measurements were made at 25°C with an

Orion Model 801 pH meter equipped with either a standard glass electrode and a fibre-junction saturated calomel reference electrode or a micro-combination electrode. Saturated potassium acid tartrate and 0.01 $\underline{M}$ sodium tetraborate solutions, pH 3.56 and 9.18 at 25°, were used to standardize the meter. For D_2O solutions, the meter readings were converted to pD values using the expression of Glascoe and Long (75)

$$pD = pH \text{ meter reading} + 0.40.$$

D. PMR MEASUREMENTS

The proton spectra were obtained at 60 MHz on a Varian A-60D, at 100 MHz on a Varian HA-100 and at 220 MHz on a Varian HR-220 spectrometer. These instruments were equipped with Varian variable temperature controllers. The temperature of the probe was determined using the standard methanol and ethylene glycol solutions and the plot of chemical shift vs. temperature prepared by Varian.

At 60 MHz, spectra were recorded at sweep rates of 0.1 Hz/sec for both the chemical shift and line-shape measurements. The chemical shifts are reported in ppm relative to the central resonance of the TMA

triplet which is 3.17 ppm downfield from the methyl

resonance of sodium 3-(trimethylsilyl)-1-propane

sulfonic acid. For linewidth measurements, each

spectrum was recorded at least four times and the

linewidths at half height of the resonances in the

individual spectra were averaged.

The HA-100 spectrometer was operated in the

frequency sweep mode with the methyl resonance of

internal t-butanol providing the lock signal. Inter-

ference from the water resonance necessitated

the use of D_2O as the solvent. Each spectrum was

recorded at least four times at sweep rates of

0.1 Hz/sec for the linewidth measurements. Fre-

quencies were measured from the differences between

the manual and sweep oscillator frequencies.

At 220 MHz the chemical shift differences and

linewidths were measured directly from the spectra.

E.   KINETIC APPLICATIONS OF NUCLEAR MAGNETIC RESONANCE

The basic theories used in the study of chemical

exchange by nuclear magnetic resonance (nmr) have

been treated extensively in several monographs and

review articles (50,76-79). Two of these theories,

the modified Bloch approach and density matrix theory,

have been utilized in the present work to extract
kinetic data from the pmr spectra. Only a brief
qualitative description of these two approaches
will be given.

Bloch (80) obtained a set of equations to describe
the variation of the components of the total nuclear
magnetic moment per unit volume for a collection
of nuclei with non-zero spins in the presence of a
varying magnetic field. The simplest chemical exchange
system which may be studied by nmr is one for which the
nuclei may interchange between two different chemical
environments, A and B with different Larmour fre-
quencies. For this case, there will be two independent
magnetic moments for environments A and B which can
be described by the Bloch equations. Addition of terms
to these equations to account for the transfer of
magnetization between the two sites leads to the
modified Bloch equations (81). From these equations
a general expression may be derived describing the
intensity of the nmr absorption at a given frequency
when there is exchange between the sites (82,83).
This general equation may be simplified under certain
limiting conditions.

One such condition is that of slow exchange for
which the spectrum consists of two separate resonances

at frequencies δ_A and δ_B (in Hz). For this situa-
tion the lifetimes τ_A and τ_B of the nuclei in each
of the sites before exchange to the other site are
large compared to the inverse of the separation of
the resonances; that is, τ_A, $\tau_B > (\delta_A - \delta_B)^{-1}$. These
lifetimes may be determined from the extent of broad-
ening of each of the resonances by an equation of the
form (76),

$$\frac{1}{\tau_A} = \pi(W'_{1/2,A} - W_{1/2,A}) \qquad\qquad \text{XVIII}$$

where $W'_{1/2,A}$ is the linewidth at half height of the
exchange—broadened resonance of nuclei at site A
and $W_{1/2,A}$ is the linewidth of the same resonance in
the absence of exchange. An analogous equation
may be written for the lifetime τ_B. The natural
linewidth $W_{1/2,A}$ is related to the effective spin-
spin relaxation time $T_{2,A}$ by the relation $1/T_{2,A} = \pi W_{1/2,A}$. The effective spin-spin relaxation time
takes into account the actual spin-spin relaxation
time and broadening due to magnetic field inhomo-
geneities.

For the condition of intermediate exchange, the
lifetimes are of the order of the inverse of the
separation of the resonances and the spectrum consists
of the transition from two resonances to one. When the

lifetimes are small compared to the inverse of the separation of the resonances, rapid exchange occurs and the spectrum consists of one resonance at an intermediate frequency between δ_A and δ_B.

Most of the ligand exchange systems studied in Chapter III are ones for which Equation XVIII is applicable. The two sites are free ligand and complexed ligand.

The modified Bloch equation approach may be extended to the many-site exchange problem by the addition of appropriate exchange terms and the derivation of an expression describing the intensity of the nmr absorption as a function of the frequency. The lifetimes in the individual sites may then be obtained by computing theoretical spectra and matching them to the experimental spectra. Such an approach was used for the Pb-1,3-PDTA exchange system which was analyzed as a four-site exchange problem.

The exchange problem becomes much more complex when there is spin-spin coupling between the nuclei at the different sites. For such systems the modified Bloch approach is no longer valid; however, a quantum mechanical method based on the use of density matrices is applicable. In this theoretical treatment (78,79), exchange and relaxation matrix

terms are added to the basic density matrix equatio
using as the basis set the spin product functions
for the spin system in question. A final lineshape
expression for the nmr absorption spectrum can then
be derived. For an AB spin system, the lifetimes
τ_A or τ_B may be obtained by computing theoretical
spectra using the above lineshape expression and
matching them to the experimental spectra. Such an
approach was used in Chapter II for determining the
lifetimes before AB interchange.

BIBLIOGRAPHY

1. R. G. Wilkins, Accounts Chem. Res., 3, 408 (1970).

2. A. K. Ahmed and R. G. Wilkins, J. Chem. Soc., 3700 (1959).

3. D. W. Margerum, D. B. Rorabacher and J. F. G. Clarke, Jr., Inorg. Chem., 2, 667 (1963).

4. D. W. Margerum, Rec. Chem. Progress, 24, 237 (1963).

5. D. W. Margerum and T. J. Bydalek, Inorg. Chem., 1, 852 (1962).

6. D. W. Margerum, D. L. Janes and H. M. Rosen, J. Amer. Chem. Soc., 87, 4463 (1965).

7. D. B. Rorabacher and D. W. Margerum, Inorg. Chem. 3, 382 (1964).

8. D. W. Margerum and H. M. Rosen, ibid., 7, 299 (1968).

9. R. J. Day and C. N. Reilley, Anal. Chem., 36, 1073 (1964).

10. S. Chan, R. J. Kula and D. T. Sawyer, J. Amer. Chem. Soc., 86, 377 (1964).

11. Y. O. Aochi and D. T. Sawyer, Inorg. Chem., 5, 2085 (1966).

12. T. J. Bydalek and D. W. Margerum, J. Amer. Chem. Soc., 83, 4326 (1961).

13. L. V. Haynes and D. T. Sawyer, Inorg. Chem., 6, 2146 (1967).

14. B. B. Smith and D. T. Sawyer, ibid., 7, 2020 (1968).

15. G. H. Reed and R. J. Kula, ibid., 10, 2050 (1971).

16. G. L. Blackmer and J. L. Sudmeier, ibid., 10, 2019 (1971).

17. J. L. Sudmeier, A. J. Senzel, and G. L. Blackmer, ibid., 10, 90 (1971).

18. R. J. Day and C. N. Reilley, *Anal. Chem.*, **37**, 1326 (1965).

19. T. J. Bydalek and D. W. Margerum, *Inorg. Chem.*, **2**, 678 (1963).

20. R. J. Kula, *Anal. Chem.*, **39**, 1171 (1967).

21. J. I. Legg and D. W. Cooke, *Inorg. Chem.*, **4**, 1576 (1965).

22. D. W. Cooke, *ibid.*, **5**, 1141 (1966).

23. P. Letkeman and J. B. Westmore, *Can. J. Chem.*, **49**, 2073 (1971).

24. J. L. Sudmeier and C. N. Reilley, *Inorg. Chem.*, **5**, 1047 (1966).

25. M. Saunders and F. Yamada, *J. Amer. Chem. Soc.*, **85**, 1882 (1963).

26. C. H. Bushweller and J. W. O'Neal, *ibid.*, **92**, 2159 (1970).

27. W. R. Morgan and D. E. Leyden, *ibid.*, **92**, 4527 (1970).

28. D. E. Leyden and W. R. Morgan, *J. Phys. Chem.*, **75**, 3190 (1971).

29. D. L. Rabenstein and B. J. Fuhr, *Inorg. Chem.*, **11**, 2430 (1972).

30. D. L. Rabenstein, G. Blakney and B. J. Fuhr, submitted for publication.

31. M. Eigen, *Z. Elektrochem.*, **64**, 115 (1960).

32. M. Eigen in "Advances in the Chemistry of Coordination Compounds", S. Kirschner, Ed., MacMillan, New York, N.Y., 1961, p.371.

33. M. Eigen and K. Tamm, *Z. Electrochem.*, **66**, 93, 107 (1962).

34. N. Tanaka, R. Tamanushi and M. Kodama, *Z. Physik. Chem.* (Frankfurt), **14**, 141 (1958).

35. J. W. Emsley, J. Feeney and L. H. Sutcliffe, "High Resolution Nuclear Magnetic Resonance", Vol. 1, Pergamon Press, Oxford, 1965, pp. 357-363.

36. N. Tanaka, H. Osawa and M. Kamada, Bull. Chem. Soc. Japan, 36, 67 (1963).

37. N. Tanaka, H. Osawa and M. Kamada, ibid., 36, 530 (1963).

38. D. W. Margerum and B. A. Zabin, J. Phys. Chem., 66, 2214 (1962).

39. R. J. Kula and D. L. Rabenstein, J. Amer. Chem. Soc., 89, 552 (1967).

40. R. J. Kula and G. H. Reed, Anal. Chem., 38, 697 (1966).

41. T. J. Bydalek and M. L. Blomster, Inorg. Chem., 3, 667 (1964).

42. N. Tanaka, K. Ebata, T. Takahari and T. Kumagai, Bull. Chem. Soc. Japan, 35, 1836 (1962).

43. D. L. Rabenstein, J. Amer. Chem. Soc., 93, 2869 (1971).

44. D. L. Rabenstein and R. J. Kula, ibid., 91, 2492 (1969).

45. J. C. Cassatt and R. G. Wilkins, ibid., 90, 6045 (1968).

46. D. B. Rorabacher, Ph.D. Dissertation, Purdue University, Lafayette, Ind., 1963.

47. K. Kustin, R. F. Pasternack and E. M. Weinstock, J. Amer. Chem. Soc., 88, 4610 (1966).

48. A. Kowalak, K. Kustin, R. F. Pasternack and S. Petrucci, ibid., 89, 3126 (1967).

49. B. J. Fuhr and D. L. Rabenstein, Inorg. Chem., 12, 1868 (1973).

50. Reference 35, pp. 481-488.

51. B. W. Goodwin, Master's Thesis, University of Manitoba, Winnipeg, Manitoba, 1969.

52. R. J. Kula, Anal. Chem., 37, 989 (1965).

53. J. C. Bailar, J. Inorg. Nucl. Chem., 8, 165 (1958).

54. M. Eigen, Pure Appl. Chem., 6, 97 (1963).

55. J. P. Jones, E. J. Billo and D. W. Margerum, J. Amer. Chem. Soc., 92, 1875 (1970).

56. M. W. Grant, H. W. Dodgen and J. P. Hunt, ibid., 93, 6828 (1971).

57. M. Rabinovitz and A. Pines, ibid., 91, 1585 (1969).

58. H. Hoffmann, Ber. Bunsenges. Phys. Chem., 73, 432 (1969).

59. W. Byers and B. E. Douglas, Inorg. Chem., 11, 1470 (1972).

60. P. F. Coleman, J. I. Legg and J. Steele, ibid., 9, 937 (1970).

61. G. Schwarzenbach and H. Ackermann, Helv. Chim. Acta, 31, 1029 (1948).

62. R. J. Kula, D. T. Sawyer, S. I. Chan and C. M. Finley, J. Amer. Chem. Soc., 85, 2930 (1963).

63. D. Chapman, D. R. Lloyd and R. Prince, J. Chem. Soc., 3645 (1963).

64. F. L'Eplattenier and G. Anderegg, Helv. Chim. Acta, 47, 1792 (1964).

65. G. Anderegg, ibid., 47, 1801 (1964).

66. S. Chaberek and A. E. Martell, J. Amer. Chem. Soc., 74, 6228 (1952).

67. D. L. Rabenstein, Can. J. Chem., 50, 1036 (1972).

68. J. L. Sudmeier and C. N. Reilley, Anal. Chem., 36, 1698 (1964).

69. R. G. Pearson and D. G. de Wit, J. Coord. Chem., 2, 175 (1973).

70. M. Eigen and R. G. Wilkins, "Mechanisms of Inorganic Reactions", in Advances in Chemistry Series, No. 49, R. K. Murmann, R. T. M. Fraser and J. Bauman, eds., American Chemical Society, Washington, D.C., 1965, pp. 55-65.

71. L. G. Sillen and A. E. Martell, "Stability Constants of Metal Ion Complexes", The Chemical Society, London, 1964.

72. M. Sheinblatt and H. S. Gutowsky, J. Amer. Chem. Soc., 86, 4814 (1964).

73. J. D. Carr, R. A. Libby and D. W. Margerum, Inorg. Chem., 6, 1083 (1967).

74. J. A. Weyh and R. E. Hamm, ibid., 7, 2431 (1968).

75. P. K. Glascoe and F. A. Long, J. Phys. Chem., 64, 188 (1960).

76. J. A. Pople, W. G. Schneider and H. J. Bernstein, "High Resolution Nuclear Magnetic Resonance," McGraw-Hill Book Co. Inc., New York, N.Y., 1959, pp. 218-225.

77. C. S. Johnson, Jr., in "Advances in Magnetic Resonance", Vol. 1, J. S. Waugh, Ed., Academic Press Inc., New York, N.Y., 1965, pp. 33-102.

78. R M. Lynden-Bell, in "Progress in Nuclear Magnetic Resonance Spectroscopy", Vol. 2, J. W. Emsley, J. Feeney and L. H. Sutcliffe, Eds., Pergamon Press Ltd., Oxford, 1967, pp. 163-204.

79. G. Binsch, in "Topics in Stereochemistry", Vol. 3, E. L. Eliel and N. L. Allinger, Eds., John Wiley and Sons Inc., New York, N.Y., 1968.

80. F. Bloch, Phys. Rev., 70, 460 (1946).

81. H. S. Gutowsky, D. W. McCall and C. P. Slichter, J. Chem. Phys., 21, 279 (1953).

82. H. S. Gutowsky and C. H. Holm, ibid., 25, 1228 (1956).

83. H. M. McConnell, ibid., 28, 430 (1958).

PART II

THE BINDING OF METAL IONS BY GLUTATHIONE

111

CHAPTER 7

INTRODUCTION

The binding of metal ions by molecules such as peptides and proteins is of fundamental interest in view of the importance of metal ions in biological systems (1-4). For example, the catalytic function of many enzymes is dependent upon the presence of metal ions which may be coordinated to certain functional groups of the enzyme or substrate. In an enzyme many groups are available as potential coordination sites, but only certain ones are actually metal-coordinated in an enzymatic reaction.

Metal-peptide complexes are potential models for metal-enzyme interactions since peptides can be synthesized which contain the functional groups involved at the active sites of enzymes. Moreover, peptides are relatively small molecules making them more amenable to study by a variety of techniques. Freeman has summarized X-ray crystallographic data for many metal-peptide complexes (5). Even though these data refer to solid state structures they may be useful for at least sugges ng possible metal binding sites and conformations of the complexes in solution. A great deal of research has also been devoted to the solution

chemistry of metal-peptide complexes. Several of these studies will be reviewed briefly below.

Representative of the early work in this area are the studies in which the formation constants of the cadmium, zinc, and lead complexes of a series of polyglycine peptides were determined (6-8) using potentiometric measurements. By comparing the formation constant data, it was proposed that the binding sites in these complexes consist of the terminal amino group and the adjacent peptide linkage, but it was not possible to establish any carboxyl coordination. The copper and nickel complexes of the polyglycine peptides have also been extensively investigated (9-12,18) using pH titration, infrared and spectrophotometric methods in order to determine formation constants. Ionization of the peptide protons and subsequent metal binding to the negative nitrogen atoms was proposed by some of the workers for these complexes. pH titration and spectrophotometric studies have also been carried out on the copper complex of β-alanyl-L-histidine (carnosine) (9,13,14). From this work it was suggested that ionization of the peptide proton takes place with subsequent copper binding to the negatively charged peptide nitrogen, but there was lack of agreement as to the binding sites and the structure of

the complex.

The techniques used in the above examples have the disadvantage that they measure macroscopic properties and hence, do not provide definitive information at the molecular level. Pmr spectroscopy has proven useful for elucidating the binding of metal ions by simple peptides at the molecular level. For example the functional groups of polyglycine peptides involved in coordination to diamagnetic cadmium, zinc, lead and nickel (15-17) have been established from changes in the chemical shifts of carbon-bonded protons close to the binding site. The groups of polyglycine peptides involved in binding to paramagnetic copper and nickel (16,17) and of carnosine with copper (38) have been identified from the dependence of the line-widths of the pmr resonances on their proximity to the binding site. This application of pmr is limited, however, to those peptides whose spectra are relatively simple because of the need for distinct, well resolved resonances for monitoring interactions at the potential binding sites. Spectra which consist of overlapping peaks and complex multiplet patterns are of limited use in metal binding studies.

Carbon-13 magnetic resonance (cmr) spectroscopy is potentially more useful than pmr for the study of

metal-peptide interactions. First of all, proton-decoupled cmr spectra are comprised of single resonances for each of the nonequivalent carbon atoms of peptides. Secondly, the range of chemical shifts in cmr is at least an order of magnitude greater than in pmr, so that often a resonance can be resolved for each of the carbon atoms. In addition, carbon atoms are bonded directly to the possible binding sites in peptides making cmr potentially more sensitive as a probe for studying binding at the molecular level.

In Chapter VI, the results of a cmr investigation of the binding of cadmium, zinc, lead and mercury by the tripeptide γ-L-glutamyl-L-cysteinyl-glycine (glutathione) are presented and discussed (23). This peptide was chosen to evaluate the

$$H_2NCHCH_2CH_2CONHCHCONHCH_2COOH$$
$$|\qquad\qquad\qquad\quad |$$
$$COOH\qquad\qquad\quad CH_2$$
$$\qquad\qquad\qquad\qquad |$$
$$\qquad\qquad\qquad\qquad SH$$
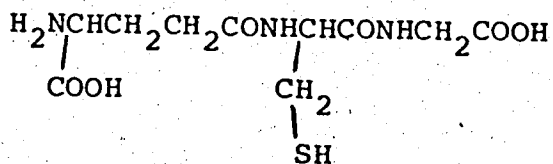
GLUTATHIONE

potential of cmr for the elucidation of metal binding by peptides because there is a lack of agreement as to which of the six possible coordination sites are involved in binding to these metal ions (19-22).

CHAPTER VI

THE BINDING OF ZINC, CADMIUM, LEAD AND MERCURY

BY GLUTATHIONE

The tripeptide glutathione, which is widely distributed in nature, contains the following six potential sites for metal ion coordination: the sulfhydryl group, the amino group, the two carboxyl groups and the two peptide linkages. Formation constants for the zinc, cadmium and lead complexes of glutathione have been determined previously using the pH titration method (19-22), but the results are different in each case because of the lack of agreement as to which of the sites are involved in metal ion coordination. The validity of microscopic formation constants determined from pH titration data is questionable when the binding sites are not known because the method is based on the competition between the metal ion and the proton for the site. Furthermore, microscopic ionization constants must be used in the calculations and only in one instance (21) was this done.

Li and coworkers (19,20) obtained formation constants for the zinc, cadmium and lead complexes of glutathione by assuming that all ionizable protons are removed from the peptide when it binds

to these metal ions. They suggested that in these
complexes the metal ion is bound to the ionized
sulfhydryl and amino groups. Martin and Edsall (21)
on the other hand, considered that divalent metal
ions could be bound to glutathione either through
the amino and carboxyl groups of the glutamyl residue
or to the sulfhydryl group of the cysteinyl residue
with possible chelate formation through a peptide
bond. By assuming that sulfur binding could be
excluded in S-methylglutathione and that bonding to
the glutamyl residue would be equivalent in gluta-
thione and its S-methyl derivative, they assigned
stability constant values to the sulfhydryl bound
and to the glutamyl bound complexes of zinc. At
pH < 8 these workers postulated that zinc binding
could take place at a peptide bond, but that ioniza-
tion of a peptide proton was unlikely. Perrin and
Watt (22) considered a number of different zinc and
cadmium complexes of glutathione of the type ML^-,
ML_2^{4-}, MHL, $ML(HL)^{3-}$, and calculated formation con-
stants for each of these species. These workers
proposed structures involving simultaneous coordina-
tion of sulfhydryl and glutamyl groups to the same
metal ion, and suggested that ionization of the
peptide protons can occur on complex formation.

Because of the differing results of the previous
studies of the metal complexes of glutathione, this
particular peptide was chosen to evaluate the potential
of cmr for the elucidation of metal binding by pep-
tides. The results of a cmr investigation of the
binding of zinc, cadmium, lead and mercury by gluta-
thione are reported in this chapter. Binding to
mercury has been studied previously by the polaro-
graphic method (24), and binding to CH_3Hg^+ has been
studied by pmr (25). In addition, the acid-base
chemistry of the four acidic groups of glutathione,
which is necessary for quantitative studies of metal
binding, has already been characterized at the
molecular level (25,26).

A. RESULTS

Glutathione

Cmr spectra of glutathione were obtained over
a pD range 1 to 13 for a 0.30 $\underline{M}$ solution of the tri-
peptide in D_2O using 1,4-dioxane as an internal
reference. The spectrum obtained at pD 7.37 is the
one designated (a) in Figure 15. The carbon atoms
are identified by Glu, Cys or Gly to specify the
amino acid residue glutamyl, cysteinyl or glycyl in
which the carbon is located and C_α, C_β, C_γ, CONH or
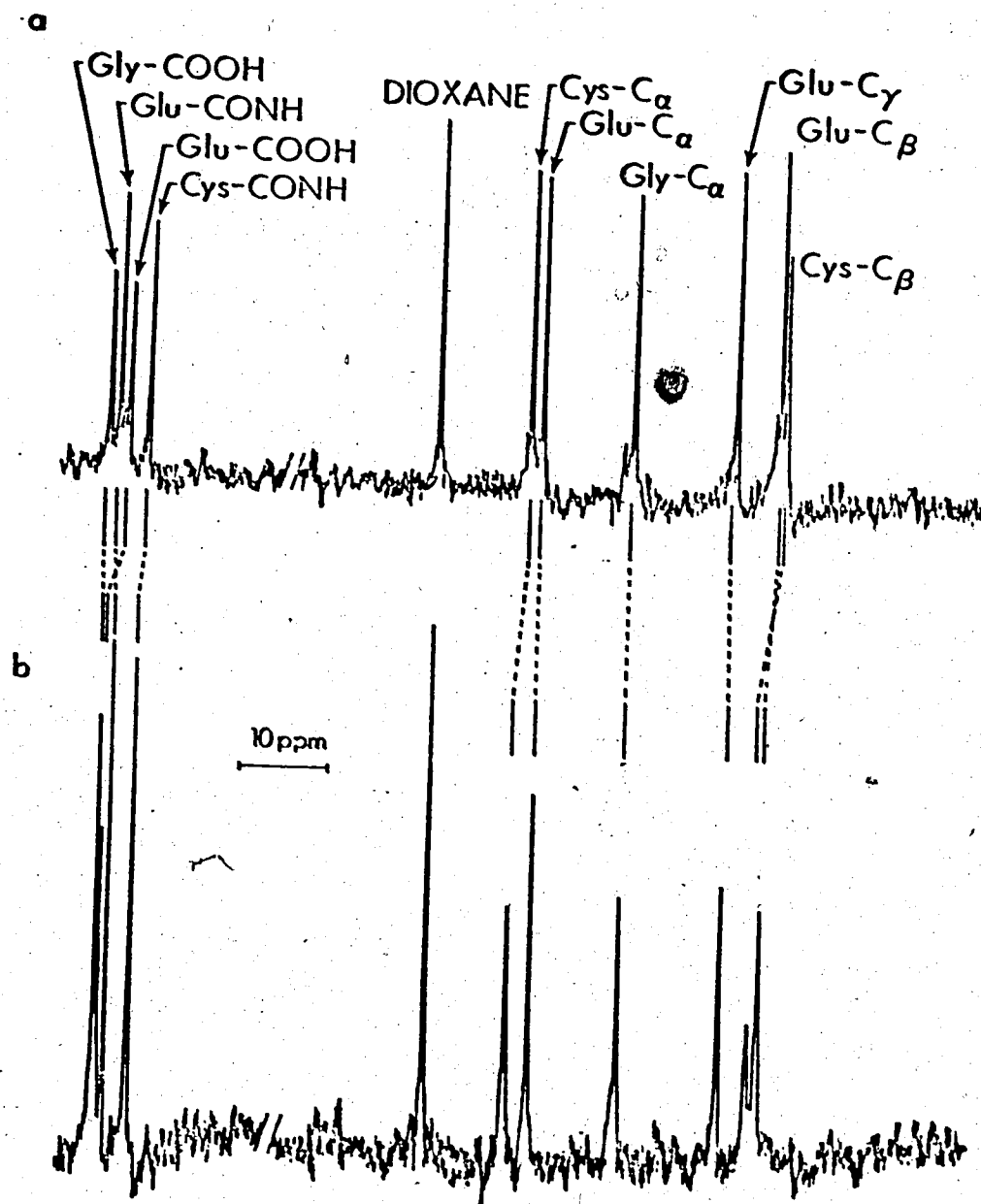
Figure 15: ^{13}C magnetic resonance spectra of glutathione.

(a) D_2O solution containing 0.30 $\underline{M}$ glutathione at pD 7.37.

(b) D_2O solution containing 0.30 $\underline{M}$ glutathione and 0.15 $\underline{M}$ $Zn(NO_3)_2$ at pD 7.84.

COOH to indicate the particular carbon of that residue. The assignments of the carbon resonances were made by comparison with the chemical shifts of the constituent amino acids (27,28), and from the chemical shift d endence of each of the resonances on the pD. These assignments are in agreement with those reported by Jung and coworkers who have previously given the cmr spectrum of glutathione (29), and have presented chemical shift vs. pH curves for each of the carbon atoms (30).

Zinc-glutathione

Addition of zinc to a solution of glutathione causes the chemical shifts of selected resonances to change, as illustrated by spectrum (b) in Figure 15. This spectrum was obtained from a solution 0.30 $\underline{M}$ in glutathione and 0.15 $\underline{M}$ in $Zn(NO_3)_2$ in D_2O at pD 7.84 and indicates that the ^{13}C chemical shifts are sensitive to metal binding. The resonances were assigned by following their pD dependence from low pD values where little metal binding takes place. The chemical shifts of the three cysteinyl carbon resonances are shown as a function of pD for a zinc to glutathione ratio of 1:2 by the solid curves in Figure 16, while the chemical shifts of selected carbon atoms of the glutamyl and glycyl residues
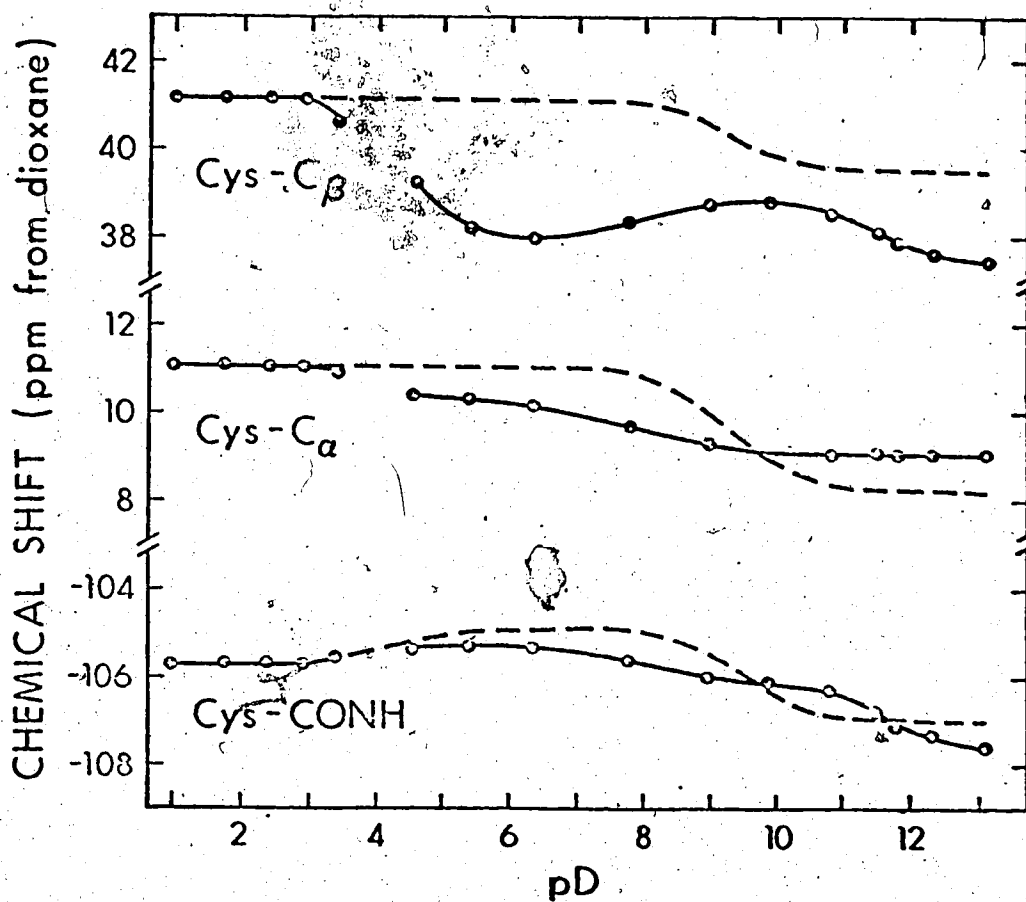
Figure 16: pD dependence of the chemical shifts of the cysteinyl carbons for a D_2O solution containing 0.30 M glutathione and 0.15 M $Zn(NO_3)_2$. The dashed curves represent the chemical shift behavior of the same carbon atoms for a solution of glutathione containing no complexing metal ion.

are shown for the same solution conditions in Figure

17. The discontinuity in these solid curves indicates

the pD region over which precipitation occurred.

The dashed curves in Figures 16 and 17 represent the

chemical shift vs. pD behaviour of the indicated

carbon resonances in the absence of coordinating

metal ion.

The lack of any large dependence of the chemical

shifts plotted in Figures 16 and 17 on the presence

of zinc at pD < 3 indicates no strong coordination

in this pD range. A small amount of binding to both

carboxylic acid groups, which previous studies (25)

have shown to be partially ionized at pD > 0, is

indicated by the small chemical shift differences

observed for the Gly-C_α, Gly-COOH, Glu-C_α and Glu-COOH

carbons. A chemical shift difference for a given

carbon atom refers to the difference between the solid

and dotted curves in Figures 16 and 17 and in sub-

sequent figures, and is assumed to be indicative

of some degree of metal binding to a specific site

near the given carbon atom. Some carboxylic acid

group coordination is consistent with the known

binding of zinc by the carboxylic acid groups of

acetylglycine and the C-terminal end of polyglycine

peptides (15,31).
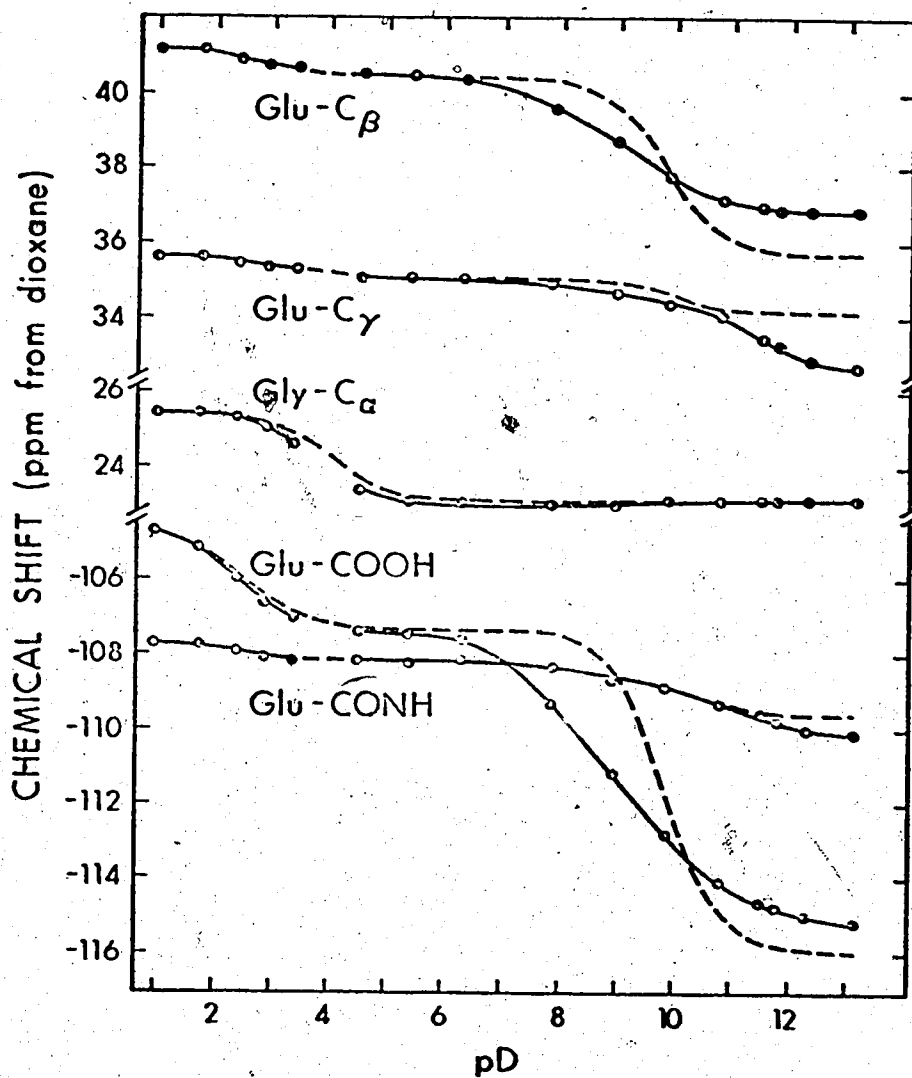
Figure 17: pD dependence of the chemical shifts of
selected glutamyl and glycyl carbons
for a D_2O solution containing 0.30 $\underline{M}$
glutathione and 0.15 $\underline{M}$ $Zn(NO_3)_2$.

Between pD 3.0 and 13.2, the large chemical shift differences exhibited by all three cysteinyl carbon resonances indicate that zinc is bound to some extent to the sulfhydryl group and possibly to the peptide linkage between the cysteinyl and glycyl residues. The lack of any chemical shift difference for the Glu-CONH carbon at pD < 10.5 indicates no binding to the peptide linkage between the glutamyl and cysteinyl residues. The Glu-COOH resonance indicates a small amount of binding to the glutamyl residue up to pD 6, presumably involving only the carboxyl group. An increase in the binding to the glutamyl residue at pD > 6, indicated by the chemical shift differences for the Glu-COOH, $-C_\alpha$, $-C_\beta$ and $-C_\gamma$ carbon resonances, probably involves simultaneous zinc coordination to the amino and carboxyl groups by analogy with the coordination of zinc by glycine. The small chemical shift differences observed for the Gly-C_α and Gly-COOH resonances over the pD range 3 to 9 are consistent with a small amount of binding to the glycyl carboxylic acid group.

The rather large downfield shifts exhibited by the Cys-CONH, Cys-C_β, Glu-CONH and Glu-C_γ carbon resonances at pD > 10.5 indicate a change in the nature of the binding to the peptide linkages. If

binding does take place at the peptide linkages at pD < 10.5, it is presumably to the carbonyl oxygen of the neutral peptide linkage, since it is known to be the more basic site (5,32-34). The downfield shift behaviour suggests that, in the presence of zinc, ionization of one or both of the peptide protons might occur at pD > 10.5 with subsequent binding of zinc to a negatively charged nitrogen atom. Separate resonances for the free amino acids of which glutathione is comprised were not observed, indicating that hydrolysis of the peptide bonds had not occurred under the given solution conditions.

The specificity of the zinc binding in the pD range 3 to 6 was investigated further by monitoring the chemical shifts as a function of the zinc to glutathione ratio for an H_2O solution at a constant pH of 5.51; the results of this study are presented in Figure 18. It can be seen that the chemical shift of the Cys-C_β carbon varies continuously as the ratio is increased from 0.0 to 0.5 and then levels out at a constant value of 38.2 ppm; the total chemical shift variation is 2.7 ppm. This indicates that at a ratio of 0.5 and a pH of 5.51, the main species in solution is a complex consisting of one zinc and two glutathione molecules. The chemical shift
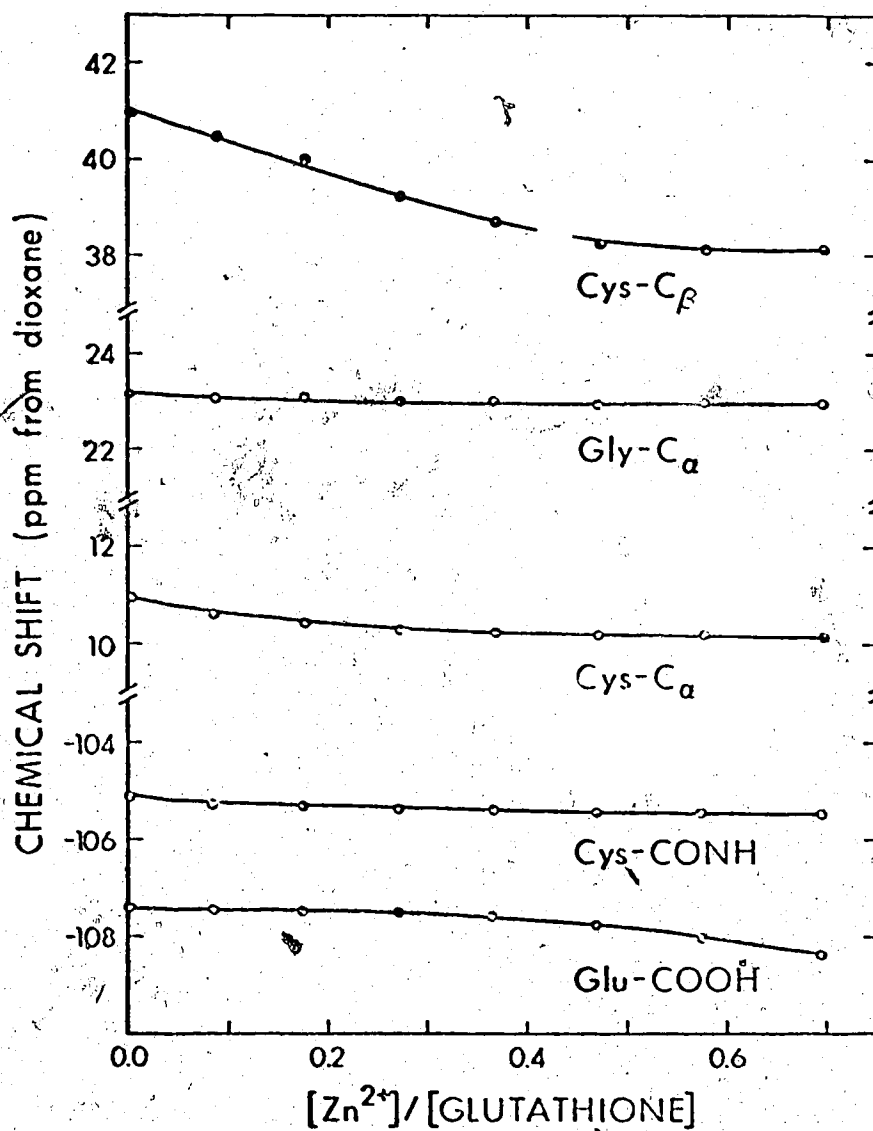
Figure 18: The chemical shifts of selected carbons
as a function of the zinc to glutathione
ratio for an aqueous solution at pH 5.51.

change of only 0.3 ppm for the Glu-COOH carbon up
to a ratio of 0.5 suggests that only a small amount
of binding takes place at the glutamyl end. For
comparison, ionization of the glutamyl ammonium
proton results in a change of 8.4 ppm for this carbon
resonance. On changing the ratio from 0.5 to 0.7,
however, when the sulfhydryl group is presumably com-
pletely complexed, the additional chemical shift
change of 0.6 ppm for the Glu-COOH carbon indicates
that the glutamyl end is becoming more important as
a binding site. The chemical shift variation of only
0.1 ppm for the Gly-C_α carbon in Figure 18 indicates
very weak glycyl carboxyl binding at the given pH.
Precipitation occurred at ratios greater than 0.7.

Cadmium-glutathione

The chemical shifts of the three cysteinyl
carbons for a cadmium to glutathione ratio of 1:2
are shown as a function of pD in Figure 19 by the
solid curves. The corresponding curves for selected
carbon atoms of the glutamyl and glycyl residues are
shown in Figure 20. The dotted curves in these
figures represent the data points for a glutathione
solution containing no complexing metal ion. At
pD < 2, evidence for a small amount of cadmium
binding to the two carboxyl groups is given by the
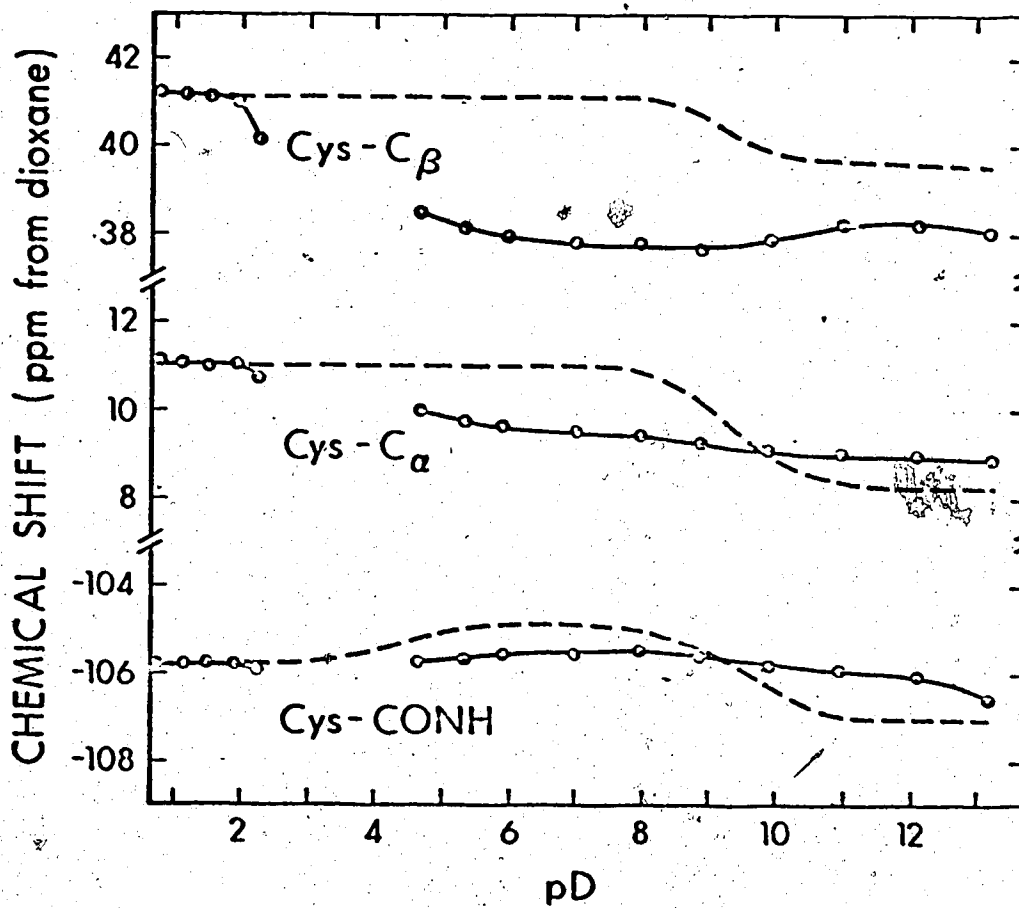
Figure 19: pD dependence of the chemical shifts of the cysteinyl carbons for a D_2O solution containing 0.30 $\underline{M}$ glutathione and 0.15 $\underline{M}$ $Cd(NO_3)_2$.
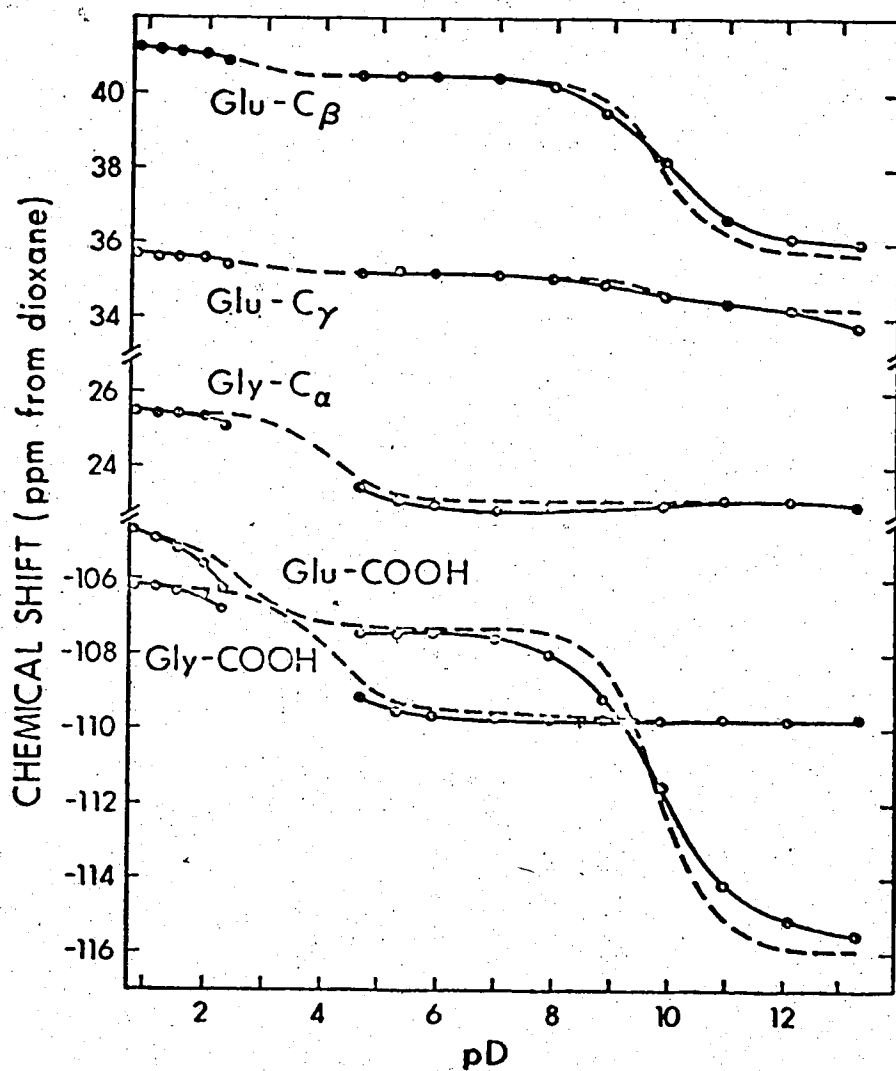
Figure 20: pD dependence of the chemical shifts
of selected glutamyl and glycyl carbons
for a D_2O solution containing 0.30 $\underline{M}$
glutathione and 0.15 $\underline{M}$ Cd(NO_3)$_2$.

small chemical shift differences observed for the
Gly-C_α, Gly-COOH, Glu-C_α and Glu-COOH carbons. As
in the zinc system, this type of binding is consistent
with the known binding of cadmium by the carboxylic
acid groups in certain peptides (31).

Between pD 2.0 and 13.2, the large chemical
shift differences observed for the three cysteinyl
carbon resonances indicate that cadmium is bound
to the sulfhydryl group and possibly to the peptide
linkage between the cysteinyl and glycyl residues.
No detectable binding to the other peptide linkage
is indicated by the fact that the chemical shift of
the Glu-CONH carbon resonance is not changed by the
presence of cadmium. The chemical shift curves
for the Glu-COOH carbon suggest that a small amount
of glutamyl binding takes place up to pD 7, probably
involving the carboxyl group. An increase in glutamyl
binding at pD > 7, indicated by the chemical shift
behaviour of the Glu-COOH, $-C_\alpha$, $-C_\beta$ and $-C_\gamma$ carbon
resonances, most likely involves simultaneous
coordination of cadmium to both the glutamyl amino
and carboxyl groups. Finally, the small chemical
shift differences observed for the Gly-C_α and Gly-COOH
carbons over the pD range 2 to 9 indicates weak
glycyl carboxyl coordination.

The above results indicate that, in the pD range 2 to 7, cadmium binding occurs almost exclusively at the cysteinyl residue of glutathione. This specificity was further investigated by monitoring the chemical shifts as a function of the cadmium to glutathione ratio for an H_2O solution at a constant pH of 6.59. The chemical shifts of selected carbon resonances are plotted as a function of the ratio in Figure 21. The cysteinyl residue is the principal coordination site up to a ratio of 0.5, as evidenced by the chemical shift variations of the cysteinyl carbons. In particular, the chemical shift of the Cys-C_β carbon changes by 3.2 ppm and then levels out above a ratio of 0.5. The chemical shift of the Glu-COOH carbon changes by only 0.3 ppm up to this ratio, indicating very little glutamyl binding. However, an increase in this interaction takes place at ratios greater than 0.5, when presumably the sulfhydryl group is fully coordinated. Finally, the chemical shift change of only 0.2 ppm for the Gly-C_α resonance indicates weak binding to the glycyl carboxyl group under these conditions. Precipitation occurred at ratios greater than 0.7.

Figure 21: The chemical shifts of selected carbons as a function of the cadmium to glutathione ratio for an aqueous solution at pH 6.59.

Lead-glutathione

The chemical shift curves of the three cysteinyl, the Gly-C_α and the Glu-COOH carbons are shown as a function of pD in Figure 22 for a lead to glutathione ratio of 1:2. Precipitation from pD 2.3 to 5.4 and above pD 12 limited the range over which binding could be studied.

At pD < 2.3, weak coordination to the two carboxyl groups is indicated by the small chemical shift differences for the Gly-C_α and Glu-COOH carbons. Between pD 5.4 and 12, the chemical shift curves provide evidence for lead binding to only the cysteinyl and glycyl residues. The large differences between the solid and dotted curves for the three cysteinyl carbon resonances indicate lead coordination to the sulfhydryl group and possibly the peptide linkage between the cysteinyl and glycyl residues. Evidence for weak glycyl carboxyl binding between pD 5.4 and 9.0 is also provided by the chemical shift curves for the Gly-C_α and Gly-COOH carbons. The extent of this binding decreases at pD > 9 presumably due to carboxyl displacement by hydroxide ions with the formation of lead-hydroxy-glutathione mixed complexes. The lack of any change in the chemical shifts due to the presence of lead for all the glutamyl carbon resonances is evidence
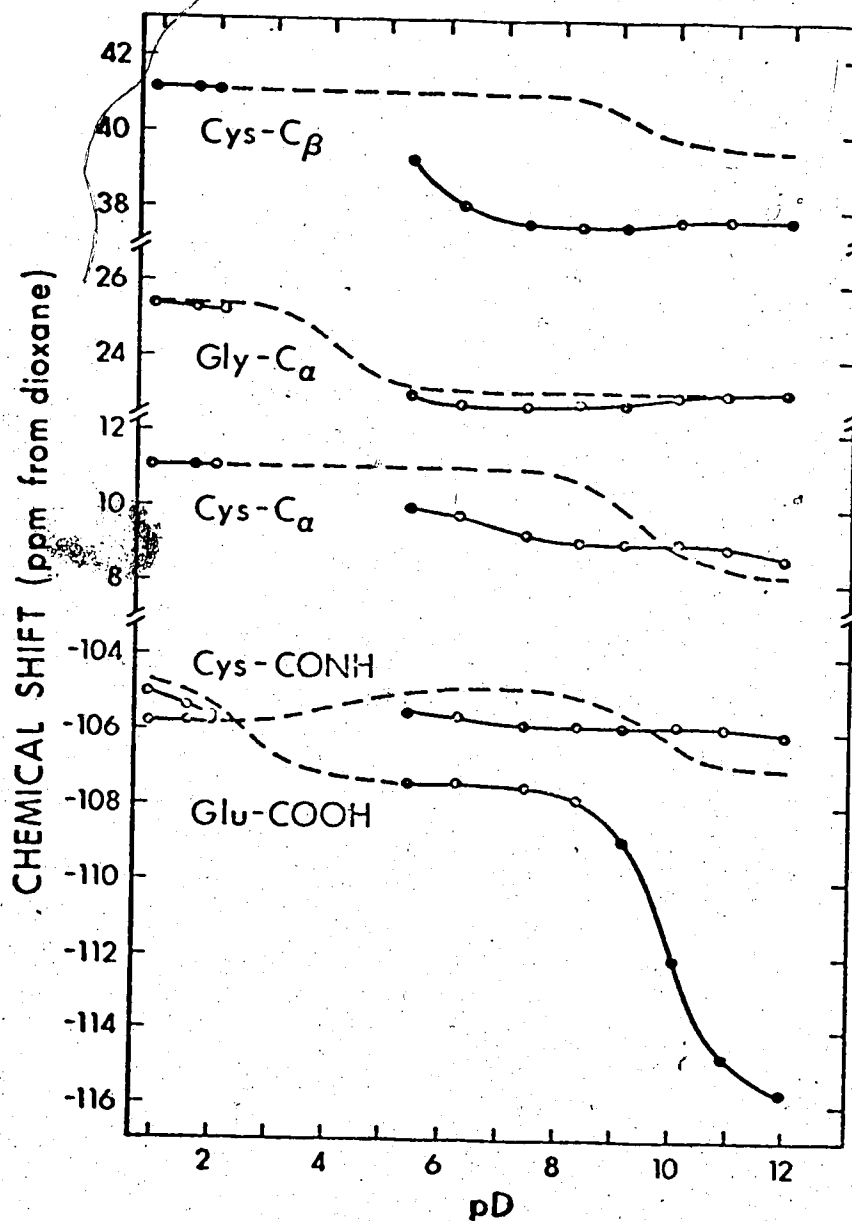
Figure 22: pD dependence of the chemical shifts of selected carbons for a D_2O solution containing 0.30 $\underline{M}$ glutathione and 0.15 $\underline{M}$ Pb$(NO_3)_2$.

that the glutamyl functional groups do not act as
binding sites in the pD range 5.4 to 12.

Mercury-glutathione

The chemical shift curves for the three cysteinyl
carbons as a function of pD, shown in Figure 23 for a
mercury to glutathione ratio of 1:2, are seen to be
nearly constant over the entire accessible pD range.
The chemical shifts for all the other carbon atoms of
glutathione are identical with those obtained from
solutions containing no mercury ions. Therefore, the
binding of mercury appears to take place exclusively
to the sulfhydryl group at a mercury to glutathione
ratio of 0.5. The results of further experiments, in
which the ratio was varied from 0.0 to 0.5 for an H_2O
solution at a constant pH of 5.01 are presented in
Figure 24. These plots confirm the specificity of the
sulfhydryl group for mercury. Precipitation prevented
investigations at mercury to glutathione ratios
greater than 0.5.

B. DISCUSSION

The cmr results show that all of the metal ions
studied in this work bind to the sulfhydryl group of
glutathione at metal to peptide ratios of 1:2 and, at
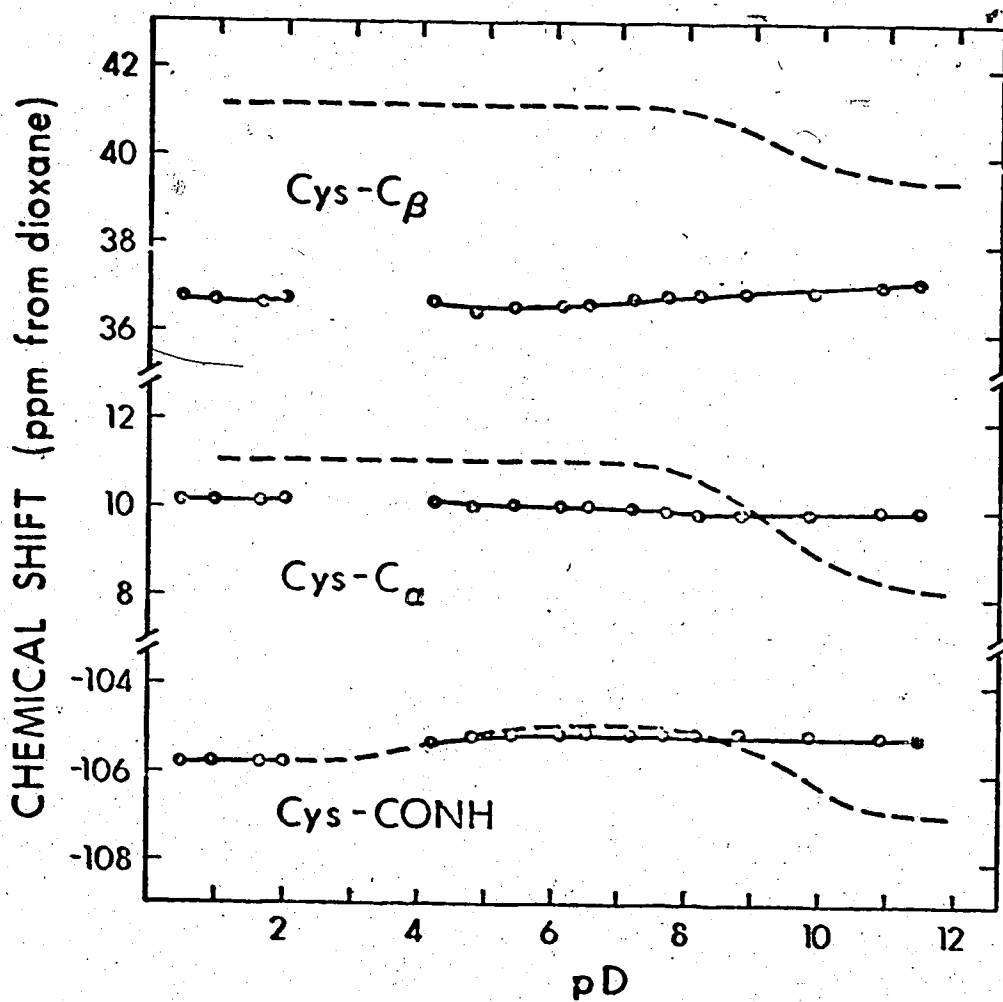
Figure 23: pD dependence of the chemical shifts of the cysteinyl carbons for a D_2O solution containing 0.30 $\underline{M}$ glutathione and 0.15 $\underline{M}$ Hg $(NO_3)_2$.
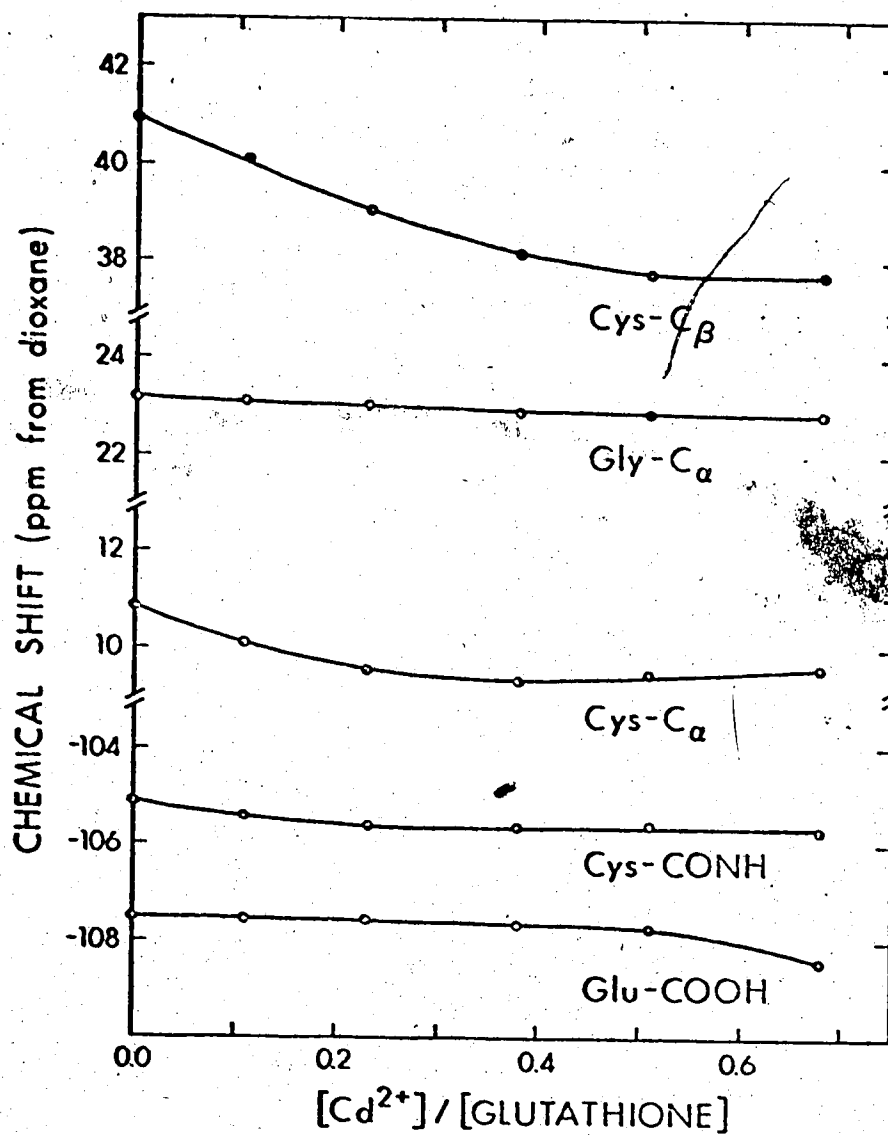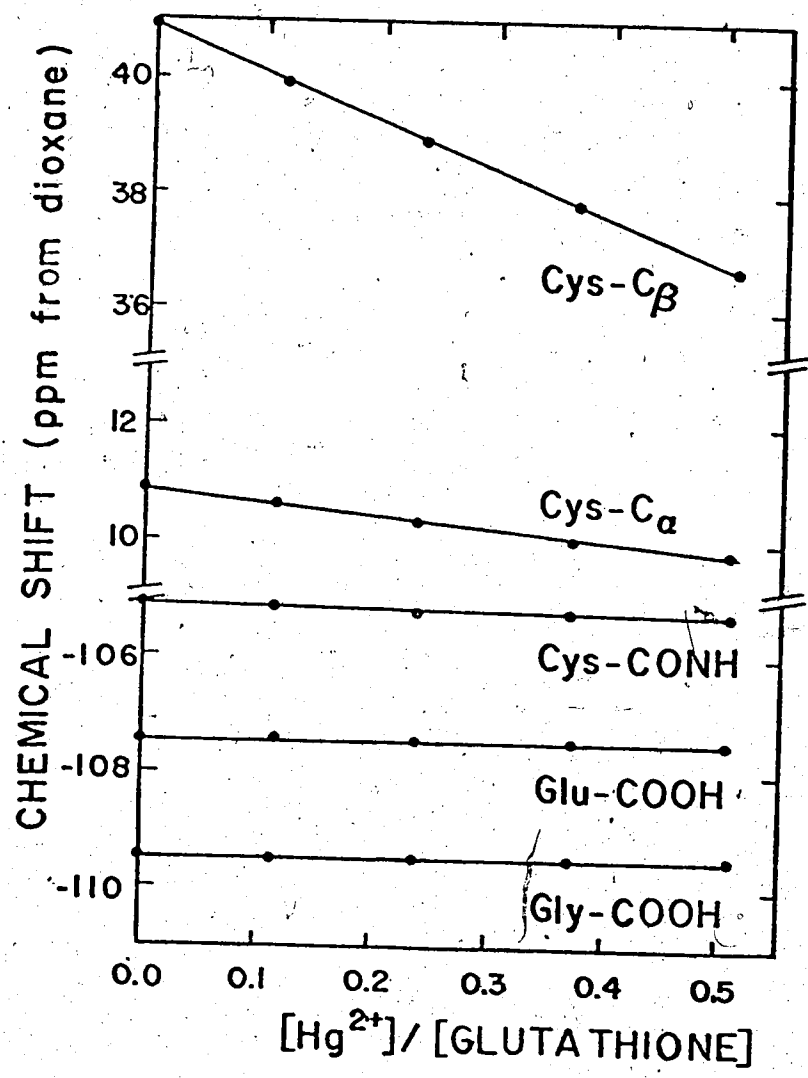
Figure 24: The chemical shifts of selected carbons as a function of the mercury to gluta-thione ratio for an aqueous solution at pH 5.01.

pD > 3. Also, all of the metal ions except mercury coordinate rather weakly to the glycyl and glutamyl carboxyl groups, while only zinc and cadmium bind to the glutamyl amino group. The extent of binding to the various sites is dependent upon the solution pD, except in the case of mercury which is bound strongly to the sulfhydryl group over the entire accessible pD range.

Zinc and Cadmium Binding to the Sulfhydryl and Glutamyl Groups

Because of the similarity in the binding of cadmium and zinc, the results for these systems will be discussed together. The strongest binding of these two metal ions occurs to the sulfhydryl group, as evidenced by the fact that the metal ions bind to this group at a much lower pD than to the glutamyl amino group, even though the pK_A of the sulfhydryl group is only 0.2 units less than that of the amino group (25). The chemical shifts of the Cys-C_β carbon indicate that, for a metal to glutathione ratio of 0.5, all the sulfhydryl groups are complexed at pD 6 in the zinc system and at pD 7 in the cadmium system. The results of experiments in which the metal to glutathione ratio was varied at pH 5.51 for the zinc system and at pH 6.59

for the cadmium system also indicate that binding

occurs almost exclusively to the sulfhydryl group at

these pH values up to a ratio of 0.5. Thus, a 1:2

complex such as that shown below is the major species

in solution for these conditions.

$$\overset{\ominus}{O_2}CCHCH_2CH_2CONHCHCONHCH_2-CO_2 \ominus$$
$$\overset{\oplus}{NH_3} \qquad CH_2$$
$$S$$
$$M$$
$$S$$
$$CH_2$$
$$\overset{\ominus}{O_2}CCHCH_2CH_2CONHCHCONHCH_2CO_2\overset{\ominus}{}$$
$$\overset{\oplus}{NH_3}$$
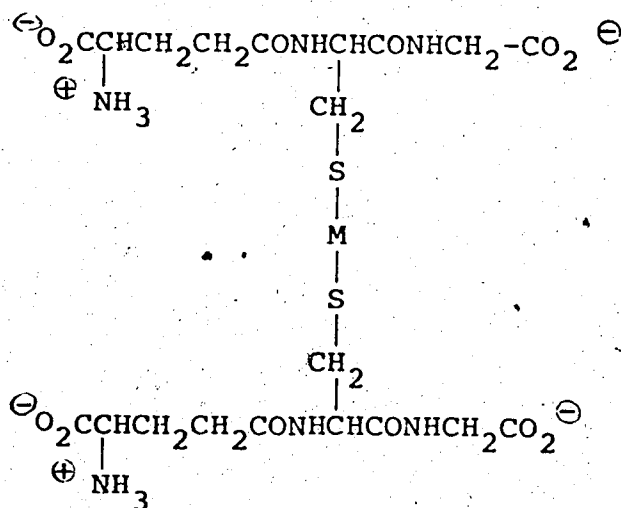
This 1:2 complex is analogous to the complex

$M(HL)_2^{2-}$, where M^{2+} is Cd^{2+} or Zn^{2+} and HL^{2-} represents

monoprotonated glutathione, proposed by Perrin and

Watt (22). These workers were unable to assign the

binding sites due to the uncertainty in the pK_A

values of the amino and sulfhydryl groups. The amino

group is still protonated as evidenced by the chemical

shift curves for the Glu-COOH, $-C_\alpha$ and $-C_\beta$ carbons. Li

and coworkers (19,20) interpreted pH titration data

for the binding of cadmium and zinc by glutathione in

terms of complexes in which the two carboxyl, the amino

and the sulfhydryl groups are all ionized. The present
chemical shift data show this not to be the case, but
rather that several different complexes may form and in
some, those functional groups which are not coordinated
are protonated.

It is possible that, in the zinc and cadmium
complexes discussed above, binding might also occur
to the peptide linkage between the cysteinyl and glycyl
residues. Of the two sites in this linkage, protonated
nitrogen and carbonyl oxygen, the oxygen is the more
basic (5,32-34) and hence a more probable binding site.
Such binding occurring simultaneously with sulfhydryl
group coordination would result in a six-membered
chelate ring. The cysteinyl carbon chemical shift
data for the zinc system at pD 7 are consistent with
carbonyl oxygen binding.

As shown by the chemical shift vs. pD curves,
observable metal binding to the glutamyl amino group
takes place at pD > 6 for the zinc system and at pD > 7
for the cadmium system. The extent of this binding is
pD dependent, as illustrated by the results in Table
XVII which were calculated from the chemical shift data
for the Glu-COOH and Glu-C_β carbon resonances using
the equation,

$$f = \frac{\delta_{OBS} - \delta_f}{\delta_c - \delta_f}$$

Table XVII

Fraction of Glutamyl Groups of Glutathione
Complexed by Zn^{2+} and Cd^{2+} as a Function of pD [a]

	Zn^{2+}		Cd^{2+}	
pD	Glu-COOH[b]	Glu-C_β[c]	Glu-COOH	Glu-C_β
6.0	0.03	0.00	0.03	0.00
7.0	0.10	0.12	0.05	0.00
8.0	0.34	0.29	0.14	0.06
8.5	0.49	0.41	0.21	0.14
9.0	0.58	0.53	0.35	0.36
10.5	0.63	0.55	0.37	0.32
11.0	0.58	0.56	0.27	0.21

(a) Data obtained from solutions of metal to glutathione
ratio of 1:2.

(b) Glu-COOH carbon chemical shift data.

(c) Glu-C_β carbon chemical shift data.

where f is the fraction of glutamyl groups complexed, δ_{OBS} is the observed chemical shift of a glutamyl carbon in the presence of complexing metal ion, δ_f is the chemical shift in the absence of metal ion and δ_c is the chemical shift of glutamyl complexed glutathione. The value of δ_c used in these calculations was obtained from the point where the solid and dashed curves cross in Figures 17 and 20 (31). The δ_{OBS} values were obtained from the chemical shift vs. pD curves for solutions of a metal to glutathione ratio of 1:2, and those for δ_f from the corresponding curves for a solution of glutathione. The fractions shown in Table XVII reveal that cadmium is bound less strongly to the glutamyl end of glutathione than is zinc.

A change in the nature of the zinc binding to the cysteinyl residue in the pD range 6 to 10.5 is indicated by the chemical shift data for the cysteinyl carbon resonances shown in Figure 16. Simultaneous coordination to the sulfhydryl group and the peptide carbonyl oxygen, as suggested above, would be expected to have a different effect on all three cysteinyl carbons than coordination to the sulfhydryl group alone. Therefore, it is suggested that at pD < 6, simultaneous sulfhydryl-peptide oxygen binding takes place, and at pD > 6 the amount of binding to the peptide oxygen decreases. Presumably

the decreased peptide binding is due to glutamyl group

competition for the coordination sites on the zinc.

The smaller affinity of cadmium for the glutamyl group

probably causes a smaller decrease in peptide binding

and hence, the effect on the cysteinyl carbon chemical

shifts is less than in the zinc system.

At pD > 6 for the zinc-glutathione system and pD > 7

for the cadmium system, the principal binding sites are

the glutamyl residue and the cysteinyl residue. Glutamyl

binding most likely involves simultaneous metal co-

ordination to the amino and carboxyl groups by analogy

with the coordination of these two metal ions by glycine.

As indicated above, cysteinyl binding could involve

simultaneous coordination to the sulfhydryl group and

the oxygen of the peptide linkage between the cysteinyl

and glycyl residues. In any case, it is unlikely that

both the cysteinyl and glutamyl residues of a glutathione

molecule are simultaneously coordinated to the same

metal ion; this would involve an unstable 10-membered

ring (35), since the present chemical shift data have

shown that the peptide linkage between the glutamyl and

cysteinyl residues is not bonded to cadmium nor to

zinc at pD < 10.5. The structure proposed by Perrin and

Watt (22) for the ML^- complexes, where M^{2+} is Cd^{2+} or

Zn^{2+} and L^{3-} represents fully ionized glutathione,

involves simultaneous coordination to the glutamyl amino and carboxyl groups, the glutamyl peptide linkage and the sulfhydryl group. This clearly is not in agreement with the ^{13}C chemical shift data. In the structure proposed for the ML_2^{4-} complexes by these workers, the second glutathione molecule was assumed to be bonded to the metal only through the glutamyl carboxyl and amino groups. More likely structures for these complexes are ones in which the cysteinyl or glutamyl group of one glutathione molecule and the cysteinyl or glutamyl group of another are bound to the same metal ion, as considered by Martin and Edsall (21) in the analysis of pH titration data. Another likely structure might be one in which the cysteinyl and glutamyl groups of a glutathione molecule are bound to different metal ions, resulting in polynuclear complexes which have been proposed previously for polyglycine peptide complexes (15,16). Molecular models indicate that polynuclear complexes in which a metal is bonded to the sulfhydryl groups of two glutathione ligands and the glutamyl amino and carboxyl dentates of two other sulfhydryl-complexed glutathione molecules are possible.

Ionization of the Peptide Protons

It is known that, in certain metal-peptide complexes, the metal ion promotes the ionization of peptide protons with subsequent binding to the negatively charged nitrogen atom (9,10,16,18,33,36,37). The large downfield shifts observed for the Glu-CONH, Glu-C_γ, Cys-CONH, and Cys-C_β carbon resonances for the zinc system at pD > 10.5 suggest that zinc might promote ionization of the peptide protons of glutathione. After such ionization the most basic site is the nitrogen atom (5,34) where zinc binding could take place. Simultaneous zinc coordination to the sulfhydryl group and glutamyl peptide nitrogen would result in a five-membered ring and to the cysteinyl peptide nitrogen would result in a six-membered ring. Ionization of a peptide proton and binding of the negatively charged nitrogen atom to a zinc ion presumably have different effects on the chemical shifts of the neighbouring carbon atoms. The fact that the chemical shift of the Cys-C_α carbon, which is near both peptide nitrogens, experiences no change at pD > 10.5 might be due to the combined effects of ionization and binding cancelling each other out. The chemical shift data for the cadmium, lead and mercury systems provide no evidence for peptide proton ionization.

Perrin and Watt (22), from pH titration data, suggested that ionization of the peptide protons of glutathione can occur upon complex formation with both zinc and cadmium and that the metal-peptide bond interaction is slightly greater in the zinc system. However, the pK_A of 9.86 which they interpreted as corresponding to ionization of a peptide proton from a coordinated peptide group in the ZnL_2^{4-} complex, is approximately two orders of magnitude too low to be consistent with the present chemical shift data. Martin and Edsall (21) found that their pH titration data for zinc-glutathione did not necessitate the postulation of the ionization of peptide protons; however, their experiments were carried out at pH < 8. These same workers have suggested that zinc ion does promote peptide ionization in the zinc-glycylhistidine complex (13).

Mercury and Lead Binding to the Sulfhydryl Group

The binding of mercury and lead to glutathione is somewhat different from that of zinc and cadmium; neither mercury nor lead binds to the glutamyl end at pD > 3 for metal to peptide ratios of 0.5. Mercury binds exclusively to the sulfhydryl group at ratios up to 0.5 over the pD range 0.5 to 12, resulting in 1:2

complexes with the protonation state of the carboxyl and amino groups dependent on the solution pD. No binding to any of the other potential coordination sites is indicated by the chemical shift data. This is in agreement with the results of Stricks and Kolthoff (24) who found that in the complex HgL_2, where L represents glutathione in any of its protonation states, mercury is firmly bound to glutathione as a mercaptide.

Since mercury and CH_3Hg^+ (25,39) bind to the sulfhydryl group with such a high degree of specificity and since such binding results in large chemical shift changes in the $Cys-C_\alpha$ and $-C_\beta$ resonances, it may be possible to identify these two resonances in the cmr spectra of proteins by observing changes in the spectrum as the protein is titrated with mercury or CH_3Hg^+ at constant pH.

The binding of lead to the sulfhydryl group of glutathione is not as strong as that of mercury, as evidenced by the decrease in the extent of binding at pD < 7 and by the fact that no binding to the sulfhydryl group is observed at pD < 2.3 for the lead-glutathione system. The chemical shift data for the Cys-CONH carbon indicate that lead might be simultaneously bound to the sulfhydryl group and to the oxygen of the peptide linkage between the cysteinyl and

glycyl residues. The chemical shift data also indicate that the glutamyl amino group is not a binding site for a lead to glutathione ratio of 0.5 over the accessible pD range.

Chemical Shift Differences

Addition of metal ions to a solution of glutathione causes the chemical shifts of selected carbons close to the binding site to change. Results of quantitative measurements of the magnitudes of the differences between the chemical shifts of selected carbon atoms, when a given functional group is complexed and when the group is not complexed, are given in Table XVIII. The magnitudes of these chemical shift differences are denoted by Δ.

In the determination of the Δ values for the cysteir i carbon resonances, the chemical shifts when the sulfhydryl group is complexed were obtained from the chemical shift vs. pD curves for the metal complex solutions at pD 7. The chemical shifts when the sulfhydryl group is not complexed were obtained from the chemical sh . pD curves for glutathione solutions at pD 7, where the sulfhydryl group is protonated. The order of decreasing Δ values for the Cys-C_β carbon is $Hg^{2+} > Pb^{2+} > Cd^{2+} > Zn^{2+}$, in agree-

Table XVIII

^{13}C Chemical Shift Changes for Selected Carbon

Resonances of Glutathione upon Complexation

CARBON	Δ (ppm)			
	Zn^{2+}	Cd^{2+}	Pb^{2+}	Hg^{2+}
Cys-C$_\beta$	3.1	3.3	3.5	4.4
Cys-C$_\alpha$	1.0	1.5	1.6	1.0
Cys-CONH	0.5	0.5	0.8	0.2
Glu-COOH	6.0	3.9	a	a
Glu-C$_\beta$	2.6	1.8	a	a
Gly-C$_\alpha$	0.1	0.2	0.3	b

(a) No coordination of Hg^{2+} or Pb^{2+} to the glutamyl amino group was detected.

(b) No coordination of Hg^{2+} to the glycyl carboxyl group was detected.

ment with the order of decreasing affinity of the sulfhydryl group of bovine serum albumin for these metal ions (40). The data in Table XVIII also illustrate that the Δ values decrease as the number of bonds separating the carbon atom from the sulfhydryl group increases. The much greater decrease for the Cys-C_α and Cys-CONH carbons in the mercury system is consistent with no binding of this metal ion to the oxygen of the peptide linkage between the cysteinyl and glycyl residues.

The Δ values for the Glu-COOH and Glu-C_β carbon resonances are presented in Table XVIII for the cadmium and zinc systems; no glutamyl amino coordination by mercury or lead was detected by the chemical shift data. The chemical shifts for the glutamyl complexed species were obtained from the points where the solid and dashed curves intersect in Figures 17 and 20 (31), whereas the corresponding values for noncomplexed glutamyl species were obtained from the chemical shift vs. pD curves for glutathione at pD 7 where the amino group is protonated and the glutamyl carboxyl group is ionized. It can be seen from Table XVIII that the values are larger for zinc than for cadmium, in agreement with the relative order of stabilities of the corresponding glutamic acid complexes of these metal

ions (41). · It is also evident that binding at the glutamyl end of glutathione affects the chemical shift of the Glu-COOH carbon more than that of the Glu-C_o carbon, which in turn experiences a larger effect than the Glu-C_α carbon. The order of these chemical shift effects is similar to that observed on protonation of the amino group in amino acids and peptides (27).

The Δ values for the Gly-C_α carbon listed in Table XVIII were obtained from the differences between the solid and dashed curves at pD 7 in Figures 17, 20, and 22, and reflect the extent of binding of the glycyl carboxyl group of glutathione by these metal ions. It can be seen that the order of decreasing Δ values is $Pb^{2+} > Cd^{2+} > Zn^{2+}$, the same as the relative order of the formation constants of the complexes of these metal ions with acetylglycine and the carboxyl group of polyglycine peptides (15,31). These carboxyl interactions are very weak as evidenced by the small Δ values, which are all less than 0.3 ppm. Binding of zinc to the carboxyl groups of glutathione has not been previously detected in pH titration experiments (19-22), presumably because the formation constants are so small.

Conclusions

^{13}C chemical shift data indicate that the metal ions zinc, cadmium, lead and mercury bind to the potential coordination sites of glutathione with a high degree of specificity. All four metal ions bind to the sulfhydryl group while only zinc and cadmium bind to the glutamyl amino group under the conditions used in this work. These results demonstrate the potential of cmr as a technique for elucidating the binding of metal ions by peptides. The technique should also be applicable to similar studies for other multidentate biological molecules.

CHAPTER VII

EXPERIMENTAL

A. CHEMICALS AND SOLUTIONS

Reduced glutathione (Nutritional Biochemicals Corp. and Terochem Laboratories) was washed with a water-ethanol solution and dried at 110° before using. Reagent grade metal nitrate salts were used as received.

The solutions were prepared in D_2O or triply distilled water under an atmosphere of nitrogen to minimize oxidation of the sulfhydryl group of glutathione. For the chemical shift vs. pD measurements, the pD of D_2O solutions, 0.30 $\underline{M}$ in glutathione and 0.15 $\underline{M}$ in metal nitrate, was adjusted with a 40% KOD solution and concentrated nitric acid and samples of about 2 ml each were withdrawn at the appropriate pD values. 1,4-dioxane was added to the solutions as an internal reference at a concentration of about 0.1 $\underline{M}$. For making chemical shift vs. mole ratio measurements at constant pH, the requisite amount of metal nitrate was added to an H_2O solution of glutathione, the pH adjusted and a sample withdrawn. More metal nitrate was added to the solution and the same procedure followed for all samples at this pH.

B. POTENTIOMETRIC AND CMR MEASUREMENTS.

All pH and pD measurements were carried out as described in Chapter IV.

The ^{13}C spectra were obtained using a Bruker HFX-90 spectrometer operating at a frequency of 22.63 MHz and equipped with a Nicolet 1085 computer. The Fourier transform mode was used with proton decoupling. When D_2O was the solvent, the deuterium resonance from the D_2O was used for the heteronuclear lock signal. When H_2O was the solvent, the ^{19}F resonance from hexafluorobenzene in a coaxial capillary was used for the lock. For each free induction decay signal, 8K data points were collected in the computer and 4K accumulations were carried out to achieve an adequate signal-to-noise ratio. The frequency range of the transformed spectra was 5000 Hz. Chemical shifts are reported in ppm relative to the resonance of internal 1,4-dioxane which is 67.4 ppm downfield from the TMS resonance. Positive chemical shifts correspond to greater shielding than in 1,4-dioxane. The chemical shift measurements are considered accurate to within 0.1 ppm. For all measurements the sample temperature was 32 ± 2°.

BIBLIOGRAPHY

1. R. J. P. Williams, <u>Roy. Inst. Chem. Rev.</u>, <u>1</u>, 13 (1968).

2. B. L. Vallee and R. J. P. Williams, <u>Chem. in Britain</u>, <u>4</u>, 397 (1968).

3. A. E. Dennard and R. J. P. Williams, <u>Transition Metal Chem.</u>, <u>2</u>, 115 (1967).

4. H. Sigel and D. B. McCormick, <u>Accounts Chem. Res.</u>, <u>3</u>, 201 (1970).

5. H. C. Freeman, <u>Adv. Protein Chem.</u>, <u>22</u>, 257 (1967).

6. C. B. Monk, <u>Trans. Faraday Soc.</u>, <u>47</u>, 285, 292, 297 (1951).

7. W. P. Evans and C. B. Monk, <u>ibid.</u>, <u>51</u>, 1244 (1955).

8. N. C. Li and M. C. M. Chen, <u>J. Amer. Chem. Soc.</u>, <u>80</u>, 5678 (1958).

9. H. Dobbie and W. O. Kermack, <u>Biochem. J.</u>, <u>59</u>, 246, 257 (1955).

10. R. B. Martin, M. Chamberlin and J. T. Edsall, <u>J. Amer. Chem. Soc.</u>, <u>82</u>, 495 (1960).

11. M. K. Kim and A. E. Martell, <u>ibid.</u>, <u>88</u>, 914 (1966).

12. M. K. Kim and A. E. Martell, <u>ibid.</u>, <u>89</u>, 5138 (1967)

13. R. B. Martin and J. T. Edsall, <u>ibid.</u>, <u>82</u>, 1107 (1960).

14. G. R. Lenz and A. E. Martell, <u>Biochem.</u>, <u>3</u>, 750 (1964).

15. D. L. Rabenstein and S. Libich, <u>Inorg. Chem.</u>, <u>11</u>, 2960 (1972).

16. M. K. Kim and A. E. Martell, <u>J. Amer. Chem. Soc.</u>, <u>91</u>, 872 (1969).

17. R. Mathur and R. B. Martin, <u>J. Phys. Chem.</u>, <u>69</u>, 668 (1965).

18. G. K. Pagenkopf and D. W. Margerum, <u>J. Amer. Chem. Soc.</u>, <u>90</u>, 6963 (1968).

19. N. C. Li, O. Gawron and G. Bascuas, _ibid._, _76_, 225 (1954).

20. N. C. Li and R. A. Manning, _ibid._, _77_, 5225 (1955).

21. R. B. Martin and J. T. Edsall, _ibid._, _81_, 4044 (1959).

22. D. D. Perrin and A. E. Watt, _Biochem. Biophys. Acta_, _230_, 96 (1971).

23. B. J. Fuhr and D. L. Rabenstein, _J. Amer. Chem. Soc._, in press.

24. W. Stricks and I. M. Kolthoff, _ibid._, _75_, 5673 (1953).

25. D. L. Rabenstein, _ibid._, _95_, 2797 (1973).

26. R. B. Martin and J. T. Edsall, _Bull. Soc. Chim. Biol._, _40_, 1763 (1958)

27. M. Christl and J. D. Roberts, _J. Amer. Chem. Soc._, _94_, 4565 (1972).

28. W. J. Horseley and H. Sternlicht, _ibid._, _90_, 3738 (1968).

29. G. Jung, E. Breitmaier, W. Voelter, T. Keller, and C. Tanzer, _Angew. Chem. Internat. Edit._, _9_, 894 (1970).

30. G. Jung, E. Breitmaier and W. Voelter, _Eur. J. Biochem._, _24_, 438 (1972).

31. D. L. Rabenstein, _Can. J. Chem._, _50_, 1036 (1972).

32. A. Berger, A. Loewenstein and S. Meiboom, _J. Amer. Chem. Soc._, _81_, 62 (1959).

33. P. J. Morris and R. B. Martin, _Inorg. Chem._, _10_, 964 (1971).

34. J. D. Bell, H. C. Freeman, A. M. Wood, R. Driver, and W. R. Walker, _Chem. Comm._, 1441 (1959).

35. A. E. Martell and M. Calvin, "Chemistry of the Metal Chelate Compounds," Prentice Hall, New York, 1952, p. 134.

36. W. L. Koltun, M. Fried and F. R. N. Gurd, J. Amer. Chem. Soc., 82, 233 (1960).

37. E. W. Wilson, Jr. and R. B. Martin, Inorg. Chem., 9, 528 (1970).

38. M. Ihnat and R. Bersohm, Biochem., 9, 4555 (1970).

39. D. L. Rabenstein and M. T. Fairhurst, unpublished results.

40. I. M. Klotz, J. M. Urquhart and H. A. Friess, J. Amer. Chem. Soc., 74, 5537 (1952).

41. L. G. Sillen and A. E. Martell, "Stability Constants of Metal Ion Complexes," Special Publication No. 17, The Chemical Society, London, 1964.